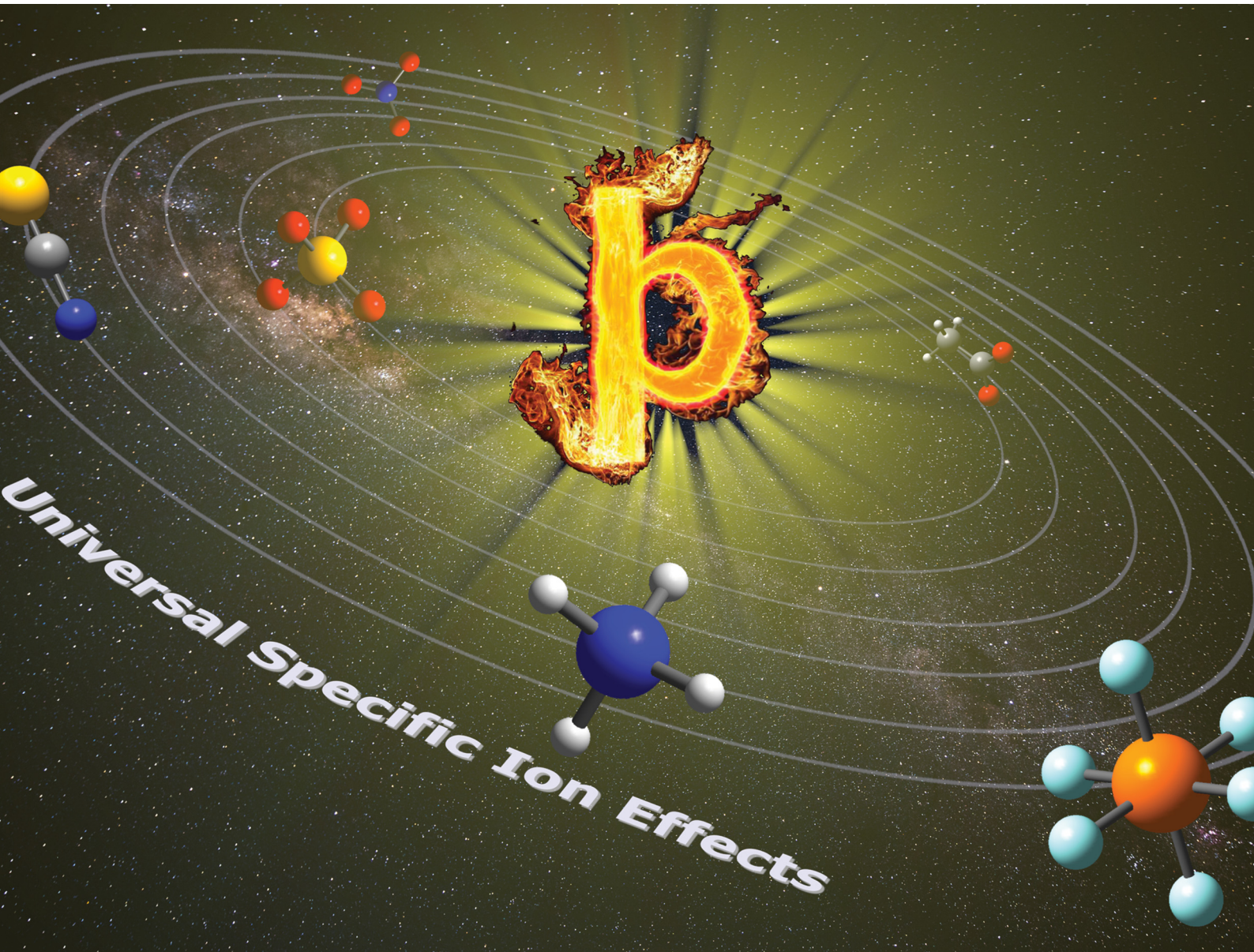


# PCCP

Physical Chemistry Chemical Physics

[rsc.li/pccp](http://rsc.li/pccp)



ISSN 1463-9076



Cite this: *Phys. Chem. Chem. Phys.*, 2022, 24, 12682

## Understanding specific ion effects and the Hofmeister series†

Kasimir P. Gregory, <sup>ab</sup> Gareth R. Elliott, <sup>a</sup> Hayden Robertson, <sup>a</sup>  
 Anand Kumar, <sup>c</sup> Erica J. Wanless, <sup>a</sup> Grant B. Webber, <sup>d</sup>  
 Vincent S. J. Craig, <sup>b</sup> Gunther G. Andersson <sup>c</sup> and Alister J. Page <sup>a\*</sup>

Specific ion effects (SIE), encompassing the Hofmeister Series, have been known for more than 130 years since Hofmeister and Lewith's foundational work. SIEs are ubiquitous and are observed across the medical, biological, chemical and industrial sciences. Nevertheless, no general predictive theory has yet been able to explain ion specificity across these fields; it remains impossible to predict when, how, and to what magnitude, a SIE will be observed. In part, this is due to the complexity of real systems in which ions, counterions, solvents and cosolutes all play varying roles, which give rise to anomalies and reversals in anticipated SIEs. Herein we review the historical explanations for SIE in water and the key ion properties that have been attributed to them. Systems where the Hofmeister series is perturbed or reversed are explored, as is the behaviour of ions at the liquid–vapour interface. We discuss SIEs in mixed electrolytes, nonaqueous solvents, and in highly concentrated electrolyte solutions – exciting frontiers in this field with particular relevance to biological and electrochemical applications. We conclude the perspective by summarising the challenges and opportunities facing this SIE research that highlight potential pathways towards a general predictive theory of SIE.

Received 20th February 2022,  
 Accepted 13th April 2022

DOI: 10.1039/d2cp00847e

rsc.li/pccp

<sup>a</sup> Discipline of Chemistry, School of Environmental and Life Sciences, The University of Newcastle, Callaghan, New South Wales 2308, Australia.

E-mail: alister.page@newcastle.edu.au

<sup>b</sup> Department of Materials Physics, Research School of Physics, Australian National University, Canberra, ACT 0200, Australia

<sup>c</sup> Flinders Institute of Nanoscale Science and Technology, College of Science and Engineering, Flinders University, South Australia 5001, Australia

<sup>d</sup> School of Engineering, The University of Newcastle, Callaghan, New South Wales 2308, Australia

† Electronic supplementary information (ESI) available. See DOI: <https://doi.org/10.1039/d2cp00847e>

‡ These authors contributed equally.



**Kasimir P. Gregory**

Kasimir obtained a Bachelor of Mathematics/Bachelor of Science (Hons – Chemistry) from the University of Newcastle in 2018 and is a PhD candidate there under the supervision of Prof. Alister Page, Prof. Erica Wanless and Prof. Grant Webber. In 2022 he started a postdoctoral appointment position at the Australian National University under the guidance of Prof. Vince Craig. He is investigating specific ion effects via computational and quantum chemistry, as well as surface force measurements.



**Gareth R. Elliott**

Gareth is a PhD student studying at the University of Newcastle (Australia) under the supervision of Prof. Alister Page, Prof. Erica Wanless and Prof. Grant Webber. He received a Bachelor of Mathematics/Bachelor of Science (Hons) with first class honours from UoN. He is currently investigating specific ion effects in various solvents at high concentrations using molecular dynamics.



## 1. Introduction

The presence of ions in a solution has a direct effect on its physicochemical properties. Electrolytes, encompassing acids, bases and salts, are key components in myriad contexts: cleaning agents,<sup>1–5</sup> fertilisers,<sup>6</sup> batteries<sup>7–9</sup> and broader geophysical phenomena.<sup>10–15</sup> Even life itself runs on electrolytes, which stabilise and regulate proteins, enzymes<sup>16–27</sup> and cells,<sup>28</sup> as well as balance acidity levels<sup>29</sup> and fluid retention.<sup>30</sup> In the majority of these applications, the electrolyte's effect is dependent not only on the ions' charges or concentrations, as suggested by widely-used theories (*e.g.* Debye–Hückel theory), but also on their *identity*. For example, KF is poisonous to humans, whilst KI is used to treat hypothyroidism; clearly the identity of the anion matters here. Such phenomena, in which the ion's identity is intrinsic to its effect on the properties of a system,

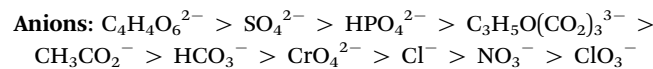


**Hayden Robertson**

*Hayden Robertson is a PhD student at the University of Newcastle under the supervision of Prof. Erica Wanless and Prof. Grant Webber. Hayden graduated from a combined degree of Bachelor of Mathematics (Pure) and Bachelor of Science (Hons)(Chemistry) from the University of Newcastle in 2019. His research includes investigating specific ion effects in complex environments using surface techniques such as neutron reflectometry and ellipsometry.*

are collectively known as specific ion effects (SIEs). Specific ion effects are the rule, rather than the exception.

SIEs were first systematically studied by Lewith and Hofmeister in the period 1887–1891, who found a consistent ordering of ions' abilities to precipitate proteins from blood serum and hen egg white in aqueous solutions:<sup>31,32</sup>



‘>’ implies a stronger ability to precipitate the protein (known as salting-out) and therefore lower “concentration” (in cation molar concentration; Fig. S1–S3, ESI<sup>†</sup>) required. This order has (perhaps erroneously) been set in stone for the anions on a



**Anand Kumar**

*Anand is a PhD student studying at Flinders University (Australia) under the supervision of Prof. Gunther Andersson and Prof. Vince Craig. He received a Bachelor in Physics/Nanotechnology with First class with distinction from SRM University (India) in 2018. For his Bachelor's final year research thesis, he worked at Flinders University and SRM research institute under supervision of Prof. Andersson where he achieved a high distinction grade. His PhD research work involves investigation of Specific ion effects at liquid surfaces employing NICISS.*



**Erica J. Wanless**

*Erica Wanless is Professor and Head of Chemistry at the University of Newcastle (Australia). She graduated with a PhD in Surface Science from the Australian National University in 1995. She then completed a postdoctoral fellowship at the University of Otago, New Zealand. She joined the University of Newcastle Chemistry Department in 1996. Erica is a colloid and interface scientist who has built an international research profile*

*for her investigations of surfactant, polymer or colloidal materials at interfaces. In recent years her research has been focussed on stimulus responsive polymer brush coatings which are tuned by changes in pH, temperature, ionic strength and/or ion identity. Erica is the current president of the Australasian Colloid and Interface Society.*



**Grant B. Webber**

*Grant Webber is a research chemist engineer, working across discipline boundaries to uncover the links between nanoscale behaviours and macroscale properties. His research combines cutting-edge experiments and precision modelling and simulation methods to study colloidal and interfacial phenomena with relevance to personal care products, pharmaceuticals, the minerals industry, water treatment, micro- and nanomechanical devices, food production and biomedical device manufacture. Grant has deployed neutron reflection and scattering, ellipsometry, atomic force microscopy and quartz crystal microbalance measurements to resolve specific ion effects in polymer brush systems with high spatial and temporal resolution.*



commemorative plaque at Charles University in Prague. SIE following the same or a very similar order have since been observed in various biological,<sup>20,29,33</sup> polymer,<sup>34–38</sup> and non-aqueous systems,<sup>24,27,39–45</sup> and has become commonly known



Vincent S. J. Craig

*Vince Craig leads the Colloids group in the Department of Materials Physics at the Australian National University. He completed both his BSc (Honours in Chemistry in 1992) and PhD degrees (jointly in the Departments of Applied Maths and Chemistry in 1997) at the ANU before postdoctoral positions at UC Davis, California and the University of Newcastle, NSW, Australia. His research interests include the measurement of surface forces in particular the long range hydrophobic interaction, adsorption of surfactants and polymers, specific ion effects, wetting and bubbles, including nanobubbles. He was awarded an ARC Postdoctoral fellowship in 1998, an ARC Research Fellowship in 2001 and an ARC Future Fellowship in 2009. He has worked with numerous industry partners as a consultant, advisor and in the provision of research. Vince was a Director and Treasurer of the Australasian Colloid and Interface Society (ACIS) from 2013 to 2018 and is currently Treasurer on the LOC for IACIS2022, to be held in Brisbane (26–29th June).*

range hydrophobic interaction, adsorption of surfactants and polymers, specific ion effects, wetting and bubbles, including nanobubbles. He was awarded an ARC Postdoctoral fellowship in 1998, an ARC Research Fellowship in 2001 and an ARC Future Fellowship in 2009. He has worked with numerous industry partners as a consultant, advisor and in the provision of research. Vince was a Director and Treasurer of the Australasian Colloid and Interface Society (ACIS) from 2013 to 2018 and is currently Treasurer on the LOC for IACIS2022, to be held in Brisbane (26–29th June).



Gunther G. Andersson

of soft matter surfaces to its current stage. He completed his Habilitation in 2006. In 2007 he was appointed at Flinders University (Australia). He is now leading as a full Professor a research group with activities in photocatalysis based on metal clusters on surfaces, and liquid and polymer surfaces and interfaces. His laboratories are equipped with instruments for electron spectroscopy (MIES, XPS, UPS, IPES), ion scattering spectroscopy (NICISS) and infrared spectroscopy (FTIR).

*In 1998 Gunther Andersson completed his PhD applying ion scattering spectroscopy on liquid surfaces at the University of Witten/Herdecke (Germany) under the supervision of Prof Harald Morgner. The following two years he was at the Technical University Eindhoven on a project on polymer based light emitting diodes. In 2000 Gunther moved to Leipzig University (Germany) where he developed the method neutral impact collision ion scattering spectroscopy (NICISS) for investigation*

as the Hofmeister series. However, there are as many reports (if not more) of SIEs that deviate from the Hofmeister series, but are nevertheless still given the same label. The Lyotropic series<sup>46</sup> (based on the heat of hydration of ions), although invariant in order, has also been used interchangeably with the Hofmeister series, due to the similarity of their orderings as shown in Fig. 1. While SIE in many contexts may share similar underlying mechanisms to those in Hofmeister's original precipitation experiments, subtle physicochemical differences induce marked deviations from Hofmeister's original ordering. Many of these deviations are either ignored or lack a comprehensive explanation, and hence we still do not fully understand the origins of SIEs. Fig. 1 also shows that, although the Hofmeister series may often be used *post hoc* as a qualitative label to explain observations, it cannot be used *a priori* to make quantitative predictions of SIEs. Such a predictor remains a 'holy-grail' in this field of research.

There are many curious disconnects between the SIE field and the broader chemical and physiological literature. For instance, Pearson's hard and soft acids and bases (HSAB) theory<sup>48</sup> has many parallels with the Hofmeister series, yet is rarely discussed in the context of SIE despite having arguably stronger theoretical foundations.<sup>49,50</sup> Similarly, the work of Wright and Diamond<sup>20</sup> is often overlooked by the field, despite its sound theoretical discussions on potential origins of SIEs in terms of electrostatic and competitive interactions.

This perspective aims to review recent advances in our theoretical understanding of SIEs and summarise the current challenges facing this fundamentally important field of research. SIEs are commonly attributed solely to the anion or cation, with disregard for the presence of a counterion. We address the



Alister J. Page

*Alister Page received his PhD from the University of Newcastle in 2008. In 2009 he was awarded a Fukui postdoctoral fellowship in the group of Prof. Keiji Morokuma at the Fukui Institute for Fundamental Chemistry, Kyoto University, and in 2012 he was appointed as a Research Fellow at the University of Newcastle. He took up a faculty position in Newcastle in 2013, where he is now Professor in the Discipline of Chemistry and leads the University of Newcastle Computational Chemistry Group. His research focuses on developing and applying quantum chemical methods to topics including self-assembly, carbon & inorganic nanomaterials, ionic liquids, deep eutectic solvents, heterogeneous & photocatalysis, and specific ion effects.*



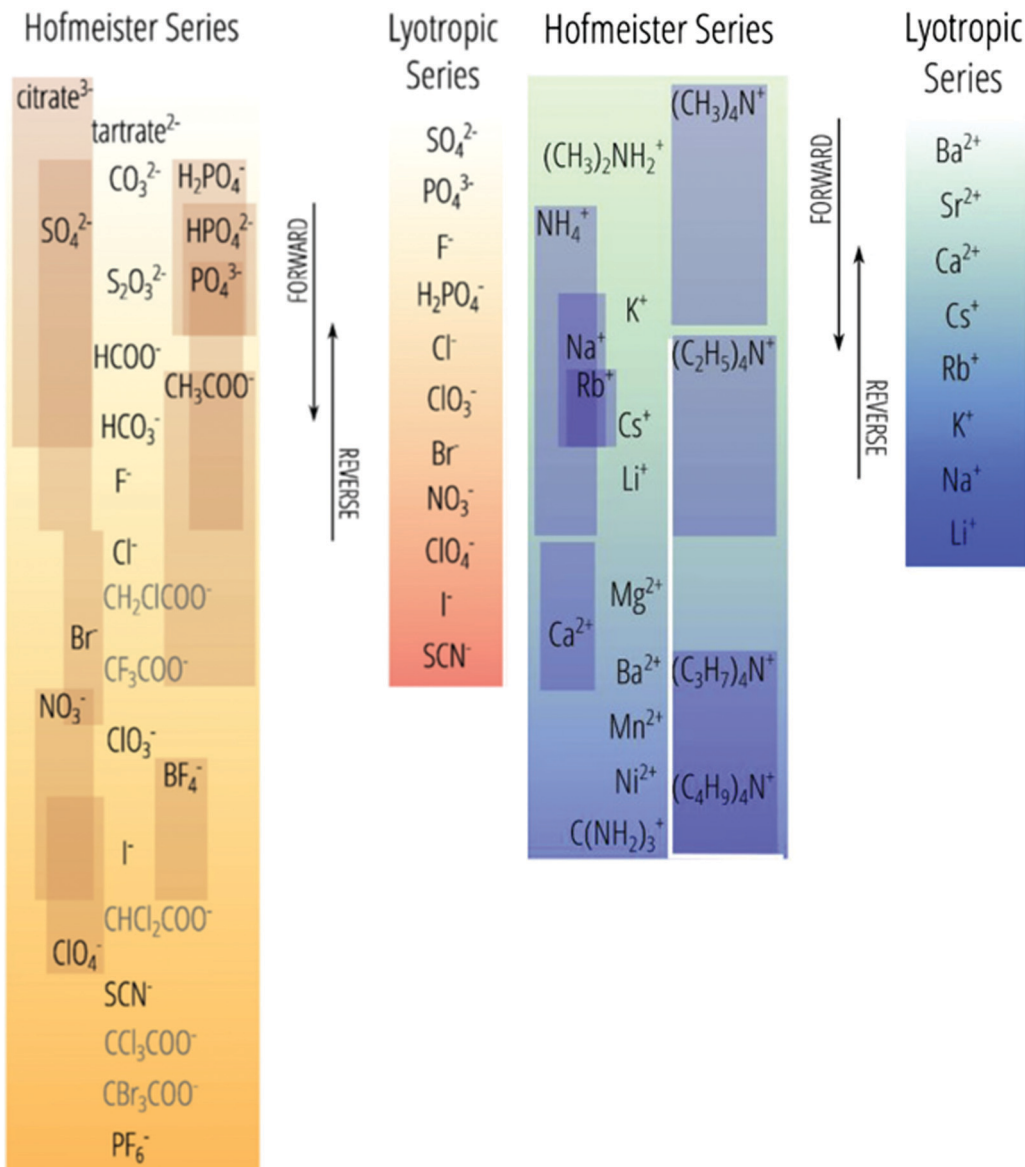


**Fig. 1** The Hofmeister series versus its deviations (with the latter indicated by individual boxes). The top(anions)/bottom(cations) end of this series, historically called kosmotropes, generally precipitate proteins from (aqueous) solution. The bottom(anions)/top(cations) ions are historically called chaotropes, which generally solubilise proteins.<sup>41</sup> We prefer the terms charge diffuse ions and charge dense ions over chaotrope and kosmotrope respectively. Reprinted with permission from ref. 41 and 47 with permission from Elsevier, copyright 2017.

shortcomings of this assumption in this perspective, and recount historical explanations, theoretical treatments, and correlations between SIEs and ionic properties in Section 2. However, SIEs are clearly counterion-dependent and are known to be responsible for deviations and even reversals in Hofmeister trends.<sup>33,44,45</sup> Counterions must be considered explicitly if SIE are to be understood completely. Counterion-induced deviations, and those caused by other relevant physico-chemical conditions, are therefore discussed in Section 3. Many SIEs occur at an interface, meaning that the synergies between SIEs and interfacial structure/properties must be elucidated carefully, if SIEs are to be fully understood; we discuss recent advances in this respect in Section 4. The complexity of SIEs is

compounded in mixed-salt systems (of particular relevance to SIEs in biochemical contexts), and so we examine the manifestation of SIEs in mixed salt systems in Section 5. The fact that SIEs occur not only in water, but in nonaqueous solvents as well suggests that SIEs occur fundamentally due to some inherent property of ions themselves that is apparently modulated by the solvent environment. With this in mind, we discuss recent advances concerning nonaqueous SIEs in Section 6. The electrostatic environments in concentrated electrolytes differ fundamentally from weak electrolytes, for instance, by exhibiting variable electrostatic decay lengths. Recent investigations have demonstrated this phenomenon to be ion specific and so Section 7 reviews recent progress in this respect. Finally, we

summarise the recent progress and current challenges for the field in Section 8.

At this point it is also important to make our conventions in terminology clear. In the manner of Mazzini and Craig,<sup>41</sup> we will use the phrase “specific ion effect” (or SIE) in reference to any physicochemical phenomenon that depends on the identity of the ion. A Hofmeister effect or series refers to a SIE that conforms to the original ion ordering reported by Hofmeister, above (either whole, or with few exceptions). A reverse Hofmeister effect or series refers to a SIE that occurs in the opposite order to that reported by Hofmeister. Similarly, Lyotropic effects or series are those that are consistent with the conventional ordering of the Lyotropic series (either whole, or in part) and the label ‘reverse’ is used in the same manner here.<sup>46</sup> When discussing general interactions between an ion and a dissolved protein, polymer, surface or other chemical species, the term cosolute is used to address these moieties.

## 2. Aqueous specific ion effects

### 2.1. Historical explanations

The genesis of the Hofmeister effect was Hofmeister’s own experiments concerning the solubility of egg proteins in aqueous electrolyte solutions.<sup>31,32</sup> Two key observations from these original experiments have had far-reaching consequence. Firstly, given the timescale over which the effects were observed by Hofmeister and Lewith (several hours or days in some circumstances), it is likely they are thermodynamic in origin (as opposed to kinetic). Secondly, trends in an ions’ abilities to precipitate five different solutes were consistent, suggesting that the effect was general. Indeed, Hofmeister effects are known to influence myriad phenomena, including surface tension,<sup>51</sup> zeta potentials,<sup>52</sup> buffers,<sup>53</sup> upper and lower critical solution temperatures (UCSTs and LCSTs respectively) of thermoresponsive polymers,<sup>36,54–56</sup> ion-binding to proteins<sup>57</sup> and membranes,<sup>58</sup> transport across membranes,<sup>59</sup> molecular forces,<sup>60,61</sup> electrolyte viscosity,<sup>62–66</sup> enzyme activity,<sup>16–27</sup> bacterial growth,<sup>67</sup> bubble stability,<sup>14</sup> and others.<sup>62,65,68–75</sup>

Hofmeister hypothesised<sup>32</sup> that the behaviour of each ion derived from its capacity to adsorb water. On this basis, ions were subsequently categorised as kosmotropes (which are strongly hydrated, thereby bringing order to the solution) and chaotropes (which are weakly hydrated, thereby disrupting order in the solution), respectively. As shown in Fig. 1, the Hofmeister series orders ions from kosmotropes (highest anions, lowest cations) to chaotropes (lowest anions, highest cations). Kosmotropes precipitate (“salt-out”) proteins, while chaotropes solubilise (“salt-in”) proteins. However, despite the pervasive historical use of the kosmotrope and chaotrope terms, they are often misleading considering the relative standard molar entropies of many ions.<sup>45,66</sup> We therefore prefer to use the terms ‘charge diffuse ion’ instead of chaotrope and ‘charge dense ion’ instead of kosmotrope. Salting-in and salting-out terms are also useful in regard to describing an ion’s impact on precipitation, yet are system dependent (Section 3), so require caution when used

more generally. Similarly, as Fig. 1 indicates, the positions of ions on this scale are not invariant; they may change based on the system and the effect in question (the most common variations are indicated by the sliding boxes containing some ions in the series).

Various models and mechanisms have been proposed since Hofmeister’s initial ion–water adsorption model. Various cavity models<sup>75,76</sup> have attempted to explain SIEs purely in terms of the ion’s influence on the solvent. These models are based on the work required to make a cavity in a liquid. On this basis, Melander and Horváth’s model<sup>75</sup> explains salting-out behaviour in terms of ion surface tension increments, and a protein salting-out constant (which is a measure of a protein’s susceptibility to being salted out, related to the “hydrophobic” and electrostatic interactions). Pica and Graziano<sup>77,78</sup> have used theories grounded in a solvent-excluded volume effect to describe the thermodynamics of poly(*N*-isopropylacrylamide) (pNIPAM) hydration. On the other hand, other models, such as Baldwin’s,<sup>79</sup> hypothesised that ions precipitate proteins *via* interactions at nonpolar functional groups, while they salt-in proteins *via* interactions at peptide groups. In polymer systems, Rogers *et al.*<sup>80</sup> have postulated that weakly hydrated ions preferentially bind to the centre of macromolecular chains where the solvation structure is most disrupted. A recognition that the counterion was important led Collins in 1997 to develop the Law of Matching Water Affinities (LMWA),<sup>81</sup> which attempts to explain SIEs *via* the fact that associated ion pairs will preferentially form if they have similar absolute enthalpies of hydration (Fig. 2). Collins also considered the relationship between the charge density and observed Hofmeister effects. More recently, Lo Nostro and Ninham<sup>29</sup> have posited that SIEs are the product of three key considerations:

- i. Cation–anion pairing and their interactions with both cosolute and solvent molecules.
- ii. “Local” interactions between the ion and the cosolute drive ions to adsorb specifically. Many-body quantum mechanical dispersion forces that are missing from standard theories can account for this. These and specific hydration are dependent on the dielectric properties of the ion, cosolutes and solvent.
- iii. Concurrent phenomena allow anomalies such as reordering the series of ionic efficacy and series inversions.

Many investigations focus on ion–protein interactions in conjunction with ion–solvent interactions.<sup>79,81,83–95</sup> Like Collins,<sup>81</sup> later work has emphasised the importance of moving “Beyond Hofmeister” to overcome the limitations of separating the anion and the cation series.<sup>33</sup>

### 2.2. Ion solvation in water

The local solvation environment around dissolved ions has long been hypothesised to be the origin of SIEs in aqueous electrolytes. Whilst ionic solvation structures have been studied extensively in this context, both experimental and theoretical approaches have revealed the aqueous solvation structure of ions to be deceptively complex. Neutron diffraction experiments<sup>96</sup> have supported the now conventional explanation of the Hofmeister



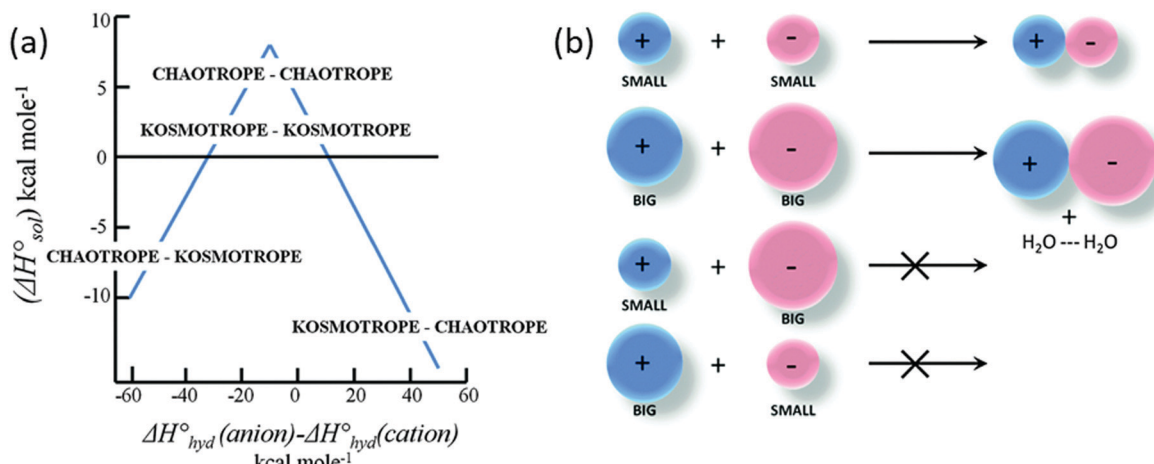


Fig. 2 The Law of Matching water affinities. (a) Plot of the enthalpy of hydration of the salt vs. the difference in the enthalpy of hydration of the anion and cation (a so-called 'volcano plot'). When the anion and cation have similar enthalpies of hydration they are likely to form ion-pairs (above the x-axis). (b) Schematics: a small (big) cation would form a contact ion pair with a small (big) anion, whereas a small (big) cation would not form a contact ion pair with a big (small) anion.<sup>82</sup> Reproduced from ref. 82 with permission from the Royal Society of Chemistry, copyright 2014.

effect for proteins, *i.e.* that salting-in or salting-out is caused by the competition between the dissolved salt and the protein for waters of hydration. Similarly, X-ray diffraction has indicated that water hydrogen bond strength changes upon NaCl dissolution.<sup>97</sup> However, there is ongoing debate regarding the influence ions have on water's native structure beyond their first solvation shell. A range of techniques indicate that ions do not significantly affect the water structure beyond their first solvation shell. These include femtosecond mid-infrared pump-probe spectroscopy,<sup>98</sup> terahertz absorption spectroscopy,<sup>99</sup> and molecular dynamics (MD)<sup>99,100</sup> studies. On the other hand, alternate conclusions, *viz.* that well hydrated ions influence the structure of water well beyond the first solvation shell, were reached on the basis of femtosecond infrared spectroscopy.<sup>101</sup> Neutron diffraction experiments<sup>102</sup> also imply that ion solvation is not limited to a single solvation shell, with salts disordering the tetrahedral structure of water in a similar manner to changes in pressure and temperature. Quantum chemical molecular dynamics<sup>103</sup> simulations indicate  $\text{Na}^+$  and  $\text{Cl}^-$  ions have distinct effects; while the disruption caused by  $\text{Na}^+$  is limited to the cation's first solvation shell,  $\text{Cl}^-$  influences hydrogen bonding within the solvent over larger length scales. A potential caveat here is that the timescale of these simulations ( $\sim 20$  ps) is comparable to the estimated residence times of water molecules around these ions.<sup>104-106</sup> The disruptions observed may therefore not truly reflect the ions' effects on experimental timescales. Thus, the range over which an ion perturbs the structure of the solvent is still to be determined, and likely to be ion specific and concentration dependent (Sections 3.1 and 7).

Classical theories regarding salt interactions in aqueous solution, such as Born energies of solution and ion transfer,<sup>107,108</sup> Debye-Hückel (DH) theory,<sup>109</sup> and the Derjaguin-Landau-Verwey-Overbeek (DLVO) theory of colloidal interaction,<sup>110-112</sup> have been developed largely to account for deviations in ideality, rather than to explain SIEs. They therefore generally fail to account for such subtle structural effects, and have significant limitations.<sup>113</sup>

DH theory treats the electrostatic potential within an electrolyte solution *via* a linearisation of the Poisson-Boltzmann equation, and assumes that ions are non-polarisable point charges that undergo complete dissociation in a featureless, homogenous dielectric "solvent". Whilst DH theory is often considered capable of only accounting for phenomena in dilute aqueous environments ( $< 10^{-3}$  M), for long-range electrostatic interactions it is often adequate up to concentrations of  $\sim 0.5$  M.<sup>114</sup> The extended DH model of Stokes and Robinson,<sup>115</sup> which includes a description of the ionic radius, is accurate up to  $\sim 0.1$  M. Similarly, specific ion interaction theory was developed from DH theory to estimate single ion activity coefficients at even higher concentrations ( $\sim 10$  M) *via* interaction coefficients.<sup>116,117</sup> The Pitzer Method<sup>118</sup> has become an increasingly popular tool for determining the thermodynamic properties of electrolytes<sup>119-122</sup> and is considered the best model for predicting ion activity coefficients to date.<sup>123,124</sup> Nevertheless, it too is based on DH theory, although it also accounts for the hydrated size of individual ions and their short-range binary and ternary interactions *via* a virial expansion (thereby requiring additional empirical parameterisation). The necessity for additional empirical parameters at high concentration in DH theory arises ultimately from the rudimentary assumptions of DH theory itself. In fact, some authors<sup>125</sup> contend that the early successes of DH theory, despite its assumptions, are responsible for our current poor understanding of electrolyte solutions at high concentrations. We discuss more advanced theoretical treatments of concentrated electrolyte solutions in Section 7. The fact that properties such as ion size, shape, polarisability and charge density are ignored in DH theory fundamentally limits its utility in the context of SIEs.

### 2.3. Correlations with electrolyte properties

The nature of an ion's effect on a system is determined by the properties of the ion as well as the solute and solvent. In fact, the ubiquity of the Hofmeister series indicates that the properties of the ion are fundamental to its origin. Collins and



Washabaugh<sup>126</sup> had listed 30 properties of salt solutions by 1985, which has since expanded, with many, such as ion size, polarisability and hydration free energy following Hofmeister trends to some extent.<sup>124,127,128</sup> Variations and exceptions are frequent however, meaning well-defined Hofmeister ion parameters have not been well established. Leontidis<sup>129</sup> covered these properties in a recent review, positing that the Hofmeister series originates from a combination of ionic charge distribution, size, shape, and hydrophobicity (Fig. 3). A study by Mazzini and Craig<sup>42</sup> showed consistent trends for anions (Hofmeister series)

and cations (reverse Hofmeister series) with respect to their electrostrictive volume in eleven different protic and aprotic solvents. This suggests ions alone exhibit a SIE series that is independent of the solvent; that is, there exists a fundamental SIE series. Investigations<sup>128,130–133</sup> of the intermolecular forces<sup>134</sup> driving SIEs have elucidated and aided the search for relevant ion properties. The discussion below considers the correlation of fundamental ion properties with observed SIEs.

**2.3.1. Ion polarisability.** Polarisability has been used as a direct correlator to experimental SIE on multiple occasions,<sup>19,25</sup>

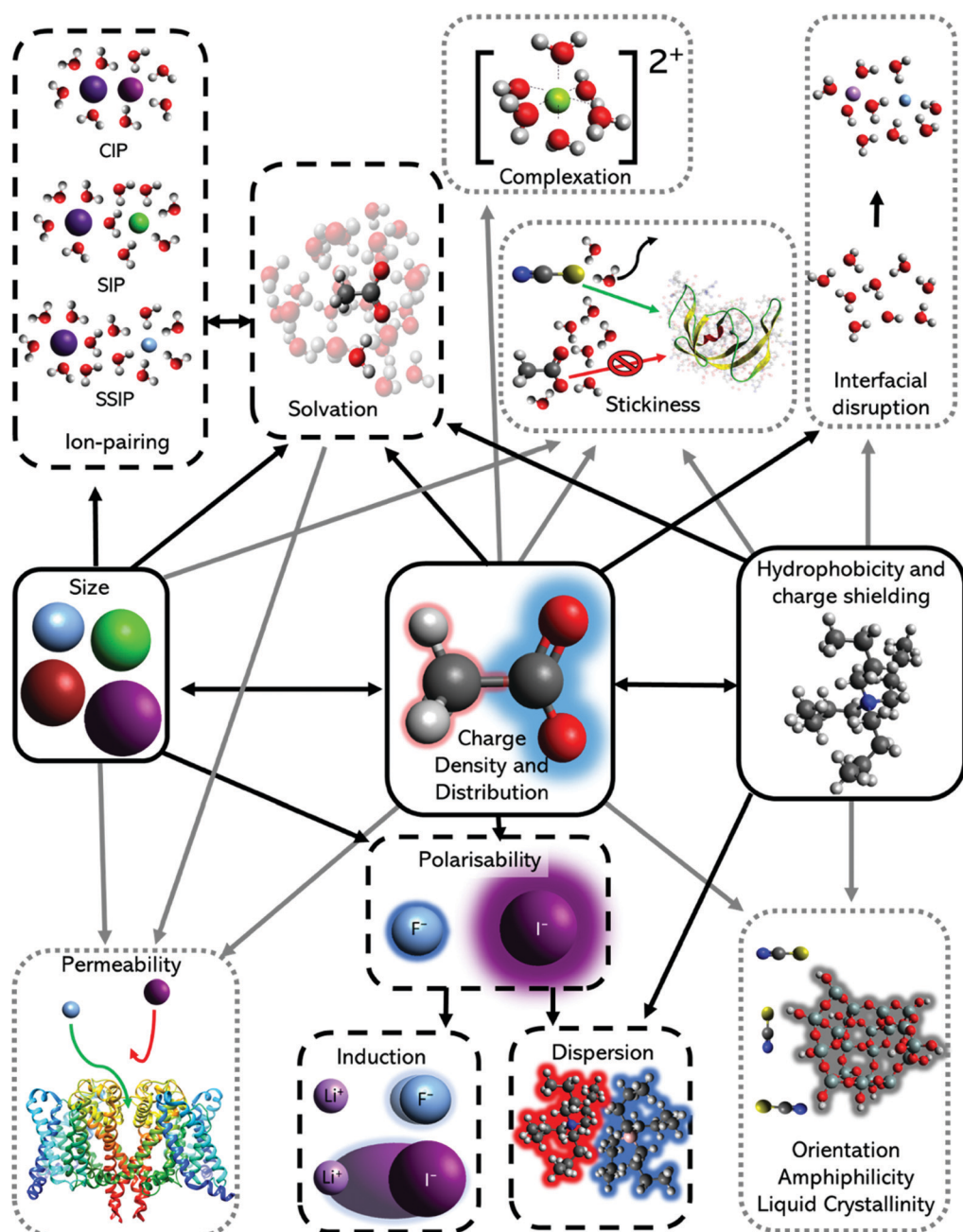


Fig. 3 The major ion properties (solid black box) linked to the effects studied widely (dashed black box) and sparsely (dotted grey box). Stickiness is a term to describe the ease at which an ion can lose or share their hydration shells, and therefore adhere to interfaces. It is resultant from a combination of ion hydration, complexation ability and surface polarity. Adapted from ref. 129 with permission from Elsevier, copyright 2017.



and correlations can be drawn between ion polarisabilities, ionic Gaussian radii and the ion ordering within the Hofmeister series. Parsons and Ninham<sup>135</sup> calculated the hard sphere radii, static (and dynamic) polarisabilities and the Gaussian radii and volume of common ions reported in SIE. The Gaussian radius is a relevant property when explaining the Hofmeister series in terms of electron density, as it can be used for non-spherical ions. However, it is still limited in its consideration of the whole ion. Thus, the correlation between these ion properties and Hofmeister effects is most obvious for monatomic, monovalent ions. However, discrepancies appear when considering polyatomic ions such as acetate ( $\text{CH}_3\text{COO}^-$ ). This is likely due to inclusion of the non-interacting methyl group in the Gaussian radius calculation making the Gaussian radius larger than those for neighbouring ions in the Hofmeister series. The interaction strength of acetate in solution remains primarily driven by the charge-dense carboxyl moiety. This indicates that unravelling these trends may require separation based on localised charge; for anions at least, electrostatic strength will dominate strong interactions (compared to polarisability). A similar example is the more ‘kosmotropic’ nature of  $\text{IO}_3^-$  ions, compared to structurally similar  $\text{ClO}_3^-$  ions.<sup>46,136</sup> In the former case, the surface charge density on the oxygens is higher due to the reduced electronegativity of the iodine atom in comparison to chlorine.<sup>128</sup>  $\text{IO}_3^-$  ions are also more polarisable than  $\text{ClO}_3^-$  which would suggest they should exhibit more ‘chaotropic’ behaviour, similar to ions such as  $\text{SCN}^-$  or  $\text{I}^-$ , but this is not the case.

**2.3.2. Ion size, shape and hydrophobicity.** Ion size is important for polarisability and ion pairing in Collin’s LMWA.<sup>81,82,135</sup> It also correlates with the Hofmeister series to some extent.<sup>135</sup> Large symmetrical ions (*e.g.*,  $\text{I}^-$ ) have a more delocalised and polarisable electron density, making them weaker at orientation-dependent binding (such as hydrogen bonding). Small ions (*e.g.*,  $\text{F}^-$ ), on the other hand, have a high charge density allowing for strong, orientational interactions. As a consequence, large ions often have weaker solvation shells,<sup>83</sup> and so they can partially desolvate more readily to interact with a cosolute. Furthermore, size can be a determining factor in non-Hofmeister SIE such as permeability of a pore<sup>137,138</sup> or binding to macrocyclic receptors and cucurbiturils.<sup>139</sup> Ion shape is also an important consideration, as it potentially leads to multiple binding locations on the ion (*e.g.*,  $\text{C}_4\text{H}_4\text{O}_6^{2-}$ ), coexisting binding and non-binding moieties (*e.g.*,  $\text{C}_n\text{H}_{2n+1}\text{COO}^-$ ), or anisotropic charge densities (*e.g.*,  $\text{SCN}^-$ ) not present in monatomic ions.

The location of the charge within a polyatomic ion is of utmost importance. When the maximal charge density of an ion is located on a distal moiety, the magnitude of the interaction strength appears to be directed through this site (*e.g.*,  $\text{CH}_3\text{COO}^-$ ). This is discussed in detail below in Section 2.3.3. However, in cases where the charge density has a maximum on an internal atom, this can effectively cause a shielding of charge. The latter is evident in tertiary ammonium cations (which often show a reverse Hofmeister series),<sup>41</sup> and also for tetraphenylphosphonium and tetraphenylarsonium cations

and tetraphenylborate anions. In these cases, higher order interactions (*e.g.* dispersion, induction, exchange) become the driving intermolecular force governing their effects.<sup>128</sup> Notably, for the tetraphenyl ions, both the cationic and anionic derivatives show little difference in common measures of the strength of specific ion interactions such as viscosity  $B$  coefficients, limiting molar conductivities, enthalpies of hydration and Gibbs energies of transfer, indicating a charge independence for these ions.<sup>66,128,140</sup>

**2.3.3. Ion radial charge density ( $\beta$ ).** Recently, Gregory *et al.*<sup>128</sup> proposed a site-specific radial charge density parameter for quantifying SIEs. This density is based on Coulomb’s Law of electrostatic interactions ( $U_E \sim q_1 q_2 / R$ ) and constitutes a system-independent approximation of an ion’s electrostatic interaction with its solvent environment (Fig. 4). For anions, this site-specific radial charge density ( $\beta$ , ‘sho’) appears to be applicable to both fundamental aqueous electrolyte properties (in the absence of cosolutes), such as hydration enthalpies (Fig. 4(e)) and viscosity  $B$  coefficients, as well as a variety of other phenomena including colloidal stability, the relative activities of viruses (Fig. 4(f)) and enzymes, and nonaqueous chemical reaction rates and Gibbs’ energy of transfers (Fig. 4(g)).

The utility of the  $\beta$  parameter is greater for anions than it is for cations (even when accounting for the increased atomic radii at a solvent’s negative dipole in the Coulomb’s Law approximation).<sup>128</sup> This suggests that electrostatic interactions are more determinant in aqueous solutions for anions than cations. This is somewhat counterintuitive, considering their generally larger size and hence greater polarisability. For the cations there is more pronounced competitive behaviour between distinct components of the ion–solvent interactions (*viz.* electrostatics, dispersion, induction, exchange). The result is that cation-induced SIEs are increasingly subject to non-Coulombic phenomena (especially when additional co-solutes are present). Notably, the dispersion and electrostatic components of the cation–solvent interaction are generally inversely related and charge-dependent, whereas for anions, these components are directly related and charge independent.

**2.3.4. Viscosity  $B$  coefficients.** Poiseuille,<sup>141</sup> in perhaps one of the earliest studies of salt specific effects, noted that the addition of some salts to water increases viscosity, whereas other salts decrease viscosity. Jones and Dole<sup>64</sup> sought a relationship between the viscosity and the concentration of electrolytes and reasoned from the work of Debye and Hückel<sup>109</sup> that the electrostatic interactions, which act to increase the viscosity, should vary with the square root of concentration. Their result was expressed in terms of the fluidity, whereas the expression is now usually cast in terms of viscosity,

$$\frac{\eta}{\eta_0} = 1 + A\sqrt{c} + Bc \quad (1)$$

Here,  $c$  is the electrolyte concentration and  $\eta$  and  $\eta_0$  are the viscosity of the solution and water respectively. The  $A$  coefficient is related to interionic forces, whereas the  $B$  term is attributed to ion–solvent interactions. This  $B$  term has come to be recognised



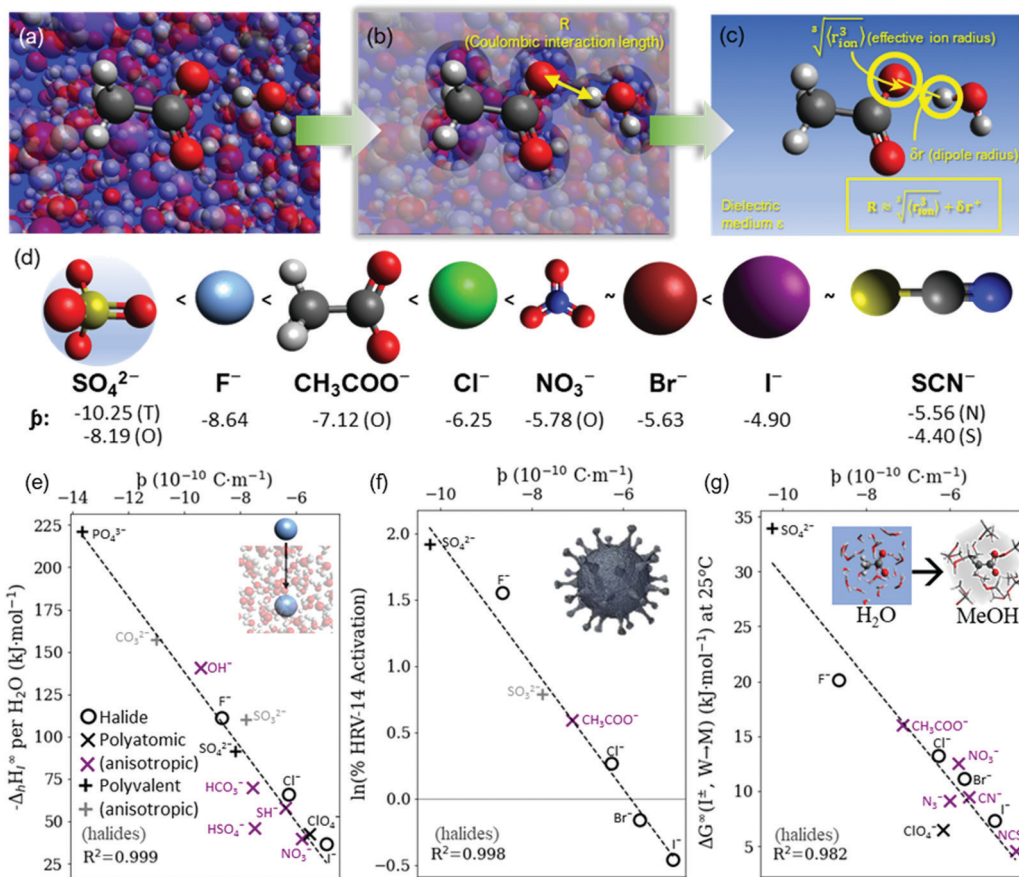


Fig. 4 (a) In bulk electrolyte solutions (b) where single ion–solvent interaction have a length of  $R$ , (c) the interaction distance may be approximated by the effective radius of the ion's charge site ( $\sqrt[3]{\langle r_{\text{ion}}^3 \rangle}$ ) and the solvent dipole ( $\delta r^+$ ). Given the partial charge on the solvent dipole is effectively constant and  $\sqrt[3]{\langle r_{\text{ion}}^3 \rangle} \gg \delta r^+$ , the electrostatic interaction as calculated by Coulomb's Law can be approximated by the radial charge density of the ion. An ion's radial charge density is calculated as  $\beta = \frac{q_{\text{ion}}}{\sqrt[3]{\langle r_{\text{ion}}^3 \rangle}}$ . (d) Example  $\beta$  values in  $10^{-10} \text{ C m}^{-1}$  are shown for commonly investigated anions. Both the total (T) and oxygen (O) values are provided for  $\text{SO}_4^{2-}$ , and both nitrogen (N) and sulfur (S) values for  $\text{SCN}^-$ . Example correlations for (e) hydration enthalpies,<sup>66</sup> (f) viral activities<sup>22</sup> and (g) Gibbs energies of transfers.<sup>66</sup> Reproduced from ref. 128 with permission from the Royal Society of Chemistry, copyright 2021.

as a quantitative measure of SIE, and was the progenitor of the “water structure breaker/maker” descriptors for ions.<sup>142</sup> Whilst the  $A$  coefficients are always positive, the  $B$  coefficients take on both positive and negative values. Notably the  $B$  coefficients are temperature dependent, which suggest a relationship between the ion's influence on solvent structure and the entropy present in the system.

Experimentally it is not possible to directly measure the contribution of each ion to the viscosity  $B$  coefficient to determine ionic  $B$  coefficients. An additivity assumption, that the contribution of each ion to the  $B$  coefficient is independent, allows ionic  $B$  coefficients to be determined relative to a reference anion or cation. In aqueous solution, KCl is often chosen as the reference salt with each of the ionic  $B$  coefficients assigned half the total  $B$  coefficient for KCl, as  $\text{K}^+$  and  $\text{Cl}^-$  have similar ionic mobilities. In other solvents, a different choice of reference ions is often required. The ionic  $B$  coefficients for simple monatomic ions correlate with the cube of the crystal

radius of ions, with smaller ions having positive  $B$  coefficients and larger ions leading to more negative ionic  $B$  coefficients. The more negative the ionic  $B$  coefficient the more “structure breaking” the ion. Ionic viscosity  $B$  coefficients have been correlated with structural hydration entropies,<sup>143</sup> partial molar entropies,<sup>144</sup> ionic partial molar volumes<sup>145</sup> and, for anions, lyotropic numbers.<sup>146</sup> Further, the variation of the  $B$  coefficients for an ion in different solvents are related to the molar volume of the solvents. Mazzini and Craig<sup>41</sup> have examined the ordering of ionic  $B$  coefficients in a number of solvents and found that the alkali metals follow a reverse lyotropic series for most solvents and the large ammonium cations follow a reverse Hofmeister series. For the anions a Hofmeister series is evident in a number of solvents but not in water.<sup>41</sup> For further details the interested reader is referred to the excellent and comprehensive review of Jenkins and Marcus on viscosity  $B$  coefficients.<sup>147</sup>

**2.3.5. Solubility,  $\text{pK}_a$  and ion pairing.** Salt solubility is an important factor for experimental investigations of SIEs and



is especially notable in nonaqueous systems (discussed in Section 6).<sup>44,148</sup> Often the relative permittivity ( $\epsilon_r$ ) is considered a key parameter for determining salt solubility in a given solvent, as it influences the Born energy of an ion, however this only has validity as a rule of thumb, considering it has limited quantitative correlation with salt solubility limits (Fig. S2, ESI†). Early experiments on protein precipitation in aqueous electrolytes were based on a limited list of salts, as saturation sometimes occurred at a lower concentration than that required to precipitate the protein.<sup>32</sup> Evidently, the protein here interacts more strongly with the water than does the salt.

The  $pK_a$  and  $pK_b$  of the respective conjugate acid and base of a salt is important to consider in understanding SIEs. Not only are they indicative of the degree of dissociation of the ions in solution, but they also describe whether hydrolysis of the ions might occur. For example, citrate buffers modulate the pH between 3.0–6.2 and  $\text{NaHCO}_3$  neutralises acids toward a pH of 8.4. This affects various components of the system, including the cosolute (whether it has an effective positive or negative charge), the ion protonation state (*i.e.*,  $\text{PO}_4^{3-}$ ,  $\text{HPO}_4^{2-}$ ,  $\text{H}_2\text{PO}_4^-$  or  $\text{H}_3\text{PO}_4$ ), and the need to account for additional ions (*i.e.*,  $\text{OH}^-$  or  $\text{H}_3\text{O}^+$ ) in any analysis, modelling or prediction.

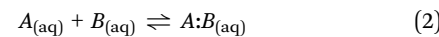
A related and common misconception is that strong electrolytes completely dissociate in water.<sup>149</sup> This is understandable considering the initial success of DH theory, and its underlying assumption that the salt is completely dissociated. However, molecular dynamics<sup>150</sup> and Monte Carlo<sup>151</sup> simulations, X-ray diffraction,<sup>152</sup> conductivity<sup>151,153</sup> and transference data,<sup>154</sup> as well as osmotic and vapour pressure measurements<sup>125,155</sup> indicate that this is not always the case in alkyl halide solutions (up to 20–30% of the ions could exist as ion-pairs or clusters at concentrations of 1 m).<sup>150</sup> Heyrovská claims that the degree of dissociation and ion hydration numbers are the two parameters required to explain activity<sup>155,156</sup> and similarly Shi and Beck<sup>157</sup> suggest a correlation exists between free energy and the ion-association affected hydration numbers. Free ions and associated ion-pairs are speculated to exhibit different SIEs, so a deeper knowledge of degree of dissociation may elucidate some SIE phenomena, especially where cation-anion interactions appear to have substantial impact (see Section 3.3).<sup>154,158</sup> Bruce and Bui *et al.*<sup>159–163</sup> have recently made substantial efforts in improving this mechanistic understanding for SIE, especially for cations and mixed salt (see Section 5) systems. Additionally, Judd *et al.*<sup>164</sup> have suggested that ion pair formation does not necessarily correlate with ion-ion binding affinity by using an eicosyl sulfate ionic surfactants as a probe.

We also note here that the concept of ion-pairing in electrolyte solutions can be ambiguous. Considering the dynamic behaviour of ions in solution, the relatively-static (statistical) picture of an ion-pair fails to encompass the range of ion-ion interactions occurring in reality, which will include contact, solvent-separated and solvent-solvent separated “ion-pairs” (CIP, SIP and SSIP respectively, see Fig. 3),<sup>165</sup> as well as larger clusters,<sup>150,152</sup> which can have lifetimes on the same timescale as ion-water interactions.<sup>104–106</sup> The term ion-ion correlations could be used to encompass this range of behaviour.

The interested reader is directed to the comprehensive review of Marcus and Hefter.<sup>165</sup>

**2.3.6. Lewis acidity/basicity.** Pearson's hard and soft acids and bases (HSAB) concept provides an alternative context for understanding SIEs in general.<sup>48</sup> According to Pearson, hard acids (cations) and bases (anions) are non-polarisable, whereas soft acids and bases are polarisable. This hard/soft categorisation (Table 1) of ions resembles the original kosmotropic/chaotropic categorisation in the Hofmeister series but is more general in the sense that it is solvent-independent due to being a property of the ion itself. Pearson's work is an extension and explanation of the previous findings of Ahrland, Chatt and Davies regarding halide affinities for particular Lewis acids.<sup>166</sup> HSAB theory posits that hard acids bind most strongly with hard bases, while soft acids bind most strongly with soft bases. This has a striking resemblance to Collins' LMWA, discussed in Section 2.1, but appeared more than 40 years earlier.<sup>81</sup>

Table 1 shows that HSAB theory encompasses not only ions that are traditionally the focus of SIE studies, but also transition metal ions and non-ionic molecules. Nevertheless, despite its generality, HSAB remains a qualitative categorisation; it does not allow for differentiation between acids and bases in the same category. Pearson<sup>167</sup> recognised a need for a two-parameter quantitative description of ions and proposed a strength factor ( $S$ , based on gas phase reaction data) paired with a “softness” parameter,  $\sigma$ , such that the equilibrium constant ( $K$ ) for an acid ( $A$ )-base ( $B$ ) reaction,



is,

$$\log K = S_A S_B + \sigma_A \sigma_B \quad (3)$$

Pearson highlighted, however, a lack of quantitative precision using this approach, despite its qualitative utility, and that parameters for the weaker aquo-ions (*e.g.*,  $\text{M}(\text{H}_2\text{O})^{n+}$ ) would be of more practical use than bare ions. This is especially relevant for strongly coordinated cations (*e.g.*,  $\text{Mg}^{2+}$ ).

Gregory *et al.*<sup>45</sup> showed that the Lewis acidity and basicity indices deduced by Marcus<sup>66,168</sup> could be correlated with observed SIE.<sup>38</sup> This hypothesis has been further investigated by Miranda-Quintana and Smiatek in terms of protein stabilisation for zwitterions and osmolytes.<sup>169</sup> For anions it appears these Lewis basic properties relate to the anion's charge density.<sup>128</sup>

### 3. Anomalous SIEs in aqueous solutions

Since so many SIE follow the Hofmeister series, it is useful to investigate those that do not – that is, those that qualitatively differ from the order of the Hofmeister series. Such ‘anomalies’ occur frequently and complicate the study of SIEs as it becomes increasingly difficult to find recurring trends. The origins of these anomalies themselves are, in many cases, not well understood. Do they deviate due to competing effects that become



**Table 1** Pearson's HSAB categorisation of neutral and ionic species. Adapted with permission from ref. 167. Copyright 1968 American Chemical Society

Classification of bases	
Hard	Soft
$\text{H}_2\text{O}$ , $\text{OH}^-$ , $\text{F}^-$ $\text{CH}_3\text{COO}^-$ , $\text{PO}_4^{3-}$ , $\text{SO}_4^-$ $\text{Cl}^-$ , $\text{CO}_3^-$ , $\text{ClO}_4^-$ , $\text{NO}_3^-$ $\text{ROH}$ , $\text{R}_2\text{O}$ , $\text{RO}^-$ $\text{NH}_3$ , $\text{RNH}_2$ , $\text{N}_2\text{H}_4$	$\text{I}^-$ , $\text{SCN}^-$ , $\text{S}_2\text{O}_3^{2-}$ $\text{R}_3\text{P}$ , $\text{R}_3\text{As}$ , $(\text{RO})_3\text{P}$ $\text{CN}^-$ , $\text{RNC}$ , $\text{CO}$ $\text{R}_2\text{S}$ , $\text{RSH}$ , $\text{RS}^-$ $\text{C}_2\text{H}_4$ , $\text{C}_2\text{H}_6$ $\text{H}^-$ , $\text{R}^-$
Borderline	
$\text{C}_6\text{H}_5\text{NH}$ , $\text{C}_5\text{H}_5\text{N}$ , $\text{N}_3^-$ , $\text{Br}^-$ , $\text{NO}_2^-$ , $\text{SO}_3^{2-}$ , $\text{N}_2$	
Classification of acids	
Hard	Soft
$\text{H}^+$ , $\text{Li}^+$ , $\text{Na}^+$ , $\text{K}^+$ $\text{Be}^{2+}$ , $\text{Mg}^{2+}$ , $\text{Ca}^{2+}$ , $\text{Sr}^{2+}$ , $\text{Mn}^{2+}$ $\text{Al}^{3+}$ , $\text{Se}^{3+}$ , $\text{Ga}^{3+}$ , $\text{In}^{3+}$ , $\text{La}^{3+}$ $\text{N}^{3+}$ , $\text{Cl}^{3+}$ , $\text{Gd}^{3+}$ , $\text{Lu}^{3+}$ $\text{Cr}^{3+}$ , $\text{Co}^{3+}$ , $\text{Co}^{3+}$ , $\text{Fe}^{3+}$ , $\text{As}^{3+}$ , $\text{CH}_3\text{Sn}^{3+}$ $\text{Si}^{4+}$ , $\text{Ti}^{4+}$ , $\text{Zr}^{4+}$ , $\text{Th}^{4+}$ , $\text{U}^{4+}$ , $\text{Pu}^{4+}$ , $\text{Ce}^{3+}$ , $\text{Hf}^{4+}$ , $\text{WO}^{4+}$ , $\text{Sn}^{4+}$ $\text{UO}_2^{2+}$ , $(\text{CH}_3)_2\text{Sn}^{2+}$ , $\text{VO}^{2+}$ , $\text{MoO}^{2+}$ $\text{BeMe}_2$ , $\text{BF}_3$ , $\text{B}(\text{OR})_3$ $\text{Al}(\text{CH}_3)_3$ , $\text{AlCl}_3$ , $\text{AlH}_3$ $\text{RPO}_2^-$ , $\text{ROPO}_2^-$ $\text{RSO}_2^+$ , $\text{ROSO}_2^+$ , $\text{SO}_3^-$ $\text{I}^+$ , $\text{I}^{5+}$ , $\text{Cl}^{7+}$ , $\text{Cr}^{6+}$ $\text{RCO}^+$ , $\text{CO}_2$ , $\text{NC}^+$ $\text{HX}$ (hydrogen bonding molecules)	$\text{Cu}^+$ , $\text{Ag}^+$ , $\text{Au}^+$ , $\text{Tl}^+$ , $\text{Hg}^+$ $\text{Pd}^{2+}$ , $\text{Cd}^{2+}$ , $\text{Pt}^{2+}$ , $\text{Hg}^{2+}$ , $\text{CH}_3\text{Hg}^+$ , $\text{Co}(\text{CN})_3^{2-}$ , $\text{Pt}^{4+}$ , $\text{Te}^{4+}$ $\text{Ti}^{3+}$ , $\text{Tl}(\text{CH}_3)_3$ , $\text{BH}_3$ , $\text{Ga}(\text{CH}_3)_3$ $\text{GaCl}_3$ , $\text{GaI}_3$ , $\text{InCl}_3$ $\text{RS}^+$ , $\text{RSe}^+$ , $\text{RTe}^+$ $\text{I}^+$ , $\text{Br}^+$ , $\text{HO}^+$ , $\text{RO}^+$ $\text{I}_2$ , $\text{Br}_2$ , $\text{ICN}$ , <i>etc.</i> Trinitrobenzene, <i>etc.</i> Chloranil, quinones, <i>etc.</i> Tetracyanoethylene, <i>etc.</i> $\text{O}^-$ , $\text{Cl}^-$ , $\text{Br}^-$ , $\text{I}^-$ , $\text{N}^-$ , $\text{RO}^-$ , $\text{RO}_2^-$ $\text{M}^0$ (metal atoms) Bulk metals $\text{CH}_2$ , carbenes
Borderline	
$\text{Fe}^{2+}$ , $\text{Co}^{2+}$ , $\text{Ni}^{2+}$ , $\text{Cu}^{2+}$ , $\text{Zn}^{2+}$ , $\text{Pb}^{2+}$ , $\text{Sn}^{2+}$ , $\text{Sb}^{3+}$ , $\text{Bi}^{3+}$ , $\text{Rh}^{3+}$ , $\text{Ir}^{3+}$ , $\text{B}(\text{CH}_3)_3$ , $\text{SO}_2$ , $\text{NO}^+$ , $\text{Ru}^{2+}$ , $\text{Os}^{2+}$ , $\text{R}_3\text{C}^+$ , $\text{C}_6\text{H}_5^+$ , $\text{GaH}_3$	

dominant given certain conditions,<sup>43</sup> or are they the product of a fundamentally different underlying mechanism? Some anomalies may in fact be a result of incomplete series reversals, or competing mechanisms (see, for instance, Fig. 5). Commonly, it is reported that SIEs are more pronounced for anions than they are for cations. This is a broad generalisation that should be taken with a grain of salt (pun intended), since in some cases the physical conditions of the system itself can be responsible, and indeed the influence or effect of cations can be more pronounced than anions.<sup>170,171</sup> In this section we examine how subtle changes within aqueous electrolytes (*e.g.*, pH, ion concentration, presence of a cosolute, counterion and

temperature), can each cause SIEs to deviate from the Hofmeister series. Understanding these phenomena remains a principal barrier preventing a complete understanding of SIEs.

### 3.1. Concentration and pH-induced series reversals

Beyond SIEs in concentrated electrolytes (see Section 7), several studies have demonstrated the delicate interplay between ion concentration and pH on Hofmeister trends (or even on 'simple' sodium chloride behaviour<sup>173</sup>). In one study the effect of pH and salt concentration on the reversal of the Hofmeister series for lysozyme was discussed by Boström *et al.*<sup>172</sup> At pH values above the isoelectric point the direct series was followed, but below this

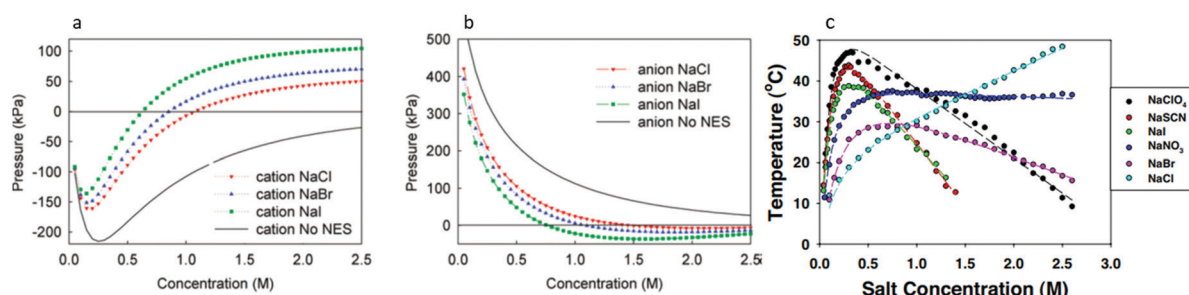


**Fig. 5** The salt concentration dependence of the double-layer pressure between two surfaces separated by 20 Å showing (a) anion and (b) cation influences.<sup>172</sup> (c) The cloud-point temperature of lysozyme as a function of anion type and concentration.<sup>25</sup> (a) and (b) reprinted from ref. 172 with permission from the American Chemical Society, copyright 2011. (c) Reprinted from ref. 25 with permission from the National Academy of Sciences, copyright 2009.



the reverse series was followed. At low salt concentrations, the adsorption of more polarisable anions was enhanced by ion-surface dispersion interactions, whereas at high concentrations there was enhanced adsorption of the cations. This is a charge reversal phenomenon; anion adsorption screens surface forces, while cation adsorption increases them (Fig. 5(a) and (b)). Boström *et al.* posit that the entropic terms, for anions at low concentration and for cations at high concentration, were the driving forces for the Hofmeister series.<sup>172</sup> Salis *et al.*<sup>174</sup> also reported electrophoretic mobility measurements on lysozyme suspensions to help explain how solution pH can invert the Hofmeister series. The reversal was predicted by a complex interplay of ionic size, hydration, and dispersion forces. Additionally, it impacted the charge on the amino acid groups, as well as the ionic composition of the solution. Specific buffer effects (a buffer subset of SIE) that can modulate Hofmeister effects in biological systems were reviewed by Salis and Monuzzi.<sup>175</sup> Fig. 5(c) displays a very rich concentration dependence on the behaviour of lysozyme in electrolyte solutions. Zhang and Cremer<sup>25</sup> claimed ionic volume and polarisability to be the properties determining the liquid–liquid phase transition, suggesting that charge diffuse ions raise the cloud point temperature sharply due to ion pairing with lysozyme. Upon saturation, however, a maximum was reached, and the behaviour reversed due to a decrease in interfacial tension. For chloride, the phase transition continues to rise due to a continual increase in the interfacial tension. pH effects have also been observed in polymer systems. For instance, in a multi-responsive poly(2-(diethylamino)ethyl methacrylate) and poly(2-(2-methoxyethoxy) ethyl methacrylate) copolymer brush system, Johnson *et al.* utilised pH effects to alter the SIE observed on the thermal response.<sup>176</sup> They indicated that the overall SIE could be quenched by a balance of competing stabilising and destabilising effects of the ions on each individual monomer identity. Section 3.2 further discusses how cosolute identity may alter SIE.

Fig. 6 shows three different concentration dependent specific ion influences on polymer behaviour.<sup>177</sup> An elastin-like polypeptide (ELP) has the general structure (VPGXG)<sub>n</sub>, where the monomeric unit is Valine-Proline-Glycine-X-Glycine, X denotes a variable amino acid and n denotes the number of monomer units. The uncharged ELP-V<sub>5</sub>A<sub>2</sub>G<sub>3</sub>-120, which has a 5:2:3 ratio of Valine, Alanine and Glycine guest residues with

120 monomer units, does not show any reversal behaviour due to salt concentration (Fig. 6(a)). The charge diffuse ions cause an increase in the LCST, while the charge dense ions show a decrease in the LCST. A positively charged KV<sub>6</sub>-112 peptide/moiety, with a 1:6 ratio of lysine to valine, shows charge diffuse ions causing the largest change in LCST at low concentrations (Fig. 6(b)), but these plateau, while charge dense ions continue decreasing the LCST causing a series inversion at ~0.4 M. This is one example of a concentration dependent Hofmeister reversal.

A similar reversal is shown in Fig. 6(c) for the positively charged poly(allylamine)-co-poly(allylurea) (PAU). At low salt concentrations, charge diffuse ions increase the cloud point temperature most significantly. However, increasing the concentration further begins to decrease the cloud point, most dramatically for the charge diffuse ions, but only minimally for charge dense ions. This results in a series inversion at ~0.5 M. This concentration reversal is explained *via* a *charge screening effect*.<sup>177</sup> At low concentrations this is described as an *ion-specific screening and bridging effect* (causing collapse) while at high concentrations (Section 7), the same strong ion specific direct interactions now govern re-entrant swelling.

### 3.2. Colute-induced series reversals

Colute-dependent Hofmeister reversal has been reviewed by Paterová *et al.*,<sup>178</sup> who state that traditional explanations of Hofmeister ordering of ions in terms of their bulk hydration properties is inadequate. NMR spectroscopy and MD simulations on a specific amino acid (triglycine) showed that uncapping the N-terminus (RNH<sub>3</sub> to RNH<sub>2</sub><sup>+</sup>) caused the ordering of the anions to reverse (Fig. 7). No appreciable binding was observed for SO<sub>4</sub><sup>2-</sup>, Cl<sup>-</sup> and Br<sup>-</sup> for the terminated triglycine, while I<sup>-</sup> and SCN<sup>-</sup> had some weak binding ( $K_D > 1000$  mM). The apparent dissociation constants ( $K_D$  in mM) for the non-terminated triglycine were in the order SO<sub>4</sub><sup>2-</sup> ( $70 \pm 30$ ) < Cl<sup>-</sup> ( $290 \pm 240$ ) < Br<sup>-</sup> ( $890 \pm 560$ ) < I<sup>-</sup> ( $> 1000$ ) < SCN<sup>-</sup> ( $> 1000$ ). This demonstrates the importance of the cosolute on the chemical and physical properties associated with SIEs and may have the same fundamental origins as those associated with pH changes.

A similar reversal was observed by Schwierz *et al.*<sup>179,180</sup> who investigated colloidal coagulation kinetics. A direct Hofmeister

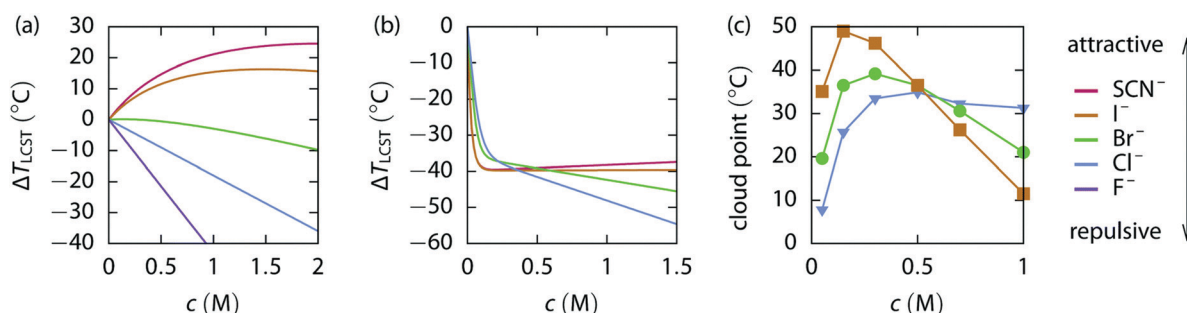


Fig. 6 LCST change vs. the concentration of various sodium salts for (a) uncharged ELP V5A2G3-120, (b) weakly positive ELP KV<sub>6</sub>-112 and (c) the UCST for weakly positive PAU.<sup>177</sup> Reproduced from ref. 177 with permission from the Royal Society of Chemistry, copyright 2018.



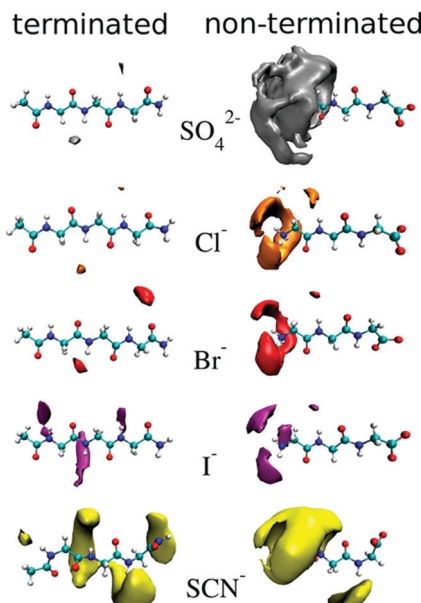


Fig. 7 Density maps of ions about terminated (left) and non-terminated (right) triglycine at an isovalue three times the aqueous bulk ion density.<sup>178</sup> Reprinted from ref. 178 with permission from the American Chemical Society, copyright 2013.

series was followed for a partial set of anions for both negatively charged hydrophobic surfaces and positively charged polar surfaces. Conversely, a reversal in the Hofmeister series was observed at negatively charged polar surfaces and positively charged non-polar surfaces. This is understood as a transient phenomenon for surfaces of intermediate polarity or charge. It implies that the surface determines whether the dominant ion will be the anion or the cation. Similar conclusions have been reached by Okur *et al.*,<sup>33</sup> who investigated Hofmeister effects on protein surfaces. Franks *et al.*, investigating zeta potentials and yield stresses, observed a forward cation Hofmeister series existing at silica surfaces<sup>181</sup> ( $\text{K}^+ > \text{Na}^+ > \text{Li}^+$ ), whilst a reverse series occurred at alumina surfaces<sup>182</sup> ( $\text{Li}^+ > \text{Na}^+ > \text{K}^+$ ). These were corroborated theoretically by Parsons *et al.*<sup>183</sup> using a modified Poisson Boltzmann analysis, indicating an interplay of hydration, non-electrostatic potentials and ion size underpinning these effects. SIE occurring at such surfaces indicates that even the vessel choice (*i.e.*, silica glassware) requires consideration. Indeed, surface functionalisation can be used as a means of masking specific ion effects (on the surface) entirely.<sup>184</sup>

### 3.3. Counterion-induced series reversals

As alluded to in the Introduction (Section 1), SIEs are not independent of the counterion despite common assumptions and the implicit assumption of the Hofmeister series itself. A simple example is provided in Fig. 8.<sup>185</sup> Here, the activity of  $\text{NaF}$  and  $\text{NaSCN}$  are vastly different across all concentrations. The activity of  $\text{NaSCN}$  is greater than the activity of  $\text{KSCN}$ , when  $\text{SCN}^-$  is the common counterion, however this is reversed when  $\text{F}^-$  is the counterion (*i.e.*,  $\gamma(\text{NaSCN}) > \gamma(\text{KSCN})$ ;  $\gamma(\text{KF}) > \gamma(\text{NaF})$ ). Also, the activity of  $\text{NaSCN}$  is greater than activity of  $\text{NaF}$  when

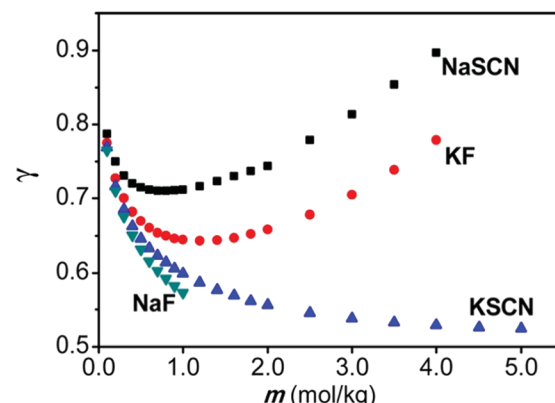


Fig. 8 Activity coefficients of  $\text{NaF}$ ,  $\text{NaF}$ ,  $\text{NaSCN}$  and  $\text{KSCN}$  electrolyte solutions. Reprinted from ref. 185 with permission from the American Chemical Society, copyright 2013.

$\text{Na}^+$  is the common counterion, but this is reversed when  $\text{K}^+$  is the counterion (*i.e.*,  $\gamma(\text{NaSCN}) > \gamma(\text{NaF})$ ;  $\gamma(\text{KF}) > \gamma(\text{KSCN})$ ).

Similarly, HSAB theory (see Section 2.3.6) recognises counterion reversals, but in a more generalised way. Soft acids form complexes with different ligand atoms in order of decreasing stability, *i.e.*  $\text{C} \sim \text{S} > \text{I} > \text{Br} > \text{Cl} \sim \text{N} > \text{O} > \text{F}$ ; whilst there is a strong, but incomplete inversion of this stability series for hard acids.<sup>186</sup> The argument for an incomplete inversion is that some soft bases are still strong proton acceptors.

Gregory *et al.*<sup>45</sup> investigated the energetic mechanisms of counterion induced reversals in a solvent cluster model *via* a density functional theory (DFT) approach using generalised Kohn-Sham energy decomposition analysis (GKS-EDA).<sup>187</sup> In the presence of a counterion that has had its energy included as part of the solvation environment, there is negligible counterion effect on the direct interaction strength between anions or cations and the model pNIPAM fragment. However, when simultaneously considering the energetics of both the cation and anion interacting at the respective  $\text{C}=\text{O}$  and  $\text{N}-\text{H}$  moieties of the pNIPAM fragment (Fig. 9(a)), a cationic reversal takes place if an ion-pair is forced at the amide  $\text{N}-\text{H}$  moiety (Fig. 9(b)), whereas an anionic reversal takes place if an ion-pair is forced at the  $\text{C}=\text{O}$  moiety (Fig. 9(c)).

Furthermore, Mazzini and Craig<sup>44</sup> showed these counterion reversals appear in nonaqueous solutions when considering the Gibbs free energy of dissolution of salts (negative values indicate solubility) *versus* the difference in the constituent ions' absolute free energies of solvation (negative values indicate the anion is more soluble than the cation, Fig. 10). In these circumstances counterion reversals can be more pronounced for aprotic solvents. In water (and other protic solvents) the inversion is most evident for the  $\text{F}^-$  anion, whilst the other cation-anion combinations fall onto the same trend. In propylene carbonate (PC) (and other aprotic solvents) no singular trend appears, but the  $\text{F}^-$  ion shows a very different trend.

### 3.4. Stimuli-induced series anomalies

Whilst there has been previous work on light-responsive polymers generally,<sup>188–190</sup> only recently<sup>191</sup> have studies investigated



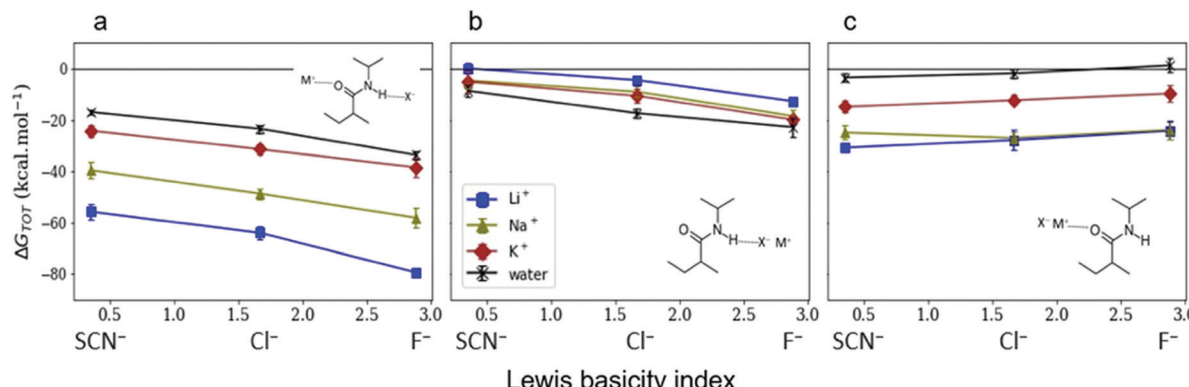


Fig. 9 GKS-EDA (M062X/cc-pVDZ) interaction energies between (a) dissociated salts and associated salts at (b) the N–H and (c) the C=O sites of a NIPAM monomer in water. Black atoms in the inset structures indicate GKS-EDA fragments considered. All data is the average of 10 independent configurations; error bars denote 1 standard deviation. Reprinted with permission from ref. 45 with permission from the American Chemical Society, copyright 2019.

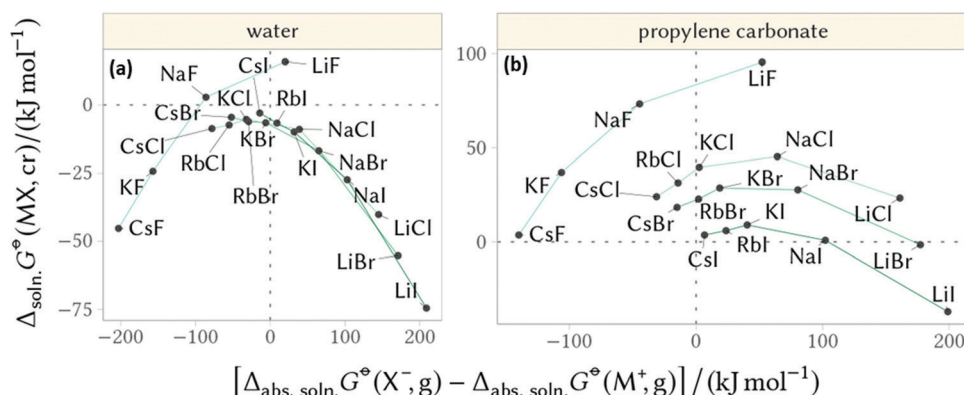


Fig. 10 Gibbs free energy of dissolution of salts versus the difference in the constituent ions' absolute free energies of solvation for (a) water and (b) propylene carbonate. Adapted from ref. 44 with permission from the American Chemical Society, copyright 2018.

the Hofmeister series in light responsive (azobenzene) salts. UV-activation causes the cation to adopt a *cis*-conformation and greatly decreases the LCST of pNIPAM (Fig. 11(a)). For azobenzene cation salts, it is difficult to distinguish the behaviour of different anions under visible light, where the cation adopts a *trans*-conformation (Fig. 11(b)). Thus, UV light acts to amplify both the ion specificity of the salts and the magnitude of their effect. This was explained as the *cis*-conformation permitting more dissociation, providing anions with more dynamic freedom. Equivalent systems for alkali metal cations, with a common light responsive anion, showed very little ion specificity and, if anything, the UV-induced *cis*-conformation decreased ion-specificity.

Senske *et al.*<sup>192</sup> reported a Hofmeister series reversal due to temperature changes using a novel thermodynamic analysis. It was found that protein stability curves,  $\Delta G_u(T)$ , for each ion were impacted by the temperature, such that their respective curves intersected, presenting temperature dependent ion rankings (Fig. 11(c)). This was attributed to differing enthalpic and entropic contributions to the excess free energy. It is claimed this classification may be extrapolated beyond ions to neutral cosolutes as well. Quartz crystal microbalance with dissipation monitoring (QCM-D) measurements performed by

Johnson *et al.*<sup>193</sup> also displayed a subtle temperature dependence on the ion ordering for the dissipation of an 80 : 20 mol% p(MEO<sub>2</sub>MA-*stat*-OEGMA<sub>300</sub>) brush (Fig. 11(d)). For example, at low temperatures lower dissipation values for the brush were observed in a 250 mM KSCN + 500 mM KCH<sub>3</sub>COO salt mixture when compared with a 250 mM KSCN + 250 mM KCH<sub>3</sub>COO salt mixture or pure 250 mM KSCN salt, however at high temperatures the opposite was observed. However, in this case it is difficult to decouple the SIEs from the effect of ionic strength and steric crowding, as noted by the authors,<sup>193</sup> as the brush in higher ionic strengths seemingly exhibits slightly higher dissipations at elevated temperatures when it is expected to be in a collapsed state. A recent study by Yao *et al.*<sup>194</sup> on ubiquitin proteins, showed both temperature and pH (Section 3.1) dependent SIE *via* static light scattering data as well as concentration dependent trends *via* differential scanning calorimetry (DSC).

#### 4. SIEs at the liquid–vapour interface

Ions at the vapour–liquid interface are of fundamental interest for understanding SIEs, and the presence of an interface

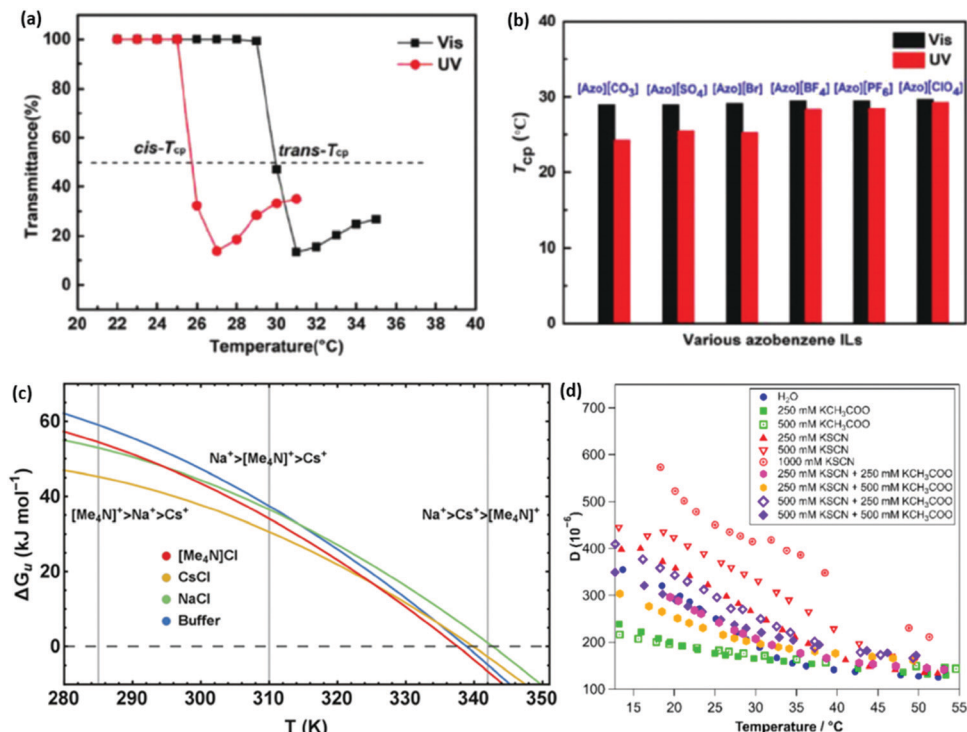


Fig. 11 (a) A large shift in the temperature of the phase transition in pNIPAM is observed depending on the light-responsive conformation of the azobenzene cation.<sup>191</sup> (b) The magnitude of the ion specific change in the temperature of the phase transition is seen to be more pronounced when the salts are in a UV-induced *cis*-conformation.<sup>191</sup> (c) Stability curves,  $\Delta G_u(T)$ , of RNase A in buffered solutions of 4 M NaCl, CsCl, and  $[\text{Me}_4\text{N}]$ Cl illustrating the temperature dependence of the Hofmeister series.<sup>192</sup> (d) The dissipation of an 80 : 20 mol% p(MEO<sub>2</sub>MA-stat-OEGMA<sub>300</sub>) brush with changing temperature in various mixtures of thiocyanate and acetate potassium salts.<sup>193</sup> (a and b) Reproduced from ref. 191 with permission from Wiley Materials, copyright 2021. (c and d) Reproduced from ref. 192 and 193 respectively, with permission from the Royal Society of Chemistry, copyright 2016 and 2019 respectively.

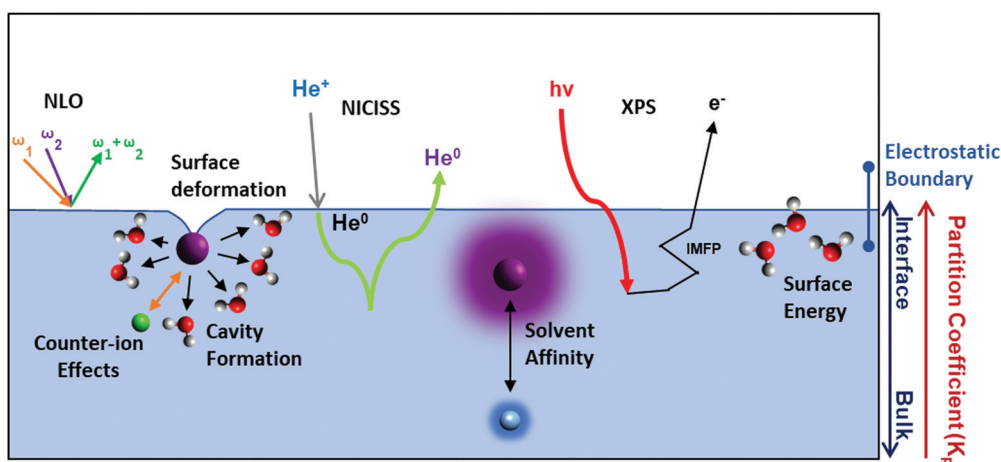


Fig. 12 Theories and techniques used to elucidate the effects of salt at liquid–vapour interfaces. NLO techniques exploit the fact that summation of the photon frequencies ( $\omega_1$  and  $\omega_2$ ) results in surface specific signals. SHG is the distinct case where  $\omega_1 = \omega_2$ . NICISS measures the energy loss experienced by ions of neutral species (e.g., He) in backscattering to infer an elemental concentration depth profile. XPS signals enable elemental identification at liquid–vapor interfaces, and hence the concentration of dissolved ions at the surface (IMFP refers to inelastic mean free path of photoelectrons through the interface). Solvent affinity, surface energy, counterion effects and cavity formation energy have all been posited to explain SIEs at the liquid–vapour interface.

increases the complexity of ion specificity (Fig. 12). In this respect the vapour–liquid interface is the simplest to consider.

Classical models of electrolytes suggest that the sharp discontinuity at the interface between two dielectric media forces



(point charge) ions away from the interface, due to image charge repulsion. This results in a depletion of ions from solvent–vapour interfaces.<sup>195</sup> As elucidated in Sections 2.2 and 7 however, treating ions as point charges ignores ion specificity completely. Experimental<sup>196</sup> and computational results<sup>197–199</sup> deviate from this classical picture, indicating that more polarisable ions have a greater affinity for the vapour–solvent interface.

Levin<sup>200</sup> explained this phenomenon *via* the cavitation energy required for an ion to reside at the water–vapour interface. Polarisable ions can redistribute their charges to stay hydrated at the interface to balance the electrostatic penalty accompanying ion adsorption. On the other hand, less-polarisable ions are less able to redistribute their charge, and so become depleted at the water–vapour interface. Nevertheless, the correlation between these ion specific trends and ion polarisability is weak,<sup>201,202</sup> and investigation of ionic adsorption at solvent surfaces remains an active area of research. Ion-specific adsorption at the liquid–vapour interface has also been explained in terms of the competition between ions' bulk solvation and interfacial affinity. Colussi *et al.*<sup>201</sup> found an inverse correlation between the dehydration free energy of an anion and its affinity for the air/water interface. Their results indicate strongly hydrated ions prefer to remain in the bulk solvent, while weakly hydrated ions will be driven to the liquid–vapour interface.

At the surface of an electrolyte solution, the Gibbs adsorption equation relates increasing<sup>203</sup> surface tension values of an electrolyte solution with a depletion of the ions from the interface (if an electrolyte is treated as a binary system).<sup>195</sup> However, separate ion contributions are essential to understand ion-specific adsorption, and it is impossible to directly infer these from surface tension measurements (which reflect the influence of both cation and anion). Pegram and Record<sup>204–206</sup> have utilised surface tension data to determine single ionic partition coefficients ( $K_p$ ) at the water–vapour interface (relative to  $\text{Na}_2\text{SO}_4$  at 0). These coefficients show similarity to reported Hofmeister series. Nevertheless, these  $K_p$  values only account for anion–cation interactions indirectly. Further, the impact of ions on the interfacial tension is not strictly additive, reflecting ion specific effects of the counterion (see Section 3.3).<sup>14</sup> Work by Craig *et al.*<sup>13,14,207</sup> with similarities to Collins' LMWA (Section 2.1)<sup>81,126</sup> suggested if the cation and anion had similar properties (*i.e.*,  $\alpha$  or  $\beta$ ) they would inhibit bubble coalescence, whilst different would allow properties would allow coalescence. The assignment of  $\alpha$  and  $\beta$  properties was related to each ions  $K_p$  values and indicates ion pairs inhibit coalescence while partitioned ions do not.<sup>14</sup> Modelling by Duignan<sup>208</sup> explained these results with a modified Poisson–Boltzmann equation. An electrostatic surface potential arises from the coexisting enhancement and depletion of each ion. This allows for bubble coalescence due to a reduced Gibbs–Marangoni pressure.

Experimentally, few techniques can quantitatively determine the presence of ions at the liquid–vapour interface and their interaction with solvent molecules. Relevant techniques include X-ray photoelectron spectroscopy<sup>209,210</sup> (XPS) and metastable induced electron spectroscopy<sup>211–213</sup> (MIES), X-ray

reflectivity (XR),<sup>214,215</sup> neutral impact collision ion scattering spectroscopy (NICISS),<sup>213,216–220</sup> and non-linear optical (NLO) techniques such as vibrational sum-frequency generation (VSFG) and second-harmonic generation (SHG) spectroscopy<sup>195,221–223</sup> (see Table S1 for descriptions in ESI†). Of these techniques however, only XPS and NICISS can directly probe concentration depth profiles of single ions at solvent surfaces. NICISS has the additional (and unique) benefit of delivering high depth resolution (down to  $\sim 0.2$  nm).

Hemminger and co-workers<sup>224–226</sup> have applied XPS at the surfaces of aqueous electrolyte solutions to measure the ratio between ionic concentrations. They reported an aqueous specific ion order in the surface-enhanced concentration of  $\text{I}^- > \text{Br}^- > \text{F}^-$ . In a separate investigation<sup>227</sup> with LiI and KI salts in water, they showed higher surface concentrations of  $\text{Li}^+$  than  $\text{K}^+$ . Additionally, the anion–cation ratio presented by the authors indicated that  $\text{I}^-$  had a higher surface concentration in LiI solutions than KI solutions. This trend agreed with Pegram and Record's<sup>204</sup> anion partition coefficient values for  $\text{I}^-$  in LiI ( $1.34 \pm 0.22$ ) and KI ( $1.0 \pm 0.14$ ) electrolyte solutions, where a higher partition coefficient value suggests higher propensity towards the water–vapour interface.

As with surface tension, NLO techniques can only measure the net ion contribution at a solvent surface. Nevertheless, NLO-based investigations have delivered several insights regarding SIE at solvent surfaces. For instance, Allen and co-workers<sup>228</sup> have employed VSFG extensively to study ionic interaction with solvent molecules at liquid–vapour interfaces, *via* the ions' influence on the solvent hydrogen-bonding network. These investigations indicate that, for monovalent salts, the degree of the ions' influence at the interface follows the orders  $\text{I}^- > \text{Br}^- > \text{Cl}^- > \text{F}^-$  for simple monovalent anions,<sup>221</sup> and  $\text{Li}^+ = \text{NH}_4^+ > \text{K}^+ > \text{Na}^+$  for cations.<sup>229</sup> This order agrees qualitatively with trends in ion partition coefficients (and size) for anions, but only partially for cations.<sup>230</sup> Peterson *et al.*<sup>210</sup> have reported the same order for monovalent anions using SHG spectroscopy. For divalent cations a largest-to-smallest size order of  $\text{Sr}^{2+} > \text{Ca}^{2+} > \text{Mg}^{2+}$  was reported by Allen and co-workers.<sup>211</sup> Various experimental techniques show a consistent largest-to-smallest size order for monovalent anions at the water–vapour surface, in accordance with computational and theoretical works. For polyatomic and anisotropic ions less consistency exists,<sup>231</sup> and many studies only investigate one or two salts.<sup>232–236</sup> MD simulations related to one of these studies<sup>233</sup> on a NaSCN salt reported an accumulation of the  $\text{SCN}^-$  and depletion of  $\text{Na}^+$  at the surface, while the subsurface (between  $\sim 5$ – $10$  Å depth) had an accumulation of  $\text{Na}^+$  and depletion of  $\text{SCN}^-$ .

Liquid–vapour interfaces have also been investigated in nonaqueous solutions (more generally discussed in Section 6). In glycerol, Allen *et al.*<sup>237</sup> found that NaI has a larger degree of disturbance on the surface hydrogen bonding network than NaBr. One possible explanation for this result is that the propensity of  $\text{I}^-$  for the interface is larger than that of  $\text{Br}^-$ . Alternatively, NICISS can be used to directly measure concentration depth profiles elementally. For instance, LiI and LiCl salts have been investigated at aqueous<sup>238–240</sup> and formamide<sup>241</sup>



solvent surfaces, and could also be useful for exploring mixed electrolyte systems.<sup>207,242,243</sup> For formamide,<sup>241</sup>  $\text{I}^-$  was reported to accumulate at the surface, whereas  $\text{Cl}^-$  had roughly the same concentration at the outermost surface layer as the bulk. In both cases however there was a subsurface depletion of the anions. The local topology around the ions was deemed important for this analysis, as ion scattering spectroscopy revealed the surface was not flat, with structural deformations particularly near the ions. In mixed electrolytes dissolved in glycerol, NICISS concentration depth profiles showed that  $\text{Br}^-$  outcompetes  $\text{Cl}^-$  in interactions with the tetrahexylammonium cations at the glycerol–vapour interface.<sup>243</sup> In water however, additional challenges arise due to its low vapour pressure, given the vacuum system. Low temperatures (e.g.,  $-13.8^\circ\text{C}$ ) and high concentrations (e.g., 7.2 m) can also enable aqueous electrolyte measurements, but this limits direct insight into standard experimental conditions.  $\text{I}^-$  showed a depletion up to  $\sim 20\text{ \AA}$  from the surface in aqueous solutions. Nonetheless, NICISS provides a means to directly measure concentration depth profiles of each element in a solution, in contrast to indirect measurements which generally require triangulation or extra-thermodynamic assumptions from indirect measurements. NICISS is especially of use in nonaqueous electrolytes solutions (Section 6) which are gaining more attention.<sup>41,244</sup>

## 5. SIEs in mixed electrolytes

Specific ion effects in simple systems (*i.e.*, single electrolytes in water) have been well studied, demonstrating the influence of ion identity on colloidal stability,<sup>245–248</sup> structure of soft matter systems<sup>14,29</sup> and response of polymer brushes and gels.<sup>36–38,193,249</sup> However, the manifestation of SIEs *in vivo* relies on the delicate balance of myriad interactions between the solvent and multiple solutes/cosolutes. In an attempt to quantify these phenomena, industry often applies the parameterised Pitzer Method (Section 2.2). Few studies have examined this intricate and complex behaviour to explicitly resolve SIEs.

To understand the behaviour between ions in a complex system, the effect of each individual ion must be considered along with their net additive or non-additive influences. In a recent investigation, Robertson *et al.*<sup>249</sup> deconvolved the net response of neutral thermoresponsive polymer brushes in complex electrolytes, consisting of two anions from the same end of the Hofmeister series (Fig. 1), into the influence of the constituent ions. The authors suggest that the change in response of a system ( $\Delta R$ ) is the difference between the response in the presence of an electrolyte with respect to the neat solvent ( $\Delta R_i = R_{\text{salt}} - R_{\text{solv}}$ ). For a responsive polymer,  $\Delta R$  may be analogous to a change in LCST or swelling state. The observed net change in response ( $\Delta R_{\text{net}}$ ) results from the simple summation of the effect of each pure component salt ( $\Delta R_{\text{net}} = \sum_i \Delta R_i$ ) and an empirical term,  $\delta$ , which accounts for deviations from pure additive behaviour (e.g., synergistic or competitive behaviour). Thus, for a binary complex electrolyte

for two salts that either both salt-in or both salt-out the polymer, the net response of the system  $\Delta R_{\text{net}}$  can be expressed as,

$$|\Delta R_{\text{net}}| = |\Delta R_1 + \Delta R_2| + \delta \quad (4)$$

where  $\Delta R_1$  and  $\Delta R_2$  are the response in the presence of the two component salts alone. This relationship quantitatively describes the behaviour of the ions in terms of magnitude (additive *vs.* non-additive) and direction of the combined effect. Robertson *et al.* thus defined for a system of two same-effect salts that  $\delta \approx 0$  represents additive behaviour, and  $\delta > 0$  non-additive and synergistic behaviour. When  $\delta < 0$  the combined behaviour is non-additive, with further distinction defined;  $\delta < 0$  and  $|\Delta R_{\text{net}}| > \max(\Delta R_1, \Delta R_2)$  is cooperative, while  $\delta < 0$  and  $|\Delta R_{\text{net}}| < \max(\Delta R_1, \Delta R_2)$  is antagonistic.

Moghaddam and Thormann utilised DSC to investigate the stability of ungrafted poly(propylene oxide) (PPO) in aqueous solutions of binary sodium electrolytes, keeping the cation constant to decode the relative influence of different anions.<sup>250</sup> They reported that the behaviour of PPO in the presence of two salts that salt-in PPO (NaSCN and NaI) or two salts that salt-out PPO (NaCl and NaBr) is dependent on the salt concentration. The authors reported a turnover in the manifested SIE with increasing concentration. That is, in the presence of a low concentration binary electrolyte,  $|\Delta R_{\text{net}}|$  is greater than the  $|\Delta R_i|$  of PPO in the presence of either pure electrolyte, while at higher concentrations the LCST ( $|\Delta R_{\text{net}}|$ ) in the mixed salt solution lies between each of the pure composite electrolytes (Fig. 13); altering from cooperative to antagonistic behaviour. We recast the data of Moghaddam and Thormann (Fig. 13(a) and (b)), showing the net change in the LCST of PPO as a function of the concentration of a second electrolyte from the same end of the Hofmeister series. Deviations from purely additive behaviour are illustrated by  $\delta$  in each inset figure. In the case of two salting-out salts (Fig. 13(a)), systematically varying the concentration of NaBr whilst maintaining a constant NaCl concentration of 0.1 M, and *vice versa*, yields approximately additive behaviour ( $\delta \approx 0$ ). Deviations from additive behaviour occur at high NaCl concentrations as  $\delta$  diverges from 0. Fig. 13(b) presents the behaviour of PPO in the presence of binary electrolytes composed of two salting-in anions. For this combination of mixed electrolytes, the behaviour is essentially additive at all concentrations.

Moghaddam and Thormann also investigated a binary electrolyte composed of two salts that salt-in and salt-out PPO, NaSCN and NaCl, Fig. 13(c).<sup>250</sup> Here approximately additive behaviour was observed, whereby both anions impart their individual (opposite) effects onto the system. No attempt is made here to extend the definition of the  $\delta$  deviation parameter to systems comprising mixtures with both salting-in and salting-out salts, owing to the non-unique range of possible relative responses for a given  $\delta$  value.

Recently, Bruce *et al.* investigated the effects of a mixed electrolyte (composed of anions from opposite ends of the Hofmeister series) on the LCST of ungrafted pNIPAM in a combined spectroscopic and MD study.<sup>160</sup> In the presence of a fixed concentration of  $\text{Na}_2\text{SO}_4$  and systematically varied NaI



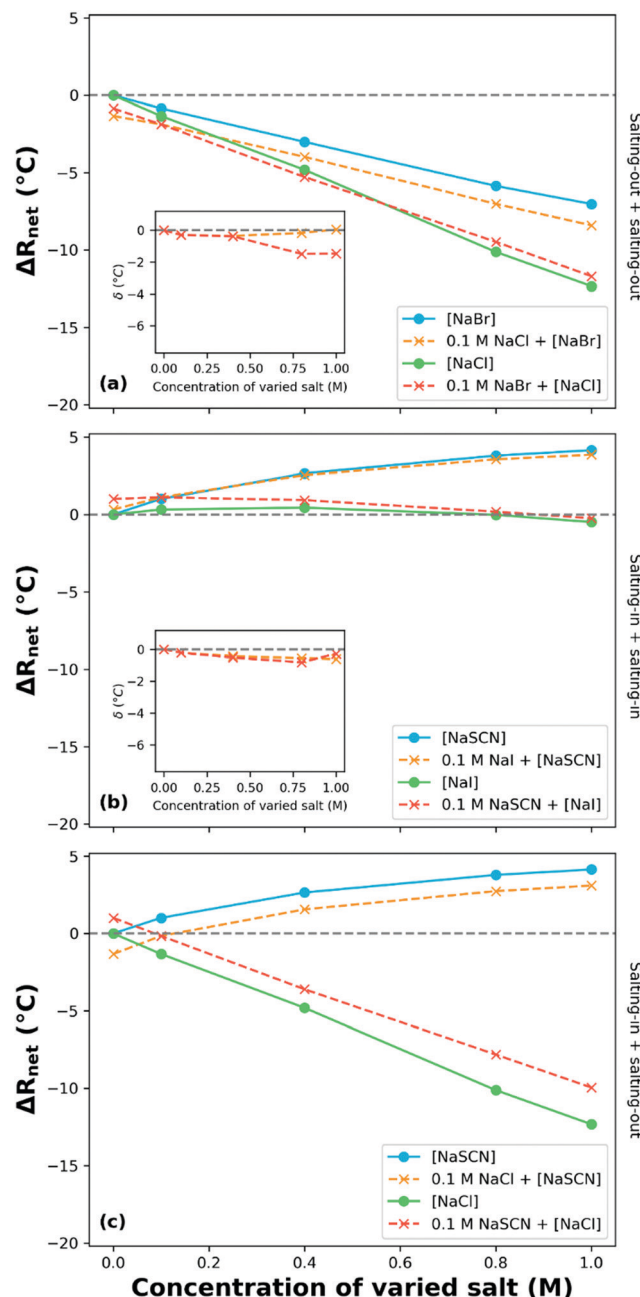


Fig. 13 The net response in LCST ( $\Delta R_{\text{net}}$ ; change relative to the LCST of PPO in water) of ungrafted PPO as a function of the concentration of varied salt species for several binary electrolyte compositions: same end of Hofmeister series anions (a) and (b); opposite end (c). The varied salt species is denoted by square brackets. Inset plots present the  $\delta$  values (deviations from purely additive behaviour) for the same effect-type binary electrolyte compositions. Data obtained and reproduced with permission from Moghaddam and Thormann,<sup>250</sup> copyright 2015.

concentration, a reduction in the LCST of pNIPAM was observed at low  $\text{I}^-$  concentrations. This non-additive, antagonistic behaviour is contrary to the PPO-based study conducted by Moghaddam and Thormann who observed near additive behaviour for all conditions (Fig. 13).<sup>250</sup> Bruce *et al.* hypothesised that the  $\text{Na}^+$  counterion preferentially interacts with the

strongly hydrated  $\text{SO}_4^{2-}$  anion, leaving a greater number of lone  $\text{I}^-$  anions in a more hydrated state. These hydrated ions compete with the polymer for water and decrease polymer solubility. However, at all concentrations of the mixed salt the MD results indicated an increase in the number of  $\text{I}^-$  ions proximal to a model oligomer compared to the pure salt, and the effects of the  $\text{SO}_4^{2-}$  anion on the solvation of the  $\text{I}^-$  anion was most notable in the second solvation shell. This may indicate other factors at play (for instance cation effects<sup>161</sup>) for  $\text{NaI}$  to further salt-out the polymer whilst  $\text{I}^-$  itself showed an increased affinity for the polymer and increased solvation in the mixed salt system. Upon further addition of  $\text{NaI}$ , a salting-in effect was observed in comparison to the lower concentrations; this turnover in behaviour is indicative of competitive behaviour occurring between the anions (*i.e.*,  $\text{I}^-$  salting-in effects manifest instead of  $\text{SO}_4^{2-}$  salting-out behaviour). Finally, in the highest iodide concentration region, it was concluded there was a depletion of ions at the surface, driving polymer collapse and thus a decrease in LCST.

Johnson *et al.*<sup>193</sup> investigated the effects of mixed aqueous electrolytes composed of anions from the two extremes of the Hofmeister series. The authors probed the behaviour of a statistical copolymer brush of di(ethylene glycol)methyl ether methacrylate ( $\text{MEO}_2\text{MA}$ ) and ethylene glycol methyl ether methacrylate ( $\text{OEGMA}_{300}$ ) ( $\text{P}(\text{MEO}_2\text{MA}-\text{stat}-\text{OEGMA}_{300})$ ) 80:20 mol% using QCM-D. In comparison to Moghaddam and Thormann<sup>250</sup> and Bruce *et al.*,<sup>160</sup> Johnson *et al.* explored the influence of temperature on the manifestation of SIEs across a wide concentration range, noting temperature-dependent SIEs (Fig. 11(d)). At low temperatures ( $< 25^\circ\text{C}$ ) and in the presence of equimolar  $\text{KSCN}$  (salting-in) and  $\text{KCH}_3\text{COO}$  (salting-out) electrolytes, the impact of the ions was approximately additive, yielding a similar brush response to that in the absence of salt. However, at higher temperatures a net salting-in effect was observed in comparison to water.

The influence of mixed electrolyte solutions on the thermo-transition of a  $\text{P}(\text{MEO}_2\text{MA}-\text{stat}-\text{OEGMA}_{300})$  80:20 mol% copolymer brush has also been studied by Robertson *et al.*<sup>249</sup> Fig. 14 presents a subset of the data collected by Robertson *et al.*:  $\Delta R_{\text{net}}$  as a function of varied salt concentration at  $15^\circ\text{C}$  (most swollen state). This study reported that for binary electrolytes composed of two salts (KF and KCl) that both individually salt-out the polymer, the influence of the ions was concentration dependent. At low and intermediate concentrations of KF (containing the more charge dense of the anions), an approximately additive ( $\delta \approx 0$ ) behaviour of the ions with increasing KCl concentration was observed, consistent with Moghaddam and Thormann.<sup>249,250</sup> At high KF concentrations (500 mM), a non-monotonic impact was observed that was dependent on the KCl concentration, which was attributed to the availability of solvent molecules.<sup>249</sup> A complementary experiment with two salting-in salts, KSCN and KI, demonstrated competitive behaviour between the salts. As shown in Fig. 14(b), all  $\Delta R_{\text{net}}$  curves corresponding to binary electrolytes are non-monotonic with increasing salt concentration. For example, in 250 mM KSCN with varied KI concentration,

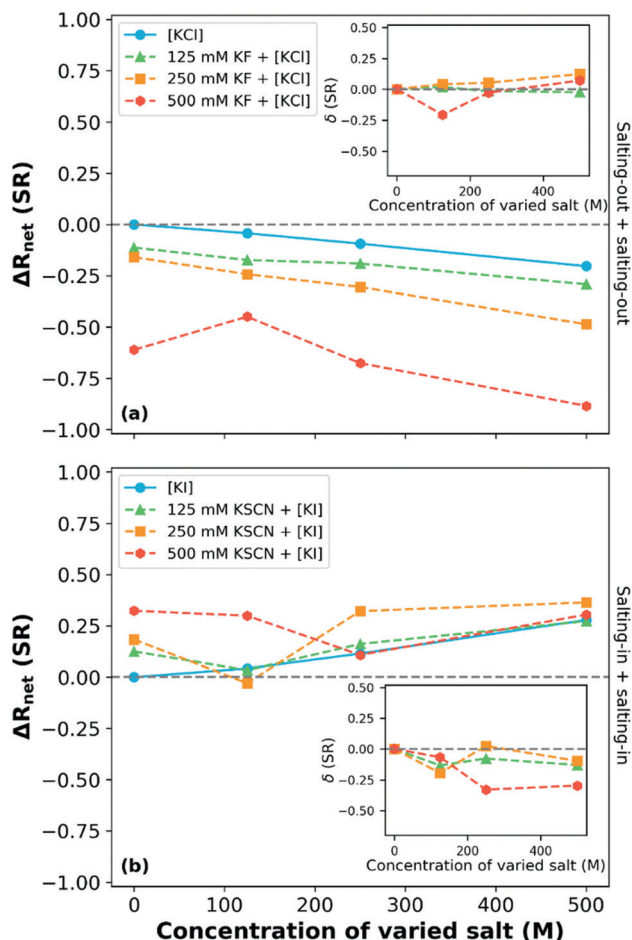


Fig. 14 The net response ( $\Delta R_{\text{net}}(\text{SR})$ ; change in swelling ratio relative to the response in water) of a P(MEO<sub>2</sub>MA-stat-OEGMA<sub>300</sub>) 80:20 mol% copolymer brush at 15 °C in binary electrolytes composed of (a) salting-out and (b) salting-in ions where the varied species is denoted by square brackets. Inset plots present the  $\delta$  values for the various binary electrolyte compositions. Adapted from ref. 249 with permission from Elsevier, copyright 2021.

antagonistic behaviour was observed at 125 mM KI, additive behaviour at 250 mM KI concentrations and again non-additive behaviour at 500 mM KI. This is similar to the three concentration regions observed by Bruce *et al.* for Na<sub>2</sub>SO<sub>4</sub> and NaI mixtures.<sup>160</sup> Robertson *et al.* note, however, that the non-monotonic behaviour between the ions (from antagonistic to cooperative) in Fig. 14(b) cannot be explained by the Moghaddam and Thormann competitive binding mechanism.<sup>250</sup> Rather, it was hypothesised that the turnover is due to the reduction in salting-in behaviour driven by the inter-anion and polymer-anion interactions. Notably, when observing the 125 mM and 500 mM KSCN solutions, at high concentrations of KI the behaviour appears to converge to that observed in the pure KI salt.

## 6. SIEs in nonaqueous solvents

The vast majority of SIE studies have employed water as the solvent (Section 2.2). This has led to the prevalent assumption that the SIEs observed originate from the properties of water

itself, or that the existence of the Hofmeister series is dependent upon water. Recent reports by Mazzini and Craig,<sup>41–44</sup> Liu *et al.*,<sup>40,251–255</sup> Gregory *et al.*,<sup>45,128,256</sup> Smiatek *et al.*,<sup>169,244,257–263</sup> and others<sup>24,27,39,264,265</sup> demonstrate however that SIEs and the Hofmeister series also exist in nonaqueous solvents. The origins of SIEs therefore cannot be solely attributed to an ion's ability to induce order in an aqueous environment; their origins must be more general in nature (*i.e.*, a property of the ions themselves). Nonetheless, the role of the solvent is important in the manifestation of SIEs. Identifying the influence of the solvent on SIEs in nonaqueous environments is not only critical for SIEs to be exploited in myriad applications employing nonaqueous solvents (*e.g.* batteries,<sup>266</sup> supercapacitors,<sup>267</sup> metal electrodeposition,<sup>268</sup> semiconductors,<sup>269</sup> fuel cells,<sup>270</sup> capillary electrophoresis,<sup>271</sup> *etc.*<sup>66,266</sup>), but also for our fundamental understanding of SIEs generally.

In this respect, nonaqueous solvents pose interesting challenges. For instance, Mazzini and Craig<sup>41</sup> have recently demonstrated that the association of anions with their solvent environment in water and methanol exhibit analogous trends; both following the Hofmeister series (measured *via* NMR molecular reorientation time). On the other hand, the standard molar heat capacities of the same anions exhibit no known SIE trend in water but follow a reverse Hofmeister trend in methanol. Comparable results were observed regarding the limiting molar conductivity. Similarly, while viscosity  $B$  coefficients of these anions in water were reported not to follow a known SIE trend (these are dependent on coordination number<sup>128</sup>), in methanol they followed a direct Hofmeister series. Solvent-induced SIE reversals have been observed in ion retention times in size exclusion chromatography and polymer swelling experiments.<sup>43</sup> For instance, a direct series was found for water and MeOH in both cases, while a reverse series was seen in dimethyl sulfoxide (DMSO) and PC. In formamide (FA) electrolyte solutions, polymer-brush swelling exhibited a reverse series, despite ion retention times exhibiting no known ion specific trend. These series inversions supported prior observations of Parker<sup>272</sup> and Pearson.<sup>273</sup>

The initial hypotheses for solvent-induced anion Hofmeister series reversal by Mazzini *et al.*<sup>43</sup> were in line with the proposed polarisability origins of SIE. This suggested that a forward Hofmeister series would be followed in low polarisability solvents, such as water and methanol, whilst a reversal would occur for high polarisability solvents such as DMSO and PC. The fact that ion retention times in FA showed no known ion-specific trend whilst known ion-specific trends were observed in polymer brush swelling, suggest that FA has properties that were on the cusp of producing ion series reversal. For these protic solvents, polarisability correlates with Lewis acidity, and other work<sup>128,274</sup> suggests that the latter is the fundamentally important property. In fact, the radial charge density of anions ( $\beta$ , Section 2.3.3) and the solvent's Lewis acidity (quantified by the Gutmann acceptor number,<sup>275</sup> AN) were correlated quantitatively with the magnitude of the Gibbs energy of transfer from aqueous to nonaqueous solutions (Fig. 15(a)). Similar correlations were observed for the S<sub>N</sub>2 reaction rate of nucleophilic



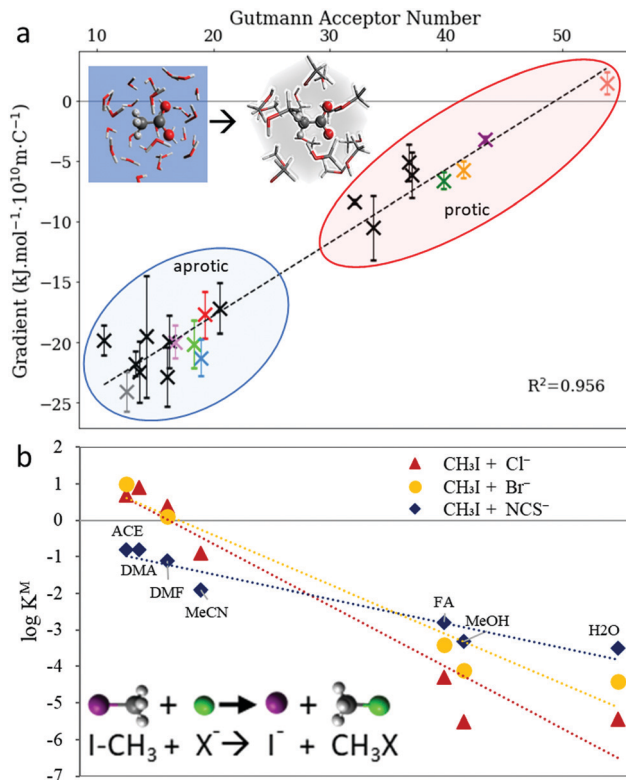


Fig. 15 The Gutmann acceptor number approximates the effect of the solvent on anion trends (a) with the Gibbs' free energy of transfer from aqueous to nonaqueous solvents and (b) the  $S_2N_2$  reaction rate with methyl iodide. Adapted from ref. 128 with permission from the Royal Society of Chemistry, copyright 2021.

anions with methyl iodide in nonaqueous environments (Fig. 15(b)).<sup>128</sup> For cations, it was hypothesised that the similarity in Lewis basicity (quantified by the Gutmann donor number, DN) between water and many nonaqueous solvents (or cosolutes) allowed for non-electrostatic interactions, such as dispersion, to instead have significant influence in (partially) aqueous SIE for cations. Considerable work to address the use of donor numbers for SIE has been performed by Smiatek *et al.* using a conceptual density functional theory approach.<sup>257,260,263,276,277</sup>

Whilst it appears AN quantifies the magnitude of anion SIE in nonaqueous solvents and DN has shown some success as a solvent parameter for cation solvation,<sup>278</sup> there are two key problems that arise from their empirical origins:

1. A solvent's DN and AN are based on completely different empirical measurements, and are defined in inconsistent units. The DN is obtained by calorimetry, and is defined as the enthalpy of formation of a solvent antimony pentachloride ( $SbCl_5$ ) 1:1 adduct (in kcal mol<sup>-1</sup>). The AN is the solvent-induced  $^{31}P$  NMR chemical shift of triethyl phosphine oxide ( $Et_3PO$ ) in the solvent (in ppm). It is therefore meaningless to quantitatively compare these parameters, or simultaneously account for cation and anion effects self-consistently.

2. A solvent's DN and AN are specific to the molecular probe ( $SbCl_5$  and  $Et_3PO$ , respectively) from which they were each derived. This may limit their transferability for predicting

solvency of Lewis acids (*e.g.*, cations) and Lewis bases (*e.g.*, anions) that are dissimilar to these molecular probes.

For these reasons, an *ab initio* unification of solvent Lewis acid and base properties is warranted. Similarly, the importance of ion solvation numbers have also been highlighted in properly understanding ion solvation in aqueous solution (Section 2.3.5),<sup>20,128,130,155,157</sup> yet there is limited information available for nonaqueous solvents.

## 7. SIEs in concentrated electrolytes

To date no theory to describe the properties of highly concentrated electrolyte solutions has gained widespread acceptance, and various effects manifest in this regime (*i.e.*, re-entrant behaviour in polyelectrolyte<sup>279–281</sup> and colloidal systems<sup>74,282,283</sup>). DH theory describes the behaviour of dilute electrolytes successfully, however its accuracy is diminished with increasing concentration for various reasons, some of which are mentioned in Section 2. The DH equation (also called the linearised Poisson–Boltzmann (PB) equation) is the following differential equation,

$$\nabla^2 \psi_i(r) = \begin{cases} 0, & 0 < r < d^h \\ \kappa_D^2 \psi_i(r), & r \geq d^h \end{cases} \quad (5)$$

where  $\nabla^2$  is the Laplace operator,  $\psi_i$  is the mean electrostatic potential at distance  $r$  from an ion  $i$  and the square root of the eigenvalue,  $\kappa_D$ , is known as the Debye parameter and its inverse ( $\lambda_D$ ) is called the Debye length. The meaning of the Debye length is the distance over which the electrostatic effect of a charge is reduced by a factor of  $e^{-1}$ ,<sup>284</sup> in a solvent with static permittivity (formerly known as the dielectric constant) value of  $\epsilon_r$ , absolute temperature  $T$ , and ionic strength  $I$ ,

$$\lambda_D = \frac{1}{\kappa_D} = \sqrt{\frac{\epsilon_r \epsilon_0 k_B T}{2q_e^2 N_A I}} = \frac{1}{\sqrt{8\pi \lambda_B N_A I}} \quad (6)$$

where  $N_A$  is the Avogadro constant and  $q_e$  is the formal charge on the ions,  $\epsilon_0$  is the static permittivity of a vacuum, and  $k_B$  is the Boltzmann constant. In the final term, the appearance of  $\lambda_B$ , is a quantity known as the (unscreened) Bjerrum length,<sup>285</sup>

$$\lambda_B = \frac{q_e^2}{4\pi\epsilon_0\epsilon_r k_B T} \quad (7)$$

which is the length scale at which the thermal ( $k_B T$ ) and electrostatic energy are equal. Both  $\lambda_D$  and  $\lambda_B$  length scales are valid at low concentrations of ions, however consider for a moment the meaning of  $\epsilon_r$ . From electrodynamics, the electric displacement ( $\mathbf{D}$ ) is given by,

$$\mathbf{D} = \epsilon_0 \mathbf{E} + \mathbf{P} \quad (8)$$

with the electric field denoted by  $\mathbf{E}$  and the polarisation by  $\mathbf{P}$ , with the latter being the response of the material to the applied electric field.<sup>286</sup> In the first-order Taylor expansion of  $\mathbf{P}$  (higher order terms apply for large electric fields, and this is relegated to lasers and optics), we obtain,

$$\mathbf{D} = \epsilon_0(1 + \chi_e)\mathbf{E} = \epsilon_0\epsilon_r\mathbf{E} \quad (9)$$



where  $\chi_e$  is the electric susceptibility;  $\chi_e$  and  $\varepsilon_r$  which are generally tensors (for anisotropic media) and are both frequency and temperature dependent. In the context of equilibrium electrolytes, there is no externally applied field, so the relative permittivity is  $\varepsilon_r = \varepsilon_r(\omega = 0, T) \in \mathbb{R}$  ( $\omega$  is the angular frequency of the applied field). This single number is often used in understanding solvation of ions in different solvents, as solvents with higher permittivity numbers have greater capacity to screen an electric field. However, it is also a function of the composition of the mixture. The electronic and geometric nature of the solvent and solute molecules, their ability to orient toward an applied field, as well as the intermolecular interactions, all contribute. At finite frequencies, different contributions have competing effects and this can lead to phenomena such as an isopermittivity point in water.<sup>287</sup> Hence  $\varepsilon_r$  is also a function of concentration. Usually, high permittivity solvents will see a decrease in the value of  $\varepsilon_r$  with the addition of a salt while lower permittivity solvents can see the reverse. The former is thought to be due to an entropic effect of locking solvent dipoles into solvation shells of ions (salt-screening of solvent–solvent correlations), and the latter due to ion pairing and polarisation of the solvent, as proposed by Grzetic *et al.*<sup>288</sup>

To illustrate the effect of adjusting the value of the static permittivity on the Debye and Bjerrum lengths, experimental values<sup>289–294</sup> were collected and fitted to a functional form provided by Gavish and Promislow<sup>295</sup> (detailed in the ESI†), and the correction is shown in Fig. 16. By increasing the NaCl concentration the Debye length decreases at a faster rate compared to the fixed  $\varepsilon_r$  form and Bjerrum length increases linearly compared to the fixed  $\varepsilon_r$  form.

The form of the Bjerrum length provided in eqn (7) is widely used. However, this form is derived from a simple unscreened Coulomb interaction and will therefore become increasingly inaccurate as the number of ions in solution (and therefore

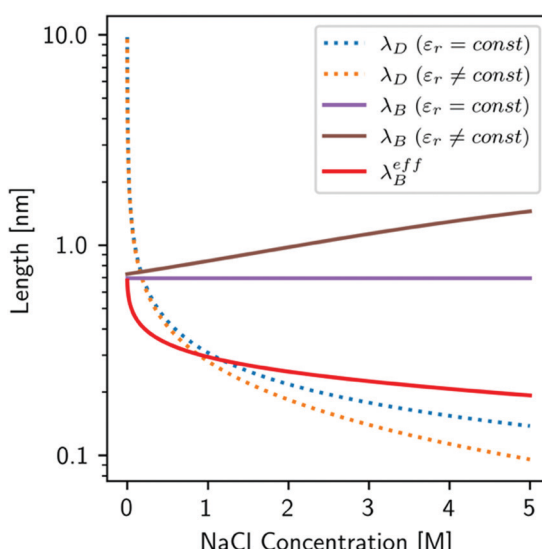


Fig. 16 The effect of varying the relative permittivity ( $\varepsilon_r$ ) due to concentration on both the Debye length ( $\lambda_D$ ) and the unscreened Bjerrum length ( $\lambda_B$ ), as well as the predicted effective (or screened) Bjerrum length ( $\lambda_B^{\text{eff}}$ ).

electrostatic screening) increases. Hence the decay will take the form of a Yukawa-like potential,<sup>296</sup> as shown by Liu *et al.*,<sup>279</sup> and results in the following transcendental equation for  $r_{ij}$  that gives the effective Bjerrum length ( $\lambda_B^{\text{eff}}$ ) in solution,

$$r_{ij} = e^{-\kappa_D r_{ij}} \quad (10)$$

The solutions to such transcendental equations are given by the real component of the Lambert  $W$  function ( $W_R(x)$ ),

$$\lambda_B^{\text{eff}} = \frac{1}{\kappa_D} W_R(\kappa_D \lambda_B) = \lambda_D W_R\left(\frac{\lambda_B}{\lambda_D}\right) \quad (11)$$

This effective Bjerrum length gives the length of the electrostatic-thermal interaction equivalence in the presence of ions, with a concentration dependence implicit in the calculation of  $\lambda_D$ . This is plotted in Fig. 16, showing the significant reduction in the Bjerrum length (compared to the increase by only adjusting the value of the static permittivity) if there are other ions present.

If these were the only extra corrections needed there would be nothing left to add. However surface force measurements<sup>297</sup> by Gebbie *et al.*<sup>298</sup> and Perkin's group,<sup>285,299,300</sup> with agreement from other techniques described by Gaddam and Ducker,<sup>301</sup> and then further critically reviewed,<sup>302</sup> showed that there were significant deviations from the Debye length at higher concentrations, despite adjustments to the value of the permittivity. This highlights a significant breakdown of the DH picture of electrolytes. This is particularly obvious in Fig. 17(a), where there is a significant deviation at higher concentrations. Note all plots in Fig. 17 use an  $x$ -axis of  $\kappa_D a = a/\lambda_D \sim \sqrt{I}$ , *i.e.*, it is proportional to the ionic strength and increases with ionic concentration. In all cases  $a$  is the diameter of the particle (sometimes  $d$  is used instead of  $a$  to denote this quantity) and  $\lambda_D = \kappa_D^{-1}$  is the predicted Debye length (*i.e.*, from eqn (6)). Fig. 17(a) shows that the ratio of the observed screening length divided by the Debye length ( $\lambda_S/\lambda_D$ ) for 1:1 aqueous electrolytes, pure room temperature ionic liquids (RTILs) and diluted ionic liquids (ILs) in PC, appear to collapse onto a single line at values of  $\kappa_D a \geq 1$ . The authors put forward the following relationship to fit the observation,

$$\frac{\lambda_S}{\lambda_D} \sim \left(\frac{a}{\lambda_D}\right)^\alpha = (\kappa_D a)^\alpha \quad (12)$$

where  $\alpha$  is an empirical exponent, which was found to be  $\sim 3$  from their surface force measurements.<sup>285,299,300</sup> They also put forward an equivalent equation,

$$\lambda_S \sim c_{\text{ion}} a^3 \lambda_B \quad (13)$$

where  $c_{\text{ion}}$  is the concentration of the ions. This suggested that the (unscreened) Bjerrum length and the ion size are important in the onset of this phenomenon. They termed this behaviour of the increase in observed screening (compared to the Debye length) as underscreening.

Statistical mechanics predicts a change in the screening behaviour when the Debye length is of the order of the ion size. Kirkwood<sup>308</sup> showed that there is a crossover point where the



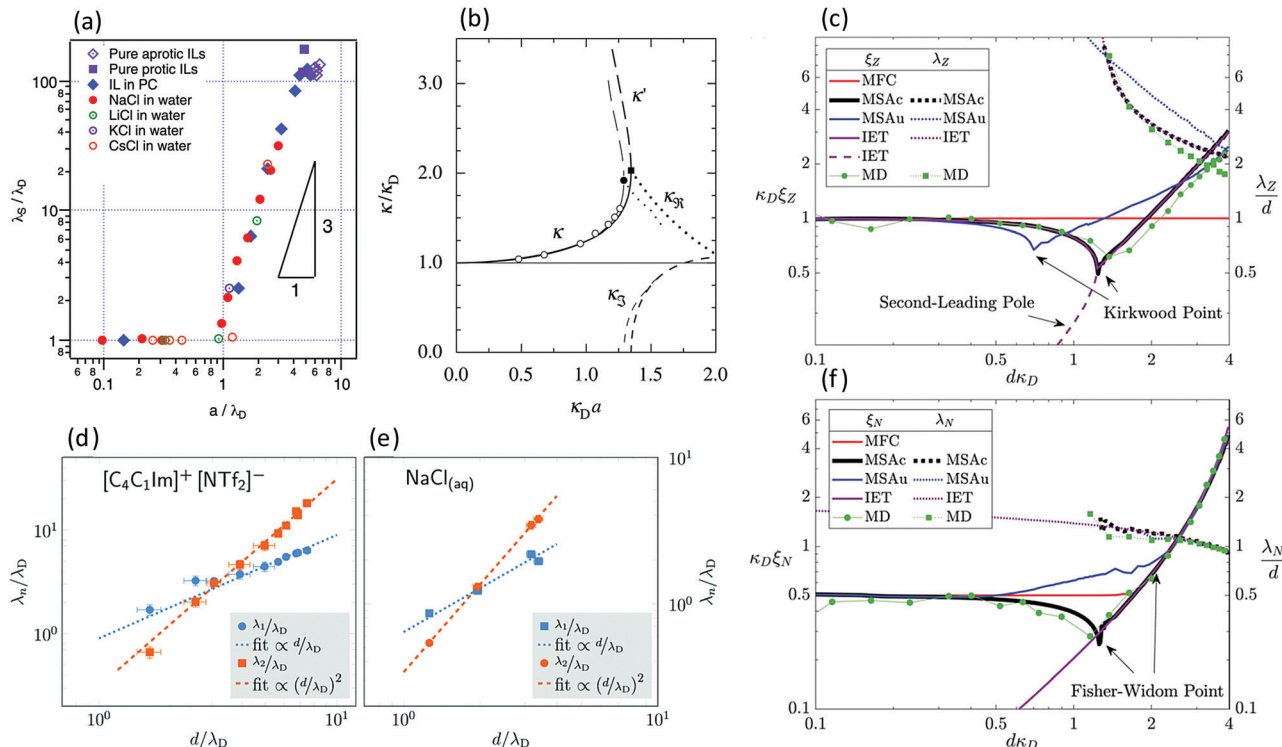


**Fig. 17** Plots of various phenomena as the concentration (i.e., ionic strength) is increased. For all plots, the x-axis is given in units of  $\kappa_D a = a/\lambda_D \sim \sqrt{I}$ , where  $I$  is the ionic strength, hence it is a measure of concentration when  $a$  is constant. (a) Experimentally measured screening of a selection of pure ILs, an IL dissolved in PC and several 1:1 inorganic salts in water. (b) The behaviour of eqn (15) (thick curves) for a 1:1 aqueous electrolyte solution at room temperature (also valid for a classical 1:1 plasma in vacuum at  $T = 23\,400$  K), showing the convergence of two solutions with decay parameters  $\kappa$  and  $\kappa'$  to the Kirkwood point (filled symbols), at which they merge into complex conjugates. The thin curves are hypernetted-chain (HNC) results from Ennis *et al.*<sup>303</sup> and open symbols are Monte Carlo (MC) simulation results from Ulander *et al.*<sup>304</sup> (c) The charge decay length ( $\xi_Z$ , solid lines) and the wavelength ( $\lambda_Z$ , dotted lines) for several models as well as MD results, showing the rough agreement of the Kirkwood point and the scaling behaviour at higher concentrations. (d) The scaling behaviour from MD simulations indicating the presence of two decay lengths with exponents  $\alpha = 1$  and  $\alpha = 2$ . (e) Similarly, but for aqueous NaCl. (f) Similar to (c) except for the number decay length ( $\xi_N$ ) and number wavelength ( $\lambda_N$ ), indicating the Fisher-Widom point. For (a), (b), (d), (e) the y-axis is in units of  $\kappa/\kappa_D = \lambda/\lambda_D$  which is the ratio of the observed screening length compared to the screening length predicted by the Debye-Hückel equation. (a) Reproduced from ref. 285 with permission from the American Physical Society, copyright 2018. (b) Reproduced from ref. 305 with permission from the Royal Society of Chemistry, copyright 2020. (c and f) Reprinted from ref. 306, with permission from AIP Publishing, copyright 2021 (d) and (e) reproduced from ref. 307 with permission from the Royal Society of Chemistry, copyright 2021 and 2020 respectively.

screening behaviour would change from pure exponential decay to a damped oscillatory decay, and Lee *et al.*<sup>299</sup> showed that it occurs at approximately  $a/\lambda_D = \sqrt{4\pi l_B c_0 a^2} > \approx \sqrt{2}$ . This oscillatory decay has the functional form,

$$f(r) = \frac{A}{r} \exp\left(-\frac{r}{\lambda}\right) \sin\left(\frac{2\pi r}{d} + \phi\right) \quad (14)$$

where  $\lambda$  is the decay length at a distance  $r$ ,  $A$ , and  $\phi$  are empirical constants and  $d$  is related to the ion size.<sup>284</sup> The oscillating behaviour appears to be related to the granular nature of the interactions becoming important, and the onset of charge-ordering which is known as overscreening.<sup>309</sup> The onset of the damped oscillatory decay is observed in both the charge-charge and number-number distribution functions, and is known as the Kirkwood<sup>308</sup> and Fisher-Widom<sup>310</sup> points respectively. The onset of this behaviour was also found in the works of Onsager,<sup>311</sup> Kjellander,<sup>284,305,312–315</sup> Carvalho and Evans,<sup>316</sup> Stillinger and Lovett,<sup>317</sup> and Attard.<sup>318</sup> Fig. 17(c) and (f)

shows the Kirkwood and Fisher-Widom points, respectively, for various classical density functional models.<sup>306</sup> Other statistical mechanical models are also plotted in a similar way,<sup>306</sup> and while they predict the same onset of the change in behaviour, they do not capture the  $\alpha = 3$  scaling behaviour at higher concentrations (i.e., values of  $\kappa_D a$ ) that was found by the surface force measurements.

Subsequent theoretical and computational work has also been unable to obtain the  $\alpha = 3$  scaling that is observed experimentally.<sup>307,319–325</sup> The exact contributing factors leading to the scaling behaviour are still unknown, with suggestions of the omission of polarisation<sup>306</sup> as well as ion-pairing and/or clustering<sup>319–321</sup> being important, with the full dissociation of “strong” 1:1 electrolytes above 0.5 M being questionable (Section 2.3.5).<sup>326,327</sup> However the degree and nature of such clustering and pairing is still debated. As was shown by Gebbie *et al.*<sup>298</sup> and more recently by Liu *et al.*,<sup>279</sup> most of the ions in the solution would need to be paired in order to get such a screening length if ion-pairing were the only explanation.

Predicted electrical double-layer capacitance for such a high degree of ion pairing was also qualitatively different from experiment.<sup>328</sup>

Kjellander has shown that, in contrast to DH and PB theory, if all the ions are treated on the same basis, the screening decay length is different from the Debye length.<sup>284,314,329</sup> The behaviour of the screening length can be observed by solving,

$$\left[ \frac{\kappa}{\kappa_D} \right]^2 = \frac{e^{\kappa a}}{1 + \kappa a} \quad (15)$$

where  $\kappa$  is the actual screening parameter, and  $a$  is the particle diameter.<sup>284</sup> This yields (at least) 2 solutions, with decay parameters  $\kappa$  and  $\kappa'$  such that  $\kappa < \kappa' (\kappa, \kappa' \in \mathbb{R})$ . The behaviour of these two solutions is shown in Fig. 17(b). When  $\kappa_D a$  is increased (*i.e.*, as concentration is increased), the two solutions approach each other and merge to become complex conjugates,

$$\begin{aligned} \kappa &= \kappa_R + i\kappa_I \\ \kappa' &= \kappa_R - i\kappa_I \end{aligned} \quad (16)$$

with  $\kappa_R, \kappa_I \in \mathbb{R}$ . This corresponds to the Kirkwood point and indicates the onset of an exponentially oscillating decay behaviour, where  $\kappa_R$  and  $\kappa_I$  are related to the  $\lambda$  and  $d$  terms in eqn (14). Kjellander also derived an exact statistical mechanical result for the screening length, given by,

$$\kappa^2 = \frac{1}{k_B T \mathcal{E}_r^* (\kappa) \varepsilon_0} \sum_j q_j q_j^* n_j^b \quad (17)$$

where  $\mathcal{E}_r^*$  is the dielectric factor (see Kjellander<sup>284</sup> for details), and  $q_j^*$  is the dressed particle charge (*i.e.*, a renormalised charge) on ion  $j$  and  $n_j^b$  is the number density of  $j$  ions in the bulk phase. While this is an exact result, calculation of  $\mathcal{E}_r^*$  and  $q_j^*$  are unknown quantities. However, the modification of the charge to an effective charge is due to the presence of other ions in the solution, which will have correlated behaviour. Hence the electrostatics are highly non-local<sup>312</sup> and points to a significant reason why the DH theory breaks down. Furthermore, this treatment also captures ion-ion correlations with the inclusion of ion-pairing (*i.e.* CIP, SIP, SSIP, clusters) as just highly correlated ions. The permittivity term,  $\mathcal{E}_r^*$ , is a quantity that depends on the presence of ions and also takes into account the granular nature of the solvent. Both of these terms will be specific to both the solvent and the ions that are involved.

The above equations also permit more than two solutions for  $\kappa$ , which would lead to a linear combination of exponential and/or oscillatory exponential decays, as shown recently by Kjellander.<sup>305</sup> This was hinted at by work by Kebinski *et al.*,<sup>330</sup> and more recently Zeman *et al.*<sup>307</sup> also examined this possibility and fitted simulation data of the potential of mean force with multiple functions similar to the one given by eqn (14). They found scaling relationships with  $\alpha = 1$  and  $\alpha = 2$  for two of the terms that they used to fit their simulation data for the diluted IL and for aqueous NaCl (Fig. 17(d) and (e)).

The addition of extra decay lengths increases the accuracy of the DH model (see Fig. 18).<sup>305</sup> The term with the smallest decay

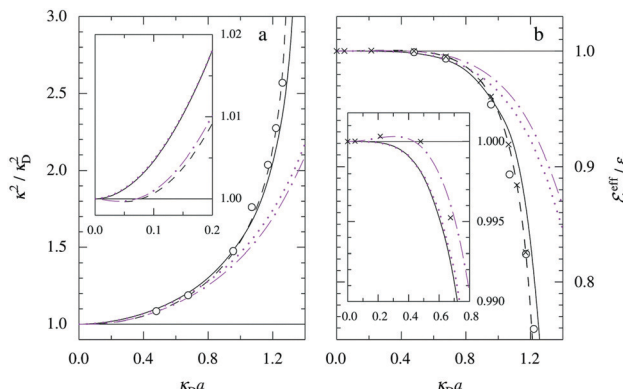


Fig. 18 The ratios (a)  $\kappa^2/\kappa_D^2$  and (b)  $\mathcal{E}_r^{\text{eff}}/\mathcal{E}_r$  plotted as functions of  $\kappa_D a \sim \sqrt{l}$ , where  $l$  is the ionic strength, for monovalent electrolytes in aqueous solution at room temperature. The inset shows the behaviour at low  $\kappa_D a$ . The dot-dashed curves are from the extended exponential DH approximation (EDHX), dotted curves from the Attard's self-consistent screening length approximation (SCSL).<sup>318</sup> The full curves are from the simple multiple-decay extended Debye–Hückel (MDE-DH) approximation, while the dashed curves and crosses show results from HNC calculations, and open circles are from MC simulations. The HNC and MC data are taken from work by Ulander<sup>304</sup> and Ennis.<sup>303</sup> Reproduced from ref. 305 with permission from the Royal Society of Chemistry, copyright 2020.

parameter (largest wavelength) is the one that dominates the behaviour at long range. Recently it has been suggested that a modified Poisson–Boltzmann model may aid in explaining large experimental decay lengths.<sup>331</sup>

Salt concentration has long been recognised as a significant factor in the study of SIE. There is much more to discuss regarding SIEs at high concentration and the so-called “4th evolution of ionic liquids”<sup>332</sup> shows there is much still to be understood about ion concentration effects in both aqueous and nonaqueous solvents. The original precipitation experiments performed by Lewith and Hofmeister required significant salt concentrations.<sup>32</sup> Many modern studies of SIE’s have also performed using high salt concentrations, leading to a prevailing assumption that SIEs are only largely relevant observed in concentrated electrolytes. In this respect it is important to highlight the study of Mazzini and Craig, who demonstrated that SIEs are observed on standard molar volumes of infinitely dilute electrolyte solutions.<sup>42</sup> Nevertheless, in concentrated solutions, the ion size, its interaction with the other ions and the solvent and the decay lengths of the electrostatics are ion specific. There is no reason to suppose that this supplants other SIEs observed in concentrated electrolytes, and it is conceivable that ion specificity in general are the result of multiple factors (we have discussed concentration-induced SIE reversals further in Section 3.1). However, the empirical relationship of eqn (12) still lacks explanation and has mostly been explored for 1:1 electrolytes, hence the impact of ion valency on these phenomena remains to be explored. We note that the re-entrant solubility of polyelectrolytes at high salt concentrations has been attributed to the extended electrostatic decay length,<sup>279</sup> the implication being that higher valency ions induce a departure in the electrostatic decay length from the



Debye length at significantly lower concentrations than those expected from eqn (12).

The implications of the ion specificity of the extended electrostatic decay length at high salt are indeed broad, as they will likely influence any solution with a high ionic strength, including nonaqueous solutions (Section 6), deep eutectic solvents,<sup>333</sup> and ionic liquids.<sup>334–339</sup> Thus, one would expect that these SIE's are manifest in fields as diverse as crystallisation,<sup>340,341</sup> the packing of DNA,<sup>342,343</sup> the colloidal stability of particles,<sup>74,282,283</sup> battery and supercapacitor technologies<sup>7,258,262,264,267,344,345</sup> and self-assembly.<sup>72,344,346</sup> In many cases this will result in re-entrant behaviour, that is the stability or properties of a system reverting to a state that is seen at low salt concentrations.<sup>279</sup>

## 8. Conclusions & outlook

There have been significant contributions to our knowledge of SIEs in recent years. The Hofmeister series itself has been quantified for anions<sup>128</sup> based solely the ionic radial charge density (Section 2.3.3) and insight into the governing intermolecular forces in SIEs has advanced more generally.<sup>128,130,131</sup> Mechanisms underpinning SIEs, particularly regarding the influence of cations on polymer systems, continue to be elucidated.<sup>38,45,161–163</sup> Circumstances where SIEs either deviate from the traditional Hofmeister series or undergo complete reversals (Section 3) are becoming more extensively understood. In particular, it is now known that SIEs can be perturbed by stimuli such as solvent,<sup>43,128</sup> temperature<sup>192,193</sup> and UV radiation,<sup>191</sup> in addition to the more well established changes induced by concentration,<sup>25,172,177</sup> pH,<sup>172,174,176,194</sup> cosolute<sup>33,178–183</sup> and counterion.<sup>44,45,185–187</sup> By contrast, the behaviour of ions at surfaces (Section 4) are still poorly understood, in part due to experimental techniques' inability to delineate the individual effects of cations and anions near the interface. However, techniques such as NLO<sup>195,221,222</sup> and NICISS<sup>213,216–220</sup> are beginning to overcome this barrier (Table S1, ESI†), as are theoretical and computational approaches. The understanding of mixed salt SIE systems, relevant for biological and industrial applications (Section 5), has also developed recently, specifically regarding the additivity (or lack-there-of) of co-dissolved anions.<sup>160,249,250</sup> Direct investigations of SIE in nonaqueous environments (Section 6) constitute a new frontier for the field,<sup>24,27,39–45,128,169,244,251–255,257–265</sup> and in doing so are generalising our understanding of SIEs and their underlying mechanisms. Similarly, a new category of SIE observed in concentrated electrolytes (Section 7) has been shown to facilitate re-entrant behaviour in polyelectrolyte<sup>279–281</sup> and colloidal systems.<sup>74,282,283</sup>

Despite these advances, the ubiquity of SIEs means there is still much to be uncovered and understood. We believe the following avenues of research may help overcome the remaining challenges for understanding and predicting SIEs:

### *Ab initio* solvent and solute properties

A multitude of factors are required for predicting an ion's behaviour in any solution (Fig. 3), given the susceptibility of

SIEs to changes in the solvent or cosolute(s). Therefore, in addition to the ion's properties (Section 2.3), those of the solvent and any cosolute(s) must be considered explicitly for SIEs to be predicted. In this respect, the static relative permittivity ( $\epsilon_r$ ) is prevalent in established electrolyte theories (Sections 2 and 7). This parameter encompasses both positive and negative dipoles of the solution medium, and while this implies an ability to simultaneously account for cation and anion solvation, there is limited relation on relevant properties (e.g. salt solubility Fig. S2, ESI†), since it does not describe explicitly the distribution of charges in an electrolyte solution. The adjusted permittivity term,  $\mathcal{E}_r^*$ , proposed by Kjellander<sup>284</sup> possibly overcomes these limitations, as it is an ion specific term that accounts for the bulk molecular structure of the solvent. However, it is currently an unknown quantity. Alternate solvent properties (Section 6) relating to the Lewis acidity (AN) and basicity (DN) appear relevant to the magnitude of observed SIE. It is tempting to use these to predict the potential point of reversal behaviour (Sections 3 and 6), or if salting-in or -out effects occur. However, this is generally not possible – their empirical nature limits their utility and transferability. Elucidation of solvent properties that can simultaneously account for SIE and be incorporated into generalised electrolyte theories ( $\epsilon_r$ ) is therefore a key requirement for a general predictive theory for SIE. Ideally, such properties would be identified in the absence of solutes, particularly considering that reliably quantifying even the most fundamental of electrolyte properties (e.g. the solubility of a salt in a solvent) remains problematic. While resolving this issue is critical for more complex SIEs to be elucidated, understanding and predicting solvent structure and properties *ab initio* will be a key approach in future. While modified Poisson–Boltzmann models can successfully explain ion behaviour in various surface<sup>208</sup> and high concentration<sup>331</sup> phenomena, we think that extending these models to include site-specific charges<sup>128</sup> (Section 2.3.3) could also provide a basis for the elusive predictive theory of specific ion effects.

### Interfacial structure

Interfacial structure and concentration in electrolyte solutions are critical for myriad chemical and biological processes, such as enzyme and protein structure and electrochemical interfaces. Next-generation electrochemical devices can more readily be realised through optimisation of the electrode interface, and in this respect the adsorption/desorption of electrolyte is the critical phenomenon. A more detailed understanding of SIEs at interfaces will also inform bulk behaviour, and the origins of non-Hofmeister ion specificity (such as those observed in bubble-bubble interactions<sup>347</sup>). In these contexts, nonaqueous solvents are of particular importance. The complete elucidation of these phenomena requires pairing elementally-resolved techniques (e.g. NICISS) and computational simulation towards answering the following questions:

- i. What (accumulation/depletion) trend do ions follow at aqueous and nonaqueous solvent surfaces?



- ii. How does the solvent identity affect these specific ion trends?
- iii. What role do counterions (Section 3.3) have on the specific ion adsorption of individual ions?

### Beyond mixed salt solutions

Studying SIEs in mixed salt solutions presents challenging test cases for any prospective SIE theory. A natural extension to mixed salt systems are buffered solutions, such as those relevant to SIE in biological systems.<sup>53,175,348–350</sup> In addition to their roles in modulating pH, buffers compete with co-existing “Hofmeister ions” to influence, both cooperatively and independently, enzyme activities, electrophoretic mobilities, antibody aggregation and protein thermal stability. The screening and competitive behaviour of buffers has recently been modelled, showing the importance of ionic strength in this respect.<sup>351</sup> The fact that mixed salt effects have also been studied in polyelectrolytes<sup>352,353</sup> and neutral polymer solutions (Section 5) presents alternative opportunities for studying SIEs *via* ionic surfactants, which are already known to influence mesophase behaviour in mixed salt-surfactant systems in an ion-specific way.<sup>354,355</sup> Ionic surfactants also enable systematic investigation and manipulation of SIEs, for instance by using a constant charge group with increasing aliphatic tail length (*i.e.* in order to maintain a constant Coulombic interaction between the surfactant and the solvent, while varying non-Coulombic effects).<sup>356</sup> Such approaches would be assisted by the fact that properties of ionic surfactant solutions (*e.g.*, critical micelle concentration, surface tension *etc.*) can be readily measured to assess SIE’s without requiring additional cosolutes. This also provides an additional approach to investigating specific counterion effects and SIEs in mixed salt solutions.<sup>357</sup>

### High salt concentrations

The ion specific re-entrant behaviour of polyelectrolyte solutions at high concentrations have recently been highlighted.<sup>279</sup> The mechanistic understanding of such behaviour is still limited however. There remain inconsistencies between experimental observation and theory (particularly with respects to electrostatic underscreening, Section 7). Atomistic simulation of bulk structure provides the most direct means forward for elucidating the driving forces behind this non-monotonic behaviour. Notably, simulation would enable the investigation of supersaturated regimes beyond what is experimentally accessible. In this respect, SIEs in ionic liquids provide an alternate avenue for exploring SIEs at high salt concentrations (Section 7), but also one that enables counterion effects to be negated (for instance, by matching one of the ions comprising the salt with the ions in the IL).

### Non-Coulombic effects

Coulombic interactions between ions, cosolutes and solvents play a significant role in SIEs, particularly for charge dense anions.<sup>45,128,133</sup> For larger, charge diffuse ions however, and/or more polarisable solvents/cosolutes, these Coulombic interactions

weaken, relative to competing non-covalent interactions (*viz.* dispersion, induction, exchange repulsion *etc.*). This is most obvious in long-chain tertiary ammonium salts, tetraphenyl borates, phosphonium or arsonium (Section 2.3.2). Whilst the electrostatic contributions of “Hofmeister ions” have largely been quantified and parameterised,<sup>128</sup> these non-Coulombic phenomena require further attention, as under certain circumstances they possibly account for SIE anomalies and reversals in general (Section 3). Indeed, compelling evidence of SIE understanding coming to maturity would be the ability to “turn off” or quench SIE by balancing these competing forces, *via* strategies such as surface functionalisation,<sup>184</sup> solution composition, solvent, counterion, *etc.*

### Data science approaches

The SIE field is somewhat unusual, in that data science and machine learning approaches have made relatively few in-roads to date (compared to some other fields). This is arguably because such approaches require large, accurate and consistent data sets, for instance, describing the ion solvation structure in aqueous and non-aqueous solvents. The recent development of data resources<sup>148,256</sup> to specifically address this issue therefore opens up exciting new opportunities for the field, relating to machine learning and deep learning approaches.

### Author contributions

K. P. G drafted Sections 1–3, 6, and 8 and reviewed and edited the entire manuscript. G. R. E. drafted Section 7 and reviewed the entire manuscript. H. R. drafted Section 5 and reviewed the entire manuscript. A. K. drafted Section 4. V. S. J. C. drafted Section 2.3.4. E. J. W., G. B. W., V. S. J. C and A. J. P. reviewed and edited the manuscript and acquired funding. G. G. A. reviewed Section 4 and acquired funding.

### Conflicts of interest

There are no conflicts to declare.

### Acknowledgements

The authors acknowledge Dr Saeed Moghaddam and Prof. Esben Thormann for providing data. A. J. P., G. B. W., E. J. W., V. S. J. C. and G. G. A. acknowledge Australian Research Council funding (ARC DP190100788). K. P. G. and H. R. acknowledge an Australian Government Research Training Program (RTP) Scholarship. H. R. would like to thank AINSE Ltd for providing financial assistance (Post Graduate Research Award). A. K. would like to acknowledge Flinders University for providing financial support through Flinders University International Tuition Fee Sponsorship and Australian Research Council (ARC DP190100788) for funding the HDR Scholarship.



## Notes and references

1 S. Lee and M. Elimelech, Salt cleaning of organic-fouled reverse osmosis membranes, *Water Res.*, 2007, **41**, 1134–1142.

2 H. Lee, S. J. Im, H. Lee, C. M. Kim and A. Jang, Comparative analysis of salt cleaning and osmotic backwash on calcium-bridged organic fouling in nanofiltration process, *Desalination*, 2021, **507**, 115022.

3 B. Zhang, X. Wang and X. Jia, Research on the mechanism of molten salt cleaning (MSC) for multiple contaminants in cylinder covers, *J. Cleaner Prod.*, 2021, **302**, 126990.

4 X. Wang, J. Li, L. Wang, X. Jia, M. Hong, Y. Ren and M. Ma, A novel de-rusting method with molten salt precleaning and laser cleaning for the recycling of steel parts, *Clean Technol. Environ. Policy*, 2021, **23**, 1403–1414.

5 S. Madeswaran and S. Jayachandran, Sodium bicarbonate: a review and its uses in dentistry, *Indian J. Dent. Res.*, 2018, **29**, 672–677.

6 N. K. Fageria, M. P.-B. Filho, A. Moreira and C. M. Guimarães, Foliar Fertilization of Crop Plants, *J. Plant Nutr.*, 2009, **32**, 1044–1064.

7 A. Eftekhari, Potassium secondary cell based on Prussian blue cathode, *J. Power Sources*, 2004, **126**, 221–228.

8 K. Xu, Electrolytes and interphases in Li-ion batteries and beyond, *Chem. Rev.*, 2014, **114**, 11503–11618.

9 D. Aurbach, Y. Talyosef, B. Markovsky, E. Markevich, E. Zinigrad, L. Asraf, J. S. Gnanaraj and H.-J. Kim, Design of electrolyte solutions for Li and Li-ion batteries: a review, *Electrochim. Acta*, 2004, **50**, 247–254.

10 S. Li, H. Li, F. N. Hu, X. R. Huang, D. T. Xie and J. P. Ni, Effects of strong ionic polarization in the soil electric field on soil particle transport during rainfall, *Eur. J. Soil Sci.*, 2015, **66**, 921–929.

11 W. Ding, X. Liu, F. Hu, H. Zhu, Y. Luo, S. Li and H. Li, How the particle interaction forces determine soil water infiltration: specific ion effects, *J. Hydrol.*, 2019, **568**, 492–500.

12 S. Wu, C. Zhu, Z. He, H. Xue, Q. Fan, Y. Song, J. S. Francisco, X. C. Zeng and J. Wang, Ion-specific ice recrystallization provides a facile approach for the fabrication of porous materials, *Nat. Commun.*, 2017, **8**, 15154.

13 V. S.-J. Craig, B. W. Ninham and R. M. Pashley, Effect of electrolytes on bubble coalescence, *Nature*, 1993, **364**, 317–319.

14 C. L. Henry and V. S.-J. Craig, The Link between Ion Specific Bubble Coalescence and Hofmeister Effects Is the Partitioning of Ions within the Interface, *Langmuir*, 2010, **26**, 6478–6483.

15 R. Tian, X. Liu, X. Gao, R. Li and H. Li, Observation of specific ion effects in humus aggregation process, *Pedosphere*, 2021, **31**, 736–745.

16 J. C. Warren and S. G. Cheatum, Effect of Neutral Salts on Enzyme Activity and Structure\*, *Biochemistry*, 1966, **5**, 1702–1707.

17 M. Hayashi, T. Unemoto and M. Hayashi, pH- and anion-dependent salt modifications of alkaline phosphatase from a slightly halophilic *Vibrio alginolyticus*, *Biochim. Biophys. Acta, Enzymol.*, 1973, **315**, 83–93.

18 V. Štěpánková, J. Paterová, J. Damborský, P. Jungwirth, R. Chaloupková and J. Heyda, Cation-Specific Effects on Enzymatic Catalysis Driven by Interactions at the Tunnel Mouth, *J. Phys. Chem. B*, 2013, **117**, 6394.

19 K. Garajová, A. Balogová, E. Dušeková, D. Sedláková, E. Sedláček and R. Varhač, Correlation of lysozyme activity and stability in the presence of Hofmeister series anions, *Biochim. Biophys. Acta, Proteins Proteomics*, 2017, **1865**, 281–288.

20 E. M. Wright and J. M. Diamond, Anion selectivity in biological systems, *Physiol. Rev.*, 1977, **57**, 109–156.

21 M. G. Cacace, E. M. Landau and J. J. Ramsden, The Hofmeister Series: Salt and Solvent Effects on Interfacial Phenomena, *Q. Rev. Biophys.*, 1997, **30**, 241.

22 Q. M. Wang and R. B. Johnson, Activation of Human Rhinovirus-14 3C Protease, *Virology*, 2001, **280**, 80–86.

23 A. Salis, D. Bilaničová, B. W. Ninham and M. Monduzzi, Hofmeister Effects in Enzymatic Activity: Weak and Strong Electrolyte Influences on the Activity of *Candida rugosa* Lipase, *J. Phys. Chem. B*, 2007, **111**, 1149.

24 D. Bilaničová, A. Salis, B. W. Ninham and M. Monduzzi, Specific Anion Effects on Enzymatic Activity in Nonaqueous Media, *J. Phys. Chem. B*, 2008, **112**, 12066–12072.

25 Y. Zhang and P. S. Cremer, The inverse and direct Hofmeister series for lysozyme, *Proc. Natl. Acad. Sci. U. S. A.*, 2009, **106**, 15249–15253.

26 C. Carucci, F. Raccis, A. Salis and E. Magner, Specific ion effects on the enzymatic activity of alcohol dehydrogenase from *Saccharomyces cerevisiae*, *Phys. Chem. Chem. Phys.*, 2020, **22**, 6749–6754.

27 M. Collu, C. Carucci and A. Salis, Specific Anion Effects on Lipase Adsorption and Enzymatic Synthesis of Biodiesel in Nonaqueous Media, *Langmuir*, 2020, **36**, 9465–9471.

28 A. Somasundar, S. Ghosh, F. Mohajerani, L. N. Massenburg, T. Yang, P. S. Cremer, D. Velegol and A. Sen, Positive and negative chemotaxis of enzyme-coated liposome motors, *Nat. Nanotechnol.*, 2019, **14**, 1129–1134.

29 P. Lo Nstro and B. W. Ninham, Hofmeister phenomena: an update on ion specificity in biology, *Chem. Rev.*, 2012, **112**, 2286–2322.

30 J. Del Coso, E. Estevez, R. A. Baquero and R. Mora-Rodriguez, Anaerobic performance when rehydrating with water or commercially available sports drinks during prolonged exercise in the heat, *Appl. Physiol. Nutr. Metab.*, 2008, **33**, 290–298.

31 F. Hofmeister, Zur Lehre Von Der Wirkung Der Salze, *Naunyn-Schmiedeberg's Arch. Pharmacol.*, 1888, **24**, 247.

32 W. Kunz, J. Henle and B. W. Ninham, 'Zur Lehre von der Wirkung der Salze' (about the science of the effect of salts): Franz Hofmeister's historical papers, *Curr. Opin. Colloid Interface Sci.*, 2004, **9**, 19–37.

33 H. I. Okur, J. Hladíková, K. B. Rembert, Y. Cho, J. Heyda, J. Dzubiella, P. S. Cremer and P. Jungwirth, Beyond the Hofmeister Series: Ion-Specific Effects on Proteins and Their Biological Functions, *J. Phys. Chem. B*, 2017, **121**, 1997–2014.

34 Y. J. Zhang, S. Furyk, D. E. Bergbreiter and P. S. Cremer, Specific Ion Effects on the Water Solubility of Macromolecules:



PNIPAM and the Hofmeister Series, *J. Am. Chem. Soc.*, 2005, **127**, 14505.

35 T. J. Murdoch, B. A. Humphreys, J. D. Willott, K. P. Gregory, S. W. Prescott, A. Nelson, E. J. Wanless and G. B. Webber, Specific Anion Effects on the Internal Structure of a Poly(N-isopropylacrylamide) Brush, *Macromolecules*, 2016, **49**, 6050–6060.

36 B. A. Humphreys, J. D. Willott, T. J. Murdoch, G. B. Webber and E. J. Wanless, Specific ion modulated thermoresponse of poly(N-isopropylacrylamide) brushes, *Phys. Chem. Chem. Phys.*, 2016, **18**, 6037–6046.

37 T. J. Murdoch, B. A. Humphreys, E. C. Johnson, G. B. Webber and E. J. Wanless, Specific ion effects on thermo-responsive polymer brushes: comparison to other architectures, *J. Colloid Interface Sci.*, 2018, **526**, 429–450.

38 B. A. Humphreys, E. J. Wanless and G. B. Webber, Effect of ionic strength and salt identity on poly(N-isopropylacrylamide) brush modified colloidal silica particles, *J. Colloid Interface Sci.*, 2018, **516**, 153–161.

39 N. Peruzzi, B. W. Ninham, P. Lo Nostro and P. Baglioni, Hofmeister Phenomena in Nonaqueous Media: The Solubility of Electrolytes in Ethylene Carbonate, *J. Phys. Chem. B*, 2012, **116**, 14398–14405.

40 L. Liu, T. Wang, C. Liu, K. Lin, G. Liu and G. Zhang, Specific Anion Effect in Water–Nonaqueous Solvent Mixtures: Interplay of the Interactions between Anion, Solvent, and Polymer, *J. Phys. Chem. B*, 2013, **117**, 10936–10943.

41 V. Mazzini and V. S. J. Craig, Specific-ion effects in non-aqueous systems, *Curr. Opin. Colloid Interface Sci.*, 2016, **23**, 82–93, DOI: [10.1016/j.cocis.2016.06.009](https://doi.org/10.1016/j.cocis.2016.06.009).

42 V. Mazzini and V. S.-J. Craig, What is the fundamental ion-specific series for anions and cations? Ion specificity in standard partial molar volumes of electrolytes and electrostriction in water and non-aqueous solvents, *Chem. Sci.*, 2017, **8**, 7052–7065.

43 V. Mazzini, G. Liu and V. S.-J. Craig, Probing the Hofmeister series beyond water: specific-ion effects in non-aqueous solvents, *J. Chem. Phys.*, 2018, **148**, 222805.

44 V. Mazzini and V. S.-J. Craig, Volcano Plots Emerge from a Sea of Nonaqueous Solvents: The Law of Matching Water Affinities Extends to All Solvents, *ACS Cent. Sci.*, 2018, **4**, 1056–1064.

45 K. P. Gregory, G. B. Webber, E. J. Wanless and A. J. Page, Lewis Strength Determines Specific-Ion Effects in Aqueous and Non-aqueous Solvents, *J. Phys. Chem. A*, 2019, **123**, 6420–6429.

46 A. Voet, Quantitative lyotropy, *Chem. Rev.*, 1937, **20**, 169.

47 V. Mazzini and V. S. J. Craig, Corrigendum to “Specific-ion Effects in Non-Aqueous Systems”, *Curr. Opin. Colloid Interface Sci.*, 2018, **38**, 214–222.

48 R. G. Pearson, Hard and soft acids and bases, *J. Am. Chem. Soc.*, 1963, **85**, 3533–3539.

49 A. Serr and R. R. Netz, Polarizabilities of hydrated and free ions derived from DFT calculations, *Int. J. Quantum Chem.*, 2006, **106**, 2960–2974.

50 T. Zemb, L. Belloni, M. Dubois, A. Aroti and E. Leontidis, Can we use area per surfactant as a quantitative test model of specific ion effects?, *Curr. Opin. Colloid Interface Sci.*, 2004, **9**, 74–80.

51 A. P. dos Santos, A. Diehl and Y. Levin, Surface Tensions, Surface Potentials, and the Hofmeister Series of Electrolyte Solutions, *Langmuir*, 2010, **26**, 10778–10783.

52 K. Wojciechowski, A. Bitner, P. Warszyński and M. Żubrowska, The Hofmeister effect in zeta potentials of CTAB-stabilised toluene-in-water emulsions, *Colloids Surf. A*, 2011, **376**, 122–126.

53 F. Cugia, S. Sedda, F. Pitzalis, D. F. Parsons, M. Monduzzi and A. Salis, Are specific buffer effects the new frontier of Hofmeister phenomena? Insights from lysozyme adsorption on ordered mesoporous silica, *RSC Adv.*, 2016, **6**, 94617–94621.

54 J. Heyda and J. Dzubiella, Thermodynamic Description of Hofmeister Effects on the LCST of Thermosensitive Polymers, *J. Phys. Chem. B*, 2014, **118**, 10979.

55 I. Shechter, O. Ramon, I. Portnaya, Y. Paz and Y. D. Livney, Microcalorimetric Study of the Effects of a Chaotropic Salt, Kscn, on the Lower Critical Solution Temperature (LCST) of Aqueous Poly(N-Isopropylacrylamide) (PNIPA) Solutions, *Macromolecules*, 2010, **43**, 480.

56 Y. Zhang, S. Furyk, L. B. Sagle, Y. Cho, D. E. Bergbreiter and P. S. Cremer, Effects of Hofmeister Anions on the LCST of PNIPAM as a Function of Molecular Weight, *J. Phys. Chem. C*, 2007, **111**, 8916.

57 K. D. Collins, Ions from the Hofmeister series and osmolytes: effects on proteins in solution and in the crystallization process, *Methods*, 2004, **34**, 300–311.

58 M. Boström, D. R.-M. Williams, P. R. Stewart and B. W. Ninham, Hofmeister effects in membrane biology: the role of ionic dispersion potentials, *Phys. Rev. E: Stat., Nonlinear, Soft Matter Phys.*, 2003, **68**, 41902.

59 A. P. Davis, D. N. Sheppard and B. D. Smith, Development of synthetic membrane transporters for anions, *Chem. Soc. Rev.*, 2007, **36**, 348–357.

60 B. W. Ninham and V. Yaminsky, Ion Binding and Ion Specificity: The Hofmeister Effect and Onsager and Lifshitz Theories, *Langmuir*, 1997, **13**, 2097–2108.

61 M. Boström, F. W. Tavares, S. Finet, F. Skouri-Panet, A. Tardieu and B. W. Ninham, Why forces between proteins follow different Hofmeister series for pH above and below pI, *Biophys. Chem.*, 2005, **117**, 217–224.

62 L. Abezgauz, K. Kuperkar, P. A. Hassan, O. Ramon, P. Bahadur and D. Danino, Effect of Hofmeister anions on micellization and micellar growth of the surfactant cetylpyridinium chloride, *J. Colloid Interface Sci.*, 2010, **342**, 83–92.

63 W. M. Cox and J. H. Wolfenden, Viscosity of Strong Electrolytes Measured by a Differential Method, *Proc. R. Soc. London, Ser. A*, 1934, **145**, 475.

64 G. Jones and M. Dole, The Viscosity of Aqueous Solutions of Strong Electrolytes with Special Reference to Barium Chloride, *J. Am. Chem. Soc.*, 1929, **51**, 2950–2964.

65 A. A. Zavitsas, Properties of Water Solutions of Electrolytes and Nonelectrolytes, *J. Phys. Chem. B*, 2001, **105**, 7805–7817.



66 Y. Marcus, *Ions in Solution and their Solvation*, 2015.

67 G. E. Holm and J. M. Sherman, Salt Effects in Bacterial Growth, *J. Bacteriol.*, 1921, **6**, 511–519.

68 P. Lo Nstro, L. Fratoni, B. W. Ninham and P. Baglioni, Water Absorbency by Wool Fibers: Hofmeister Effect, *Biomacromolecules*, 2002, **3**, 1217–1224.

69 M. Boström, D. R.-M. Williams and B. W. Ninham, The Influence of Ionic Dispersion Potentials on Counterion Condensation on Polyelectrolytes, *J. Phys. Chem. B*, 2002, **106**, 7908–7912.

70 H. P. Gregor and M. Frederick, Potentiometric titration of polyacrylic and polymethacrylic acids with alkali metal and quaternary ammonium bases, *J. Polym. Sci.*, 1957, **23**, 451–465.

71 A. V. Toktarev and G. V. Echevskii, Hofmeister Anion Effect on the Formation of Zeolite Beta, *Stud. Surf. Sci. Catal.*, 2008, **174**, 167–172.

72 E. Leontidis, Hofmeister anion effects on surfactant self-assembly and the formation of mesoporous solids, *Curr. Opin. Colloid Interface Sci.*, 2002, **7**, 81–91.

73 F. Urban, The Influence of Electrolytes on the Specific Heat of Water, *J. Phys. Chem.*, 1931, **36**, 1108–1122.

74 T. López-León, A. B. Jódar-Reyes, J. L. Ortega-Vinuesa and D. Bastos-González, Hofmeister effects on the colloidal stability of an IgG-coated polystyrene latex, *J. Colloid Interface Sci.*, 2005, **284**, 139–148.

75 W. Melander and C. Horváth, Salt effects on hydrophobic interactions in precipitation and chromatography of proteins: an interpretation of the lyotropic series, *Arch. Biochem. Biophys.*, 1977, **183**, 200–215.

76 G. Graziano, Salting out of methane by sodium chloride: a scaled particle theory study, *J. Chem. Phys.*, 2008, **129**, 84506.

77 A. Pica and G. Graziano, On the effect of sodium salts on the coil-to-globule transition of poly(*N*-isopropylacrylamide), *Phys. Chem. Chem. Phys.*, 2015, **17**, 27750–27757.

78 A. Pica and G. Graziano, Effect of sodium thiocyanate and sodium perchlorate on poly(*N*-isopropylacrylamide) collapse, *Phys. Chem. Chem. Phys.*, 2020, **22**, 189–195.

79 R. L. Baldwin, How Hofmeister Ion Interactions Affect Protein Stability, *Biophys. J.*, 1996, **71**, 2056.

80 B. A. Rogers, H. I. Okur, C. Yan, T. Yang, J. Heyda and P. S. Cremer, Weakly hydrated anions bind to polymers but not monomers in aqueous solutions, *Nat. Chem.*, 2022, **14**, 40–45.

81 K. D. Collins, Charge Density-Dependent Strength of Hydration and Biological Structure, *Biophys. J.*, 1997, **72**, 65.

82 A. Salis and B. W. Ninham, Models and mechanisms of Hofmeister effects in electrolyte solutions, and colloid and protein systems revisited, *Chem. Soc. Rev.*, 2014, **43**, 7358–7377.

83 K. D. Collins, G. W. Neilson and J. E. Enderby, Ions in Water: Characterizing the Forces That Control Chemical Processes and Biological Structure, *Biophys. Chem.*, 2007, **128**, 95.

84 J. S. Uejio, C. P. Schwartz, A. M. Duffin, W. S. Drisdell, R. C. Cohen and R. J. Saykally, Characterization of Selective Binding of Alkali Cations with Carboxylate by X-Ray Absorption Spectroscopy of Liquid Microjets, *Proc. Natl. Acad. Sci. U. S. A.*, 2008, **105**, 6809.

85 E. F. Aziz, N. Ottosson, S. Eisebitt, W. Eberhardt, B. Jagoda-Cwiklik, R. Vacha, P. Jungwirth and B. Winter, Cation-Specific Interactions with Carboxylate in Amino Acid and Acetate Aqueous Solutions: X-Ray Absorption and Ab Initio Calculations, *J. Phys. Chem. B*, 2008, **112**, 12567.

86 I. Kalcher, D. Horinek, R. R. Netz and J. Dzubiella, Ion Specific Correlations in Bulk and at Biointerfaces, *J. Phys.: Condens. Matter*, 2009, **21**, 424108.

87 B. Hess and N. F.-A. van der Vegt, Cation Specific Binding with Protein Surface Charges, *Proc. Natl. Acad. Sci. U. S. A.*, 2009, **106**, 13296.

88 J. Heyda, T. Hrobarik and P. Jungwirth, Ion-Specific Interactions between Halides and Basic Amino Acids in Water, *J. Phys. Chem. A*, 2009, **113**, 1969.

89 J. Heyda, J. C. Vincent, D. J. Tobias, J. Dzubiella and P. Jungwirth, Ion Specificity at the Peptide Bond: Molecular Dynamics Simulations of *N*-Methylacetamide in Aqueous Salt Solutions, *J. Phys. Chem. B*, 2010, **114**, 1213.

90 E. A. Algaer and N. F.-A. van der Vegt, Hofmeister Ion Interactions with Model Amide Compounds, *J. Phys. Chem. B*, 2011, **115**, 13781.

91 K. B. Rembert, J. Paterova, J. Heyda, C. Hilty, P. Jungwirth and P. S. Cremer, Molecular Mechanisms of Ion-Specific Effects on Proteins, *J. Am. Chem. Soc.*, 2012, **134**, 10039.

92 H. I. Okur, J. Kherb and P. S. Cremer, Cations Bind Only Weakly to Amides in Aqueous Solutions, *J. Am. Chem. Soc.*, 2013, **135**, 5062.

93 P. Jungwirth and P. S. Cremer, Beyond Hofmeister, *Nat. Chem.*, 2014, **6**, 261.

94 T. O. Street, D. W. Bolen and G. D. Rose, A Molecular Mechanism for Osmolyte-Induced Protein Stability, *Proc. Natl. Acad. Sci. U. S. A.*, 2006, **103**, 13997.

95 L. Vrbka, P. Jungwirth, P. Bauduin, D. Touraud and W. Kunz, Specific Ion Effects at Protein Surfaces: A Molecular Dynamics Study of Bovine Pancreatic Trypsin Inhibitor and Horseradish Peroxidase in Selected Salt Solutions, *J. Phys. Chem. B*, 2006, **110**, 7036.

96 R. M. Leberman and A. M. Soper, Effect of high salt concentrations on water structure, *Nature*, 1995, **378**, 364–366.

97 I. Waluyo, D. Nordlund, U. Bergmann, D. Schlesinger, L. G.-M. Pettersson and A. Nilsson, A different view of structure-making and structure-breaking in alkali halide aqueous solutions through x-ray absorption spectroscopy, *J. Chem. Phys.*, 2014, **140**, 244506.

98 A. W. Omta, M. F. Kropman, S. Woutersen and H. J. Bakker, Negligible Effect of Ions on the Hydrogen-Bond Structure in Liquid Water, *Science*, 2003, **301**, 347.

99 S. Funkner, G. Niehues, D. A. Schmidt, M. Heyden, G. Schwaab, K. M. Callahan, D. J. Tobias and M. Havenith, Watching the Low-Frequency Motions in Aqueous Salt Solutions: The Terahertz Vibrational Signatures of Hydrated Ions, *J. Am. Chem. Soc.*, 2012, **134**, 1030.



100 G. Stirnemann, E. Wernersson, P. Jungwirth and D. Laage, Mechanisms of Acceleration and Retardation of Water Dynamics by Ions, *J. Am. Chem. Soc.*, 2013, **135**, 11824.

101 K. J. Tielrooij, N. Garcia-Araez, M. Bonn and H. J. Bakker, Cooperativity in Ion Hydration, *Science*, 2010, **328**, 1006–1009.

102 V. A. Parsegian, *van der Waals Forces: A handbook for biologists, chemists, engineers, and physicists*, 2006.

103 A. P. Gaiduk and G. Galli, Local and Global Effects of Dissolved Sodium Chloride on the Structure of Water, *J. Phys. Chem. Lett.*, 2017, **8**, 1496–1502.

104 M. F. Kropman and H. J. Bakker, Dynamics of water molecules in aqueous solvation shells, *Science*, 2001, **291**, 2118–2120.

105 H. Dongshuai, L. Zeyu, Z. Peng and D. Qingjun, Molecular structure and dynamics of an aqueous sodium chloride solution in nano-pores between portlandite surfaces: a molecular dynamics study, *Phys. Chem. Chem. Phys.*, 2016, **18**, 2059–2069.

106 M. Kelley, A. Donley, S. Clark and A. Clark, Structure and Dynamics of NaCl Ion Pairing in Solutions of Water and Methanol, *J. Phys. Chem. B*, 2015, **119**, 15652–15661.

107 M. Born, Volumen und hydratationswärme der ionen, *Zeitschrift für Phys.*, 1920, **1**, 45–48.

108 U. Mayer and V. Gutmann, *Phenomenological approach to cation-solvent interactions, Structure and Bonding*, Springer Berlin Heidelberg, Berlin, Heidelberg, 1972, vol. 12, pp. 113–140.

109 P. Debye and E. Hückel, Debye–Hückel theory of electrolytes, *Phys. Z.*, 1923, **24**, 185.

110 B. Derjaguin and L. Landau, Theory of the stability of strongly charged lyophobic sols and of the adhesion of strongly charged particles in solutions of electrolytes, *Prog. Surf. Sci.*, 1993, **43**, 30–59.

111 E. J.-W. Verwey, Theory of the Stability of Lyophobic Colloids, *J. Phys. Colloid Chem.*, 1947, **51**, 631–636.

112 E. J.-W. Verwey and J. T.-G. Overbeek, Theory of the stability of lyophobic colloids, *J. Colloid Sci.*, 1955, **10**, 224–225.

113 B. W. Ninham, R. M. Pashley and P. Lo Nostro, Surface forces: changing concepts and complexity with dissolved gas, bubbles, salt and heat, *Curr. Opin. Colloid Interface Sci.*, 2017, **27**, 25–32.

114 G. M. Kontogeorgis, B. Maribo-Mogensen and K. Thomsen, The Debye–Hückel theory and its importance in modeling electrolyte solutions, *Fluid Phase Equilib.*, 2018, **462**, 130–152.

115 R. H. Stokes and R. A. Robinson, Ionic hydration and activity in electrolyte solutions, *J. Am. Chem. Soc.*, 1948, **70**, 1870–1878.

116 E. A. Guggenheim and J. C. Turgeon, Specific interaction of ions, *Trans. Faraday Soc.*, 1955, **51**, 747–761.

117 P. Sipos, Application of the Specific Ion Interaction Theory (SIT) for the ionic products of aqueous electrolyte solutions of very high concentrations, *J. Mol. Liq.*, 2008, **143**, 13–16.

118 K. S. Pitzer, Thermodynamics of electrolytes. I. Theoretical basis and general equations, *J. Phys. Chem.*, 1973, **77**, 268–277.

119 C. Akilan, T. Chen, T. Vielma, P. M. May, G. Senanayake and G. Hefter, Volumes and Heat Capacities of Cobalt(II), Nickel(II), and Copper(II) Sulfates in Aqueous Solution, *J. Chem. Eng. Data*, 2020, **65**, 4575–4581.

120 H. T. Kim and W. J. Frederick, Evaluation of Pitzer Ion Interaction Parameters of Aqueous Electrolytes at 25 °C. 1. Single Salt Parameters, *J. Chem. Eng. Data*, 1988, **33**, 177–184.

121 A. Lach, L. André, S. Guignot, C. Christov, P. Henocq and A. Lassin, A Pitzer Parametrization To Predict Solution Properties and Salt Solubility in the H–Na–K–Ca–Mg–NO<sub>3</sub>–H<sub>2</sub>O System at 298.15 K, *J. Chem. Eng. Data*, 2018, **63**, 787–800.

122 C. F. Weber, Calculation of Pitzer Parameters at High Ionic Strengths, *Ind. Eng. Chem. Res.*, 2000, **39**, 4422–4426.

123 B. W. Ninham, T. T. Duignan and D. F. Parsons, Approaches to hydration, old and new: insights through Hofmeister effects, *Curr. Opin. Colloid Interface Sci.*, 2011, **16**, 612–617.

124 W. Kunz, P. L. Nostro, B. W. Ninham, P. Lo Nostro and B. W. Ninham, The present state of affairs with Hofmeister effects, *Curr. Opin. Colloid Interface Sci.*, 2004, **9**, 1.

125 R. Heyrovská, Physical Electrochemistry of Strong Electrolytes Based on Partial Dissociation and Hydration Quantitative Interpretation of the Thermodynamic Properties of NaCl(aq) from “Zero to Saturation”, *J. Electrochem. Soc.*, 1996, **143**, 1789–1793.

126 K. D. Collins and M. W. Washabaugh, The Hofmeister Effect and the Behaviour of Water at Interfaces, *Q. Rev. Biophys.*, 1985, **18**, 323.

127 J. M. Berg, J. L. Tymoczko, G. J. Gatto, and L. Stryer, *Biochemistry*, W.H. Freeman & Company, a Macmillan Education Imprint, New York, Eighth edn, 1958.

128 K. P. Gregory, E. J. Wanless, G. B. Webber, V. S.-J. Craig and A. J. Page, The electrostatic origins of specific ion effects: quantifying the Hofmeister series for anions, *Chem. Sci.*, 2021, **12**, 15007–15015.

129 E. Leontidis, Investigations of the Hofmeister series and other specific ion effects using lipid model systems, *Adv. Colloid Interface Sci.*, 2017, **243**, 8–22.

130 T. T. Duignan, D. F. Parsons and B. W. Ninham, Collins's rule, Hofmeister effects and ionic dispersion interactions, *Chem. Phys. Lett.*, 2014, **608**, 55–59.

131 T. P. Pollard and T. L. Beck, Toward a quantitative theory of Hofmeister phenomena: from quantum effects to thermodynamics, *Curr. Opin. Colloid Interface Sci.*, 2016, **23**, 110–118.

132 T. T. Duignan, D. F. Parsons and B. W. Ninham, A Continuum Solvent Model of the Multipolar Dispersion Solvation Energy, *J. Phys. Chem. B*, 2013, **117**, 9412–9420.

133 R. Prasanna Misra and D. Blankschtein, Uncovering a Universal Molecular Mechanism of Salt Ion Adsorption at Solid/Water Interfaces, *Langmuir*, 2021, **37**, 722–733.



134 A. Stone, *The theory of intermolecular forces*, oUP oxford, 2013.

135 D. F. Parsons and B. W. Ninham, Ab Initio Molar Volumes and Gaussian Radii, *J. Phys. Chem. A*, 2009, **113**, 1141–1150.

136 I. Fridovich, Inhibition of Acetoacetic Decarboxylase by Anions THE HOFMEISTER LYOTROPIC SERIES, *J. Biol. Chem.*, 1963, **238**, 592–598.

137 D. A. Doyle, J. M. Cabral, R. A. Pfuetzner, A. Kuo, J. M. Gulbis, S. L. Cohen, B. T. Chait and R. MacKinnon, The Structure of the Potassium Channel: Molecular Basis of  $K^+$  Conduction and Selectivity, *Science*, 1998, **280**, 69–77.

138 B. Hille, C. M. Armstrong and R. MacKinnon, Ion channels: from idea to reality, *Nat. Med.*, 1999, **5**, 1105–1109.

139 K. Dabrowa, F. Ulatowski, D. Lichosyt and J. Jurczak, Catching the chloride: searching for non-Hofmeister selectivity behavior in systematically varied polyamide macrocyclic receptors, *Org. Biomol. Chem.*, 2017, **15**, 5927–5943.

140 Y. Marcus, The thermodynamics of solvation of ions. Part 4.—Application of the tetraphenylarsonium tetraphenylborate (TATB) extrathermodynamic assumption to the hydration of ions and to properties of hydrated ions, *J. Chem. Soc., Faraday Trans. 1*, 1987, **83**, 2985–2992.

141 J. L.-M. Poiseuille, Experimental Investigations on the Flow of Liquids in Tubes of Very Small Diameter, *Ann. Chim. Phys.*, 1847, **21**, 76.

142 H. S. Frank and M. W. Evans, Free Volume and Entropy in Condensed Systems III. Entropy in Binary Liquid Mixtures; Partial Molal Entropy in Dilute Solutions; Structure and Thermodynamics in Aqueous Electrolytes, *J. Chem. Phys.*, 1945, **13**, 507–532.

143 G. A. Krestov, *Thermodynamics of solvation*, 1991.

144 R. W. Gurney, *Ionic Processes in Solution*, 1953.

145 E. R. Nightingale Jr, Phenomenological theory of ion solvation. Effective radii of hydrated ions, *J. Phys. Chem.*, 1959, **63**, 1381–1387.

146 E. Asmus, Zur Frage des B-Koeffizienten der Jones-Dole-Gleichung, *Zeitschrift für Naturforsch. A*, 1949, **4**, 589–594.

147 H. D.-B. Jenkins and Y. Marcus, Viscosity B-Coefficients of Ions in Solution, *Chem. Rev.*, 1995, **95**, 2695–2724.

148 V. Mazzini and V. S.-J. Craig, Solubility of 1:1 electrolytes in water and non-aqueous solvents, Australian National University, 2019, DOI: [10.25911/5ca429ccb08a2](https://doi.org/10.25911/5ca429ccb08a2).

149 S. J. Hawkes, Salts are Mostly NOT Ionized, *J. Chem. Educ.*, 1996, **73**, 421.

150 A. A. Chen and R. V. Pappu, Quantitative Characterization of Ion Pairing and Cluster Formation in Strong 1:1 Electrolytes, *J. Phys. Chem. B*, 2007, **111**, 6469–6478.

151 J. Gujt, M. Bešter-Rogač and B. Hribar-Lee, An investigation of ion-pairing of alkali metal halides in aqueous solutions using the electrical conductivity and the Monte Carlo computer simulation methods, *J. Mol. Liq.*, 2014, **190**, 34–41.

152 H. Ohtaki, Dissolution and nucleation phenomena of salts in water. Molecular dynamic approaches and supporting solution X-ray diffraction measurements, *Pure Appl. Chem.*, 1993, **65**, 203.

153 A. D. Pethybridge and D. J. Spiers, Conductance of some alkali metal halides in dilute aqueous solution at 25 °C, *J. Chem. Soc., Faraday Trans. 1*, 1977, **73**, 768–775.

154 G. N. Lewis, The activity of the ions and the degree of dissociation of strong electrolytes, *J. Am. Chem. Soc.*, 1912, **34**, 1631–1644.

155 R. Heyrovská, Degrees of Dissociation and Hydration Numbers of Alkali Halides in Aqueous Solutions at 25 °C (Some up to Saturation), *Croat. Chem. Acta*, 1997, **70**, 39–54.

156 R. Heyrovská, Solution phase thermodynamics of strong electrolytes based on ionic concentrations, hydration numbers and volumes of dissolved entities, *Struct. Chem.*, 2013, **24**, 1895–1901.

157 Y. Shi and T. Beck, Deconstructing Free Energies in the Law of Matching Water Affinities, *J. Phys. Chem. B*, 2017, **121**, 2189–2201.

158 L. A. Moreira, M. Boström, B. W. Ninham, E. C. Biscaia and F. W. Tavares, Hofmeister effects: Why protein charge, pH titration and protein precipitation depend on the choice of background salt solution, *Colloids Surf., A*, 2006, **282–283**, 457–463.

159 E. E. Bruce and N. F.-A. van der Vegt, Does an electronic continuum correction improve effective short-range ion–ion interactions in aqueous solution?, *J. Chem. Phys.*, 2018, **148**, 222816.

160 E. E. Bruce, P. T. Bui, B. A. Rogers, P. S. Cremer and N. F.-A. A. Van Der Vegt, Nonadditive Ion Effects Drive Both Collapse and Swelling of Thermoresponsive Polymers in Water, *J. Am. Chem. Soc.*, 2019, **141**, 6609–6616.

161 E. E. Bruce, H. I. Okur, S. Stegmaier, C. I. Drexler, B. A. Rogers, N. F.-A. van der Vegt, S. Roke and P. S. Cremer, Molecular Mechanism for the Interactions of Hofmeister Cations with Macromolecules in Aqueous Solution, *J. Am. Chem. Soc.*, 2020, **142**, 19094–19100.

162 E. E. Bruce, P. T. Bui, M. Cao, P. S. Cremer and N. F.-A. Van Der Vegt, Contact Ion Pairs in the Bulk Affect Anion Interactions with Poly(N-isopropylacrylamide), *J. Phys. Chem. B*, 2021, **125**, 680–688.

163 P. T. Bui and P. S. Cremer, Cation Identity Affects Non-additivity in Salt Mixtures Containing Iodide and Sulfate, *J. Solution Chem.*, 2021, **50**, 1443–1456.

164 K. D. Judd, N. M. Gonzalez, T. Yang and P. S. Cremer, Contact Ion Pair Formation Is Not Necessarily Stronger than Solvent Shared Ion Pairing, *J. Phys. Chem. Lett.*, 2022, **13**, 923–930.

165 Y. Marcus and G. Hefter, Ion pairing, *Chem. Rev.*, 2006, **106**, 4585–4621.

166 S. Ahrland, J. Chatt and N. R. Davies, The relative affinities of ligand atoms for acceptor molecules and ions, *Q. Rev., Chem. Soc.*, 1958, **12**, 265–276.

167 R. G. Pearson, Hard and soft acids and bases, HSAB, part 1: Fundamental principles, *J. Chem. Educ.*, 1968, **45**, 581.

168 Y. Marcus, Linear solvation energy relationships. Correlation and prediction of the distribution of organic solutes between water and immiscible organic solvents, *J. Phys. Chem.*, 1991, **95**, 8886–8891.



169 R. Alain Miranda-Quintana and J. Smiatek, Electronic Properties of Protein Destabilizers and Stabilizers: Implications for Preferential Binding and Exclusion Mechanisms, *J. Phys. Chem. B*, 2021, **125**, 11857–11868.

170 T. A. Gmür, A. Goel and M. A. Brown, Quantifying Specific Ion Effects on the Surface Potential and Charge Density at Silica Nanoparticle–Aqueous Electrolyte Interfaces, *J. Phys. Chem. C*, 2016, **120**, 16617–16625.

171 Q. Wen, D. Yan, F. Liu, M. Wang, Y. Ling, P. Wang, P. Kluth, D. Schauries, C. Trautmann, P. Apel, W. Guo, G. Xiao, J. Liu, J. Xue and Y. Wang, Highly Selective Ionic Transport through Subnanometer Pores in Polymer Films, *Adv. Funct. Mater.*, 2016, **26**, 5796–5803.

172 M. Boström, D. F. Parsons, A. Salis, B. W. Ninham and M. Monduzzi, Possible Origin of the Inverse and Direct Hofmeister Series for Lysozyme at Low and High Salt Concentrations, *Langmuir*, 2011, **27**, 9504–9511.

173 R. Prathapan, R. Thapa, G. Garnier and R. F. Tabor, Modulating the zeta potential of cellulose nanocrystals using salts and surfactants, *Colloids Surf. A*, 2016, **509**, 11–18.

174 A. Salis, F. Cugia, D. F. Parsons, B. W. Ninham and M. Monduzzi, Hofmeister series reversal for lysozyme by change in pH and salt concentration: insights from electrophoretic mobility measurements, *Phys. Chem. Chem. Phys.*, 2012, **14**, 4343–4346.

175 A. Salis and M. Monduzzi, Not only pH. Specific buffer effects in biological systems, *Curr. Opin. Colloid Interface Sci.*, 2016, **23**, 1–9.

176 E. C. Johnson, I. J. Gresham, S. W. Prescott, A. Nelson, E. J. Wanless and G. B. Webber, The direction of influence of specific ion effects on a pH and temperature responsive copolymer brush is dependent on polymer charge, *Polymer*, 2021, **214**, 123287.

177 R. Chudoba, J. Heyda and J. Dzubiella, Tuning the collapse transition of weakly charged polymers by ion-specific screening and adsorption, *Soft Matter*, 2018, **14**, 9631–9642.

178 J. Paterova, K. B. Rembert, J. Heyda, Y. Kurra, H. I. Okur, W. S.-R. Liu, C. Hilty, P. S. Cremer and P. Jungwirth, Reversal of the Hofmeister Series: Specific Ion Effects on Peptides, *J. Phys. Chem. B*, 2013, **117**, 8150.

179 N. Schwierz, D. Horinek and R. R. Netz, Reversed Anionic Hofmeister Series: The Interplay of Surface Charge and Surface Polarity, *Langmuir*, 2010, **26**, 7370.

180 N. Schwierz, D. Horinek, U. Sivan and R. R. Netz, Reversed Hofmeister series—The rule rather than the exception, *Curr. Opin. Colloid Interface Sci.*, 2016, **23**, 10–18.

181 G. V. Franks, Zeta Potentials and Yield Stresses of Silica Suspensions in Concentrated Monovalent Electrolytes: Isoelectric Point Shift and Additional Attraction, *J. Colloid Interface Sci.*, 2002, **249**, 44–51.

182 S. B. Johnson, G. V. Franks, P. J. Scales and T. W. Healy, The Binding of Monovalent Electrolyte Ions on  $\alpha$ -Alumina. II. The Shear Yield Stress of Concentrated Suspensions, *Langmuir*, 1999, **15**, 2844–2853.

183 D. F. Parsons, M. Boström, T. J. Maceina, A. Salis and B. W. Ninham, Why Direct or Reversed Hofmeister Series? Interplay of Hydration, Non-electrostatic Potentials, and Ion Size, *Langmuir*, 2010, **26**, 3323–3328.

184 B. Katana, D. Takács, F. D. Bobbink, P. J. Dyson, N. B. Alsharif, M. Tomšič and I. Szilagyi, Masking specific effects of ionic liquid constituents at the solid–liquid interface by surface functionalization, *Phys. Chem. Chem. Phys.*, 2020, **22**, 24764–24770.

185 W. J. Xie and Y. Q. Gao, A Simple Theory for the Hofmeister Series, *J. Phys. Chem. Lett.*, 2013, **4**, 4247.

186 G. Schwarzenbach, in *Advances in Inorganic Chemistry and Radiochemistry*, ed. H. J. Emeleus and A. G. Sharpe, Academic Press, 1961, vol. 3, pp. 257–285.

187 P. Su, Z. Jiang, Z. Chen and W. Wu, Energy Decomposition Scheme Based on the Generalized Kohn–Sham Scheme, *J. Phys. Chem. A*, 2014, **118**, 2531–2542.

188 S. Juodkazis, N. Mukai, R. Wakaki, A. Yamaguchi, S. Matsuo and H. Misawa, Reversible phase transitions in polymer gels induced by radiation forces, *Nature*, 2000, **408**, 178–181.

189 Z. Li, X. Yuan, Y. Feng, Y. Chen, Y. Zhao, H. Wang, Q. Xu and J. Wang, A reversible conductivity modulation of azobenzene-based ionic liquids in aqueous solutions using UV/vis light, *Phys. Chem. Chem. Phys.*, 2018, **20**, 12808–12816.

190 X. Chen, Z. Zhan, Q. Liu and T. Wu, Modeling the response characteristics of photo-sensitive hydrogel electrolytes in Hofmeister salt solution for the development of smart energy storage devices, *Sustain. Energy Fuels*, 2020, **4**, 6112–6124.

191 S. Wei, Z. Zhang, W. Dong, T. Liang, J. Ji, W. Tian, S. Tan, Q. Zhao, C. Wang and Y. Wu, Specific Ion Effects of Azobenzene Salts on Photoresponse of PNIPAm in Aqueous Solutions, *Macromol. Rapid Commun.*, 2021, **42**, 2100232.

192 M. Senske, D. Constantinescu-Aruxandei, M. Havenith, C. Herrmann, H. Weingärtner and S. Ebbinghaus, The temperature dependence of the Hofmeister series: thermodynamic fingerprints of cosolute–protein interactions, *Phys. Chem. Chem. Phys.*, 2016, **18**, 29698–29708.

193 E. C. Johnson, T. J. Murdoch, I. J. Gresham, B. A. Humphreys, S. W. Prescott, A. Nelson, G. B. Webber and E. J. Wanless, Temperature dependent specific ion effects in mixed salt environments on a thermoresponsive poly(oligoethylene glycol methacrylate) brush, *Phys. Chem. Chem. Phys.*, 2019, **21**, 4650–4662.

194 W. Yao, K. Wang, A. Wu, W. F. Reed and B. C. Gibb, Anion binding to ubiquitin and its relevance to the Hofmeister effects, *Chem. Sci.*, 2021, **12**, 320–330.

195 P. B. Petersen and R. J. Saykally, On the nature of ions at the liquid water surface, *Annu. Rev. Phys. Chem.*, 2006, **57**, 333–364.

196 J. H. Hu, Q. Shi, P. Davidovits, D. R. Worsnop, M. S. Zahmiser and C. E. Kolb, Reactive uptake of  $\text{Cl}_2(\text{g})$  and  $\text{Br}_2(\text{g})$  by aqueous surfaces as a function of Br- and I- ion concentration: the effect of chemical reaction at the interface, *J. Phys. Chem.*, 1995, **99**, 8768–8776.



197 P. Jungwirth and D. J. Tobias, Ions at the Air/Water Interface, *J. Phys. Chem. B*, 2002, **106**, 6361–6373.

198 P. Jungwirth and D. J. Tobias, Specific ion effects at the air/water interface, *Chem. Rev.*, 2006, **106**, 1259–1281.

199 J. M. Herbert and S. K. Paul, Interaction Energy Analysis of Monovalent Inorganic Anions in Bulk Water Versus Air/Water Interface, *Molecules*, 2021, **26**, 6719.

200 Y. Levin, Polarizable Ions at Interfaces, *Phys. Rev. Lett.*, 2009, **102**, 147803.

201 C. Jie, C. D. Vecitis, M. R. Hoffmann and A. J. Colussi, Experimental anion affinities for the air/water interface, *J. Phys. Chem. B*, 2006, **110**, 25598–25602.

202 J. Noah-Vanhoucke and P. L. Geissler, On the fluctuations that drive small ions toward, and away from, interfaces between polar liquids and their vapors, *Proc. Natl. Acad. Sci. U. S. A.*, 2009, **106**, 15125–15130.

203 J. N. Israelachvili, *Intermolecular and surface forces*, Academic press, 2015.

204 L. M. Pegram and M. T. Record, Hofmeister salt effects on surface tension arise from partitioning of anions and cations between bulk water and the air-water interface, *J. Phys. Chem. B*, 2007, **111**, 5411–5417.

205 L. M. Pegram and M. T. Record, Partitioning of atmospherically relevant ions between bulk water and the water/vapor interface, *Proc. Natl. Acad. Sci. U. S. A.*, 2006, **103**, 14278–14281.

206 L. M. Pegram and M. T. Record, Quantifying accumulation or exclusion of H<sup>+</sup>, HO<sup>–</sup>, and Hofmeister salt ions near interfaces, *Chem. Phys. Lett.*, 2008, **467**, 1–8.

207 C. L. Henry, C. N. Dalton, L. Scruton and V. S.-J. Craig, Ion-Specific Coalescence of Bubbles in Mixed Electrolyte Solutions, *J. Phys. Chem. C*, 2006, **111**, 1015–1023.

208 T. T. Duignan, The surface potential explains ion specific bubble coalescence inhibition, *J. Colloid Interface Sci.*, 2021, **600**, 338–343.

209 R. Weber, B. Winter, P. M. Schmidt, W. Widdra, I. V. Hertel, M. Dittmar and M. Faubel, Photoemission from aqueous alkali-metal– iodide salt solutions using EUV synchrotron radiation, *J. Phys. Chem. B*, 2004, **108**, 4729–4736.

210 B. Winter and M. Faubel, Photoemission from Liquid Aqueous Solutions, *Chem. Rev.*, 2006, **106**, 1176–1211.

211 O. Höftt, U. Kahnert, S. Bahr and V. Kempter, Interaction of NaI with solid water and methanol, *J. Phys. Chem. B*, 2006, **110**, 17115–17120.

212 O. Höftt, A. Borodin, U. Kahnert, V. Kempter, L. X. Dang and P. Jungwirth, Surface segregation of dissolved salt ions, *J. Phys. Chem. B*, 2006, **110**, 11971–11976.

213 G. Andersson and H. Morgner, Thermodynamics and structure of liquid surfaces investigated directly with surface analytical tools, *Rev. Artic. Ann. Phys.*, 2017, **529**, 1600230.

214 E. Sloutskin, J. Baumert, B. Ocko, I. Kuzmenko, A. Checco, L. Tamam, E. Ofer, T. Gog, O. Gang and M. Deutsch, The surface structure of concentrated aqueous salt solutions, *J. Chem. Phys.*, 2007, **126**, 54704.

215 R. R. Kumal, S. Nayak, W. Bu and A. Uysal, Chemical Potential Driven Reorganization of Anions between Stern and Diffuse Layers at the Air/Water Interface, *J. Phys. Chem. C*, 2022, **126**, 1140–1151.

216 H. Niehus and G. Comsa, Features of ion scattering spectroscopy in impact collision mode: focusing and neutralization effects; ordered and disordered structure determination, *Nucl. Instrum. Methods Phys. Res., Sect. B*, 1986, **13**, 213–217.

217 G. Andersson and H. Morgner, Impact collision ion scattering spectroscopy (ICISS) and neutral impact collision ion scattering spectroscopy (NICISS) at surfaces of organic liquids, *Surf. Sci.*, 1998, **405**, 138–151.

218 G. Andersson and H. Morgner, Investigations on solutions of tetrabutylonium salts in formamide with NICISS and ICISS: concentration depth profiles and composition of the outermost layer, *Surf. Sci.*, 2000, **445**, 89–99.

219 X. Zhao, G. M. Nathanson and G. G. Andersson, Experimental Depth Profiles of Surfactants, Ions, and Solvent at the Angstrom Scale: Studies of Cationic and Anionic Surfactants and Their Salting Out, *J. Phys. Chem. B*, 2020, **124**, 2218–2229.

220 G. Andersson and C. Ridings, Ion scattering studies of molecular structure at liquid surfaces with applications in industrial and biological systems, *Chem. Rev.*, 2014, **114**, 8361–8387.

221 D. Liu, G. Ma, L. M. Levering and H. C. Allen, Vibrational Spectroscopy of Aqueous Sodium Halide Solutions and Air–Liquid Interfaces: Observation of Increased Interfacial Depth, *J. Phys. Chem. B*, 2004, **108**, 2252–2260.

222 H. C. Allen, N. N. Casillas-Ituarte, M. R. Sierra-Hernández, X. Chen and C. Y. Tang, Shedding light on water structure at air-aqueous interfaces: ions, lipids, and hydration, *Phys. Chem. Chem. Phys.*, 2009, **11**, 5538–5549.

223 R. R. Kumal, S. Nayak, W. Bu and A. Uysal, Chemical Potential Driven Reorganization of Anions between Stern and Diffuse Layers at the Air/Water Interface, *J. Phys. Chem. C*, 2022, **126**, 1140–1151.

224 M. H. Cheng, K. M. Callahan, A. M. Margarella, D. J. Tobias, J. C. Hemminger, H. Bluhm and M. J. Krisch, Ambient Pressure X-ray Photoelectron Spectroscopy and Molecular Dynamics Simulation Studies of Liquid/Vapor Interfaces of Aqueous NaCl, RbCl, and RbBr Solutions, *J. Phys. Chem. C*, 2012, **116**, 4545–4555.

225 S. Ghosal, J. C. Hemminger, H. Bluhm, B. S. Mun, E. L.-D. Hebenstreit, G. Ketteler, D. F. Ogletree, F. G. Requejo and M. Salmeron, Electron Spectroscopy of Aqueous Solution Interfaces Reveals Surface Enhancement of Halides, *Science*, 2005, **307**, 563 LP–566 LP.

226 M. A. Brown, R. D'Auria, I. F.-W. Kuo, M. J. Krisch, D. E. Starr, H. Bluhm, D. J. Tobias and J. C. Hemminger, Ion spatial distributions at the liquid–vapor interface of aqueous potassium fluoride solutions, *Phys. Chem. Chem. Phys.*, 2008, **10**, 4778–4784.

227 K. A. Perrine, K. M. Parry, A. C. Stern, M. H.-C. Van Spyk, M. J. Makowski, J. A. Freites, B. Winter, D. J. Tobias and



J. C. Hemminger, Specific cation effects at aqueous solution–vapor interfaces: surfactant-like behavior of  $\text{Li}^+$  revealed by experiments and simulations, *Proc. Natl. Acad. Sci. U. S. A.*, 2017, **114**, 13363–13368.

228 S. Gopalakrishnan, D. Liu, H. C. Allen, M. Kuo and M. J. Shultz, Vibrational Spectroscopic Studies of Aqueous Interfaces: Salts, Acids, Bases, and Nanodrops, *Chem. Rev.*, 2006, **106**, 1155–1175.

229 W. Hua, D. Verreault, Z. Huang, E. M. Adams and H. C. Allen, Cation effects on interfacial water organization of aqueous chloride solutions. I. Monovalent cations:  $\text{Li}^+$ ,  $\text{Na}^+$ ,  $\text{K}^+$ , and  $\text{NH}_4^+$ , *J. Phys. Chem. B*, 2014, **118**, 8433–8440.

230 P. B. Petersen and R. J. Saykally, Probing the Interfacial Structure of Aqueous Electrolytes with Femtosecond Second Harmonic Generation Spectroscopy, *J. Phys. Chem. B*, 2006, **110**, 14060–14073.

231 C. Tian, S. J. Byrnes, H.-L. Han and Y. R. Shen, Surface Propensities of Atmospherically Relevant Ions in Salt Solutions Revealed by Phase-Sensitive Sum Frequency Vib, *Spectrosc.*, 2011, **2**, 1946–1949.

232 P. B. Petersen, J. C. Johnson, K. P. Knutsen and R. J. Saykally, Direct experimental validation of the Jones–Ray effect, *Chem. Phys. Lett.*, 2004, **397**, 46–50.

233 P. B. Petersen, R. J. Saykally, M. Mucha and P. Jungwirth, Enhanced Concentration of Polarizable Anions at the Liquid Water Surface: SHG Spectroscopy and MD Simulations of Sodium Thiocyanide, *J. Phys. Chem. B*, 2005, **109**, 10915–10921.

234 P. B. Petersen and R. J. Saykally, Adsorption of Ions to the Surface of Dilute Electrolyte Solutions: The Jones–Ray Effect Revisited, *J. Am. Chem. Soc.*, 2005, **127**, 15446–15452.

235 P. B. Petersen and R. J. Saykally, Confirmation of enhanced anion concentration at the liquid water surface, *Chem. Phys. Lett.*, 2004, **397**, 51–55.

236 L. Piatkowski, Z. Zhang, E. H.-G. Backus, H. J. Bakker and M. Bonn, Extreme surface propensity of halide ions in water, *Nat. Commun.*, 2014, **5**, 4083.

237 Z. Huang, W. Hua, D. Verreault and H. C. Allen, Salty glycerol versus salty water surface organization: bromide and iodide surface propensities, *J. Phys. Chem. A*, 2013, **117**, 6346–6353.

238 G. Andersson, Concentration Depth Profiles of Inorganic Ions at Liquid Surfaces, *Aust. J. Chem.*, 2010, **63**, 434–437.

239 G. Andersson, Energy-loss straggling of helium projectiles at low kinetic energies, *Phys. Rev. A: At., Mol., Opt. Phys.*, 2007, **75**, 032901.

240 G. Andersson, H. Morgner and H. Pohl, Energy-loss straggling of helium projectiles at low kinetic energies: deconvolution of concentration depth profiles of inorganic salt solutes in aqueous solutions, *Phys. Rev. A: At. Mol. Opt. Phys.*, 2008, **78**, 032904.

241 G. Andersson, H. Morgner, L. Cwiklik and P. Jungwirth, Anions of Alkali Halide Salts at Surfaces of Formamide Solutions: Concentration Depth Profiles and Surface Topography, *J. Phys. Chem. C*, 2007, **111**, 4379–4387.

242 C. Ridings, G. G. Warr and G. G. Andersson, Surface Ordering in Binary Mixtures of Protic Ionic Liquids, *J. Phys. Chem. Lett.*, 2017, **8**, 4264–4267.

243 X. Zhao, G. M. Nathanson and G. G. Andersson, Competing Segregation of  $\text{Br}^-$  and  $\text{Cl}^-$  to a Surface Coated with a Cationic Surfactant: Direct Measurements of Ion and Solvent Depth Profiles, *J. Phys. Chem. A*, 2020, **124**, 11102–11110.

244 R. A. Miranda-Quintana and J. Smiatek, Specific Ion Effects in Different Media: Current Status and Future Challenges, *J. Phys. Chem. B*, 2021, **125**, 13840–13849.

245 F. Zhang, M. W.-A. Skoda, R. M.-J. Jacobs, D. G. Dressen, R. A. Martin, C. M. Martin, G. F. Clark, T. Lamkemeyer, F. Schreiber, M. W.-A. Skoda, R. M.-J. Jacobs, D. G. Dressen, R. A. Martin, C. M. Martin, G. F. Clark, T. Lamkemeyer, F. Schreiber, M. W.-A. Skoda, R. M.-J. Jacobs, D. G. Dressen, R. A. Martin, C. M. Martin, G. F. Clark, T. Lamkemeyer, F. Schreiber, Gold Nanoparticles Decorated with Oligo(ethylene glycol) Thiols: Enhanced Hofmeister Effects in Colloid–Protein Mixtures, *J. Phys. Chem. C*, 2009, **113**, 4839.

246 A. Dér, L. Kelemen, L. Fábián, S. G. Taneva, E. Fodor, T. Páli, A. Cupane, M. G. Cacace and J. J. Ramsden, Interfacial Water Structure Controls Protein Conformation, *J. Phys. Chem. B*, 2007, **111**, 5344–5350.

247 T. López-León, J. L. Ortega-Vinuesa and D. Bastos-González, Ion-Specific Aggregation of Hydrophobic Particles, *ChemPhysChem*, 2012, **13**, 2382–2391.

248 E. Braun, S. Mohamad Moosavi and B. Smit, Anomalous Effects of Velocity Rescaling Algorithms: The Flying Ice Cube Effect Revisited, *J. Chem. Theory Comput.*, 2018, **14**, 5262–5272.

249 H. Robertson, E. C. Johnson, I. J. Gresham, S. W. Prescott, A. Nelson, E. J. Wanless and G. B. Webber, Competitive specific ion effects in mixed salt solutions on a thermo-responsive polymer brush, *J. Colloid Interface Sci.*, 2021, **586**, 292–304.

250 S. Zajforoushan Moghaddam and E. Thormann, Hofmeister effect of salt mixtures on thermo-responsive poly(propylene oxide), *Phys. Chem. Chem. Phys.*, 2015, **17**, 6359–6366.

251 T. Wang, G. Liu, G. Zhang and V. S.-J. Craig, Insights into Ion Specificity in Water–Methanol Mixtures via the Reentrant Behavior of Polymer, *Langmuir*, 2012, **28**, 1893–1899.

252 L. Liu, T. Wang, C. Liu, K. Lin, Y. Ding, G. Liu and G. Zhang, Mechanistic Insights into Amplification of Specific Ion Effect in Water–Nonaqueous Solvent Mixtures, *J. Phys. Chem. B*, 2013, **117**, 2535–2544.

253 T. Wang, Y. Long, L. Liu, X. Wang, V. S.-J. Craig, G. Zhang and G. Liu, Cation-Specific Conformational Behavior of Polyelectrolyte Brushes: From Aqueous to Nonaqueous Solvent, *Langmuir*, 2014, **30**, 12850–12859.

254 Y. Xu and G. Liu, Amplification of Hofmeister Effect by Alcohols, *J. Phys. Chem. B*, 2014, **118**, 7450–7456.

255 L. Liu, R. Kou and G. Liu, Ion specificities of artificial macromolecules, *Soft Matter*, 2017, **13**, 68–80.

256 K. P. Gregory, G. R. Elliott, E. J. Wanless, G. B. Webber and A. J. Page, Ion Solvation Repository (IonSolvR), Repository, University of Newcastle, 2022, DOI: [10.25817/40r8-t633](https://doi.org/10.25817/40r8-t633).



257 A. Narayanan Krishnamoorthy, C. Holm and J. Smiatek, Specific ion effects for polyelectrolytes in aqueous and non-aqueous media: the importance of the ion solvation behavior, *Soft Matter*, 2018, **14**, 6243–6255.

258 A. Narayanan Krishnamoorthy, K. Oldiges, M. Winter, A. Heuer, I. Cekic-Laskovic, C. Holm and J. Smiatek, Electrolyte solvents for high voltage lithium ion batteries: ion correlation and specific anion effects in adiponitrile, *Phys. Chem. Chem. Phys.*, 2018, **20**, 25701–25715.

259 R. A. Miranda-Quintana and J. Smiatek, Theoretical Insights into Specific Ion Effects and Strong-Weak Acid-Base Rules for Ions in Solution: Deriving the Law of Matching Solvent Affinities from First Principles, *ChemPhysChem*, 2020, **21**, 2605–2617.

260 J. Smiatek, Specific Ion Effects and the Law of Matching Solvent Affinities: A Conceptual Density Functional Theory Approach, *J. Phys. Chem. B*, 2020, **124**, 2191–2197.

261 J. Smiatek, Theoretical and Computational Insight into Solvent and Specific Ion Effects for Polyelectrolytes: The Importance of Local Molecular Interactions, *Molecules*, 2020, **25**, 1661.

262 R. A. Miranda-Quintana and J. Smiatek, Beneficial properties of solvents and ions for lithium ion and post-lithium ion batteries: implications from charge transfer models, *Electrochim. Acta*, 2021, **384**, 138418.

263 R. A. Miranda-Quintana and J. Smiatek, Calculation of donor numbers: computational estimates for the Lewis basicity of solvents, *J. Mol. Liq.*, 2021, **322**, 114506.

264 A. E. Eisenhart and T. L. Beck, Quantum Simulations of Hydrogen Bonding Effects in Glycerol Carbonate Electrolyte Solutions, *J. Phys. Chem. B*, 2021, **125**, 2157–2166.

265 A. E. Eisenhart and T. L. Beck, Specific Ion Solvation and Pairing Effects in Glycerol Carbonate, *J. Phys. Chem. B*, 2021, **125**, 13635–13643.

266 K. Izutsu, *Electrochemistry in nonaqueous solutions*, John Wiley & Sons, 2009.

267 L. Fan, K. Lin, J. Wang, R. Ma and B. Lu, A Nonaqueous Potassium-Based Battery-Supercapacitor Hybrid Device, *Adv. Mater.*, 2018, **30**, 1800804.

268 W. Simka, D. Puszczyk and G. Nawrat, Electrodeposition of metals from non-aqueous solutions, *Electrochim. Acta*, 2009, **54**, 5307–5319.

269 J. F. Gibbons, G. W. Cogan, C. M. Gronet and N. S. Lewis, A 14% efficient nonaqueous semiconductor/liquid junction solar cell, *Appl. Phys. Lett.*, 1984, **45**, 1095–1097.

270 M. Winter and R. J. Brodd, What Are Batteries, Fuel Cells, and Supercapacitors?, *Chem. Rev.*, 2004, **104**, 4245–4270.

271 R. S. Sahota and M. G. Khaledi, Nonaqueous Capillary Electrophoresis, *Anal. Chem.*, 1994, **66**, 1141–1146.

272 A. J. Parker, The effects of solvation on the properties of anions in dipolar aprotic solvents, *Q. Rev., Chem. Soc.*, 1962, **16**, 163–187.

273 R. G. Pearson and J. Songstad, Application of the principle of hard and soft acids and bases to organic chemistry, *J. Am. Chem. Soc.*, 1967, **89**, 1827–1836.

274 N. Schmelzer, J. Einfeldt and M. Grigo, Ion–solvent interactions of some ions in dipolar aprotic solvents at 25 °C, *J. Chem. Soc., Faraday Trans.*, 1990, **86**, 489–494.

275 U. Mayer, V. Gutmann and W. Gerger, The acceptor number—A quantitative empirical parameter for the electrophilic properties of solvents, *Monatshefte für Chemie*, 1975, **106**, 1235–1257.

276 J. Smiatek, A. Wohlfarth and C. Holm, The solvation and ion condensation properties for sulfonated polyelectrolytes in different solvents—a computational study, *New J. Phys.*, 2014, **16**, 025001.

277 J. Smiatek, A. Heuer and M. Winter, Properties of ion complexes and their impact on charge transport in organic solvent-based electrolyte solutions for lithium batteries: insights from a theoretical perspective, *Batteries*, 2018, **4**, 62.

278 V. Gutmann, Empirical parameters for donor and acceptor properties of solvents, *Electrochim. Acta*, 1976, **21**, 661–670.

279 G. Liu, D. Parsons and V. S.-J. Craig, Re-entrant swelling and redissolution of polyelectrolytes arises from an increased electrostatic decay length at high salt concentrations, *J. Colloid Interface Sci.*, 2020, **579**, 369–378.

280 P. Jia and J. Zhao, Single chain contraction and re-expansion of polystyrene sulfonate: a study on its re-entrant condensation at single molecular level, *J. Chem. Phys.*, 2009, **131**, 231103.

281 R. Kou, J. Zhang, Z. Chen and G. Liu, Counterion Specificity of Polyelectrolyte Brushes: Role of Specific Ion-Pairing Interactions, *ChemPhysChem*, 2018, **19**, 1404–1413.

282 T. López-León, M. J. Santander-Ortega, J. L. Ortega-Vinuesa and D. Bastos-González, Hofmeister Effects in Colloidal Systems: Influence of the Surface Nature, *J. Phys. Chem. C*, 2008, **112**, 16060–16069.

283 Y. Luo, H. Li, X. Gao and R. Tian, Description of colloidal particles aggregation in the presence of Hofmeister effects: on the relationship between ion adsorption energy and particle aggregation activation energy, *Phys. Chem. Chem. Phys.*, 2018, **20**, 22831–22840.

284 R. Kjellander, *Statistical Mechanics of Liquids and Solutions*, CRC Press, 2019.

285 A. A. Lee, C. S. Perez-Martinez, A. M. Smith and S. Perkin, Scaling Analysis of the Screening Length in Concentrated Electrolytes, *Phys. Rev. Lett.*, 2017, **119**, 1–5.

286 D. J. Griffiths, *Introduction to Electrodynamics*, Pearson, 4th edn, 2013.

287 T. N. Tran and T. Le, Microscopic approach for low-frequency dielectric constant of liquid water, *Phys. Chem. Liq.*, 2021, **59**, 53–61.

288 D. J. Grzetic, K. T. Delaney and G. H. Fredrickson, Contrasting Dielectric Properties of Electrolyte Solutions with Polar and Polarizable Solvents, *Phys. Rev. Lett.*, 2019, **122**, 128007.

289 J. H. Christensen, A. J. Smith, R. B. Reed and K. L. Elmore, Dielectric Properties of Phosphoric Acid Solutions at 25 °C, *J. Chem. Eng. Data*, 1966, **11**, 60–63.

290 F. E. Harris and C. T. O'Konski, Dielectric properties of aqueous ionic solutions at microwave frequencies, *J. Phys. Chem.*, 1957, **61**, 310–319.



291 G. H. Haggis, J. B. Hasted and T. J. Buchanan, The dielectric properties of water in solutions, *J. Chem. Phys.*, 1952, **20**, 1452–1465.

292 A. De Ninno, E. Nikollari, M. Missori and F. Frezza, Dielectric permittivity of aqueous solutions of electrolytes probed by THz time-domain and FTIR spectroscopy, *Phys. Lett. Sect. A: Gen. At. Solid State Phys.*, 2020, **384**, 126865.

293 J. B. Hasted and G. W. Roderick, Dielectric properties of aqueous and alcoholic electrolytic solutions, *J. Chem. Phys.*, 1958, **29**, 17–26.

294 R. Buchner, G. T. Hefter and P. M. May, Dielectric relaxation of aqueous NaCl solutions, *J. Phys. Chem. A*, 1999, **103**, 8–9.

295 N. Gavish and K. Promislow, Dependence of the dielectric constant of electrolyte solutions on ionic concentration: a microfield approach, *Phys. Rev. E*, 2016, **94**, 1–7.

296 M. Muthukumar, 50th Anniversary Perspective: A Perspective on Polyelectrolyte Solutions, *Macromolecules*, 2017, **50**, 9528–9560.

297 W. Lin and J. Klein, Direct measurement of surface forces: recent advances and insights, *Appl. Phys. Rev.*, 2021, **8**, 031316.

298 M. A. Gebbie, M. Valtiner, X. Banquy, E. T. Fox, W. A. Henderson and J. N. Israelachvili, Ionic liquids behave as dilute electrolyte solutions, *Proc. Natl. Acad. Sci. U. S. A.*, 2013, **110**, 9674–9679.

299 A. A. Lee, C. S. Perez-Martinez, A. M. Smith and S. Perkin, Underscreening in concentrated electrolytes, *Faraday Discuss.*, 2017, **199**, 239–259.

300 A. M. Smith, A. A. Lee and S. Perkin, The Electrostatic Screening Length in Concentrated Electrolytes Increases with Concentration, *J. Phys. Chem. Lett.*, 2016, **7**, 2157–2163.

301 P. Gaddam and W. Ducker, Electrostatic Screening Length in Concentrated Salt Solutions, *Langmuir*, 2019, **35**, 5719–5727.

302 M. A. Gebbie, A. M. Smith, H. A. Dobbs, A. A. Lee, G. G. Warr, X. Banquy, M. Valtiner, M. W. Rutland, J. N. Israelachvili, S. Perkin and R. Atkin, Long range electrostatic forces in ionic liquids, *Chem. Commun.*, 2017, **53**, 1214–1224.

303 J. Ennis, R. Kjellander and D. J. Mitchell, Dressed ion theory for bulk symmetric electrolytes in the restricted primitive model, *J. Chem. Phys.*, 1995, **102**, 975–991.

304 J. Ulander and R. Kjellander, The decay of pair correlation functions in ionic fluids: a dressed ion theory analysis of Monte Carlo simulations, *J. Chem. Phys.*, 2001, **114**, 4893–4904.

305 R. Kjellander, A multiple decay-length extension of the Debye–Hückel theory: to achieve high accuracy also for concentrated solutions and explain under-screening in dilute symmetric electrolytes, *Phys. Chem. Chem. Phys.*, 2020, **22**, 23952–23985.

306 P. Cats, R. Evans, A. Härtel and R. Van Roij, Primitive model electrolytes in the near and far field: decay lengths from DFT and simulations, *J. Chem. Phys.*, 2021, **154**, 124504.

307 J. Zeman, S. Kondrat and C. Holm, Bulk ionic screening lengths from extremely large-scale molecular dynamics simulations, *Chem. Commun.*, 2020, **56**, 15635–15638.

308 J. G. Kirkwood, Statistical mechanics of liquid solutions, *Chem. Rev.*, 1936, **19**, 275–307.

309 M. Z. Bazant, B. D. Storey and A. A. Kornyshev, Double layer in ionic liquids: overscreening versus crowding, *Phys. Rev. Lett.*, 2011, **106**, 6–9.

310 M. E. Fisher and B. Wiodm, Decay of correlations in linear systems, *J. Chem. Phys.*, 1969, **50**, 3756–3772.

311 L. Onsager, Theories of concentrated electrolytes, *Chem. Rev.*, 1933, **13**, 73–89.

312 R. Kjellander, Decay behavior of screened electrostatic surface forces in ionic liquids: the vital role of non-local electrostatics, *Phys. Chem. Chem. Phys.*, 2016, **18**, 18985–19000.

313 R. Kjellander, Nonlocal electrostatics in ionic liquids: the key to an understanding of the screening decay length and screened interactions, *J. Chem. Phys.*, 2016, **145**, 124503.

314 R. Kjellander and D. J. Mitchell, Dressed-ion theory for electrolyte solutions: a Debye–Hückel-like reformulation of the exact theory for the primitive model, *J. Chem. Phys.*, 1994, **101**, 603–626.

315 R. Kjellander, Focus Article: oscillatory and long-range monotonic exponential decays of electrostatic interactions in ionic liquids and other electrolytes: the significance of dielectric permittivity and renormalized charges, *J. Chem. Phys.*, 2018, **148**, 193701.

316 R. J.-F. Leote De Carvalho and R. Evans, The decay of correlations in ionic fluids, *Mol. Phys.*, 1994, **83**, 619–654.

317 F. H. Stillinger and R. Lovett, Ion-Pair Theory of Concentrated Electrolytes, *J. Chem. Phys.*, 1986, **48**, 3858.

318 P. Attard, Asymptotic analysis of primitive model electrolytes and the electrical double layer, *Phys. Rev. E: Stat. Phys., Plasmas, Fluids, Relat. Interdiscip. Top.*, 1993, **48**, 3604–3621.

319 Y. Avni, R. M. Adar and D. Andelman, Charge oscillations in ionic liquids: a microscopic cluster model, *Phys. Rev. E*, 2020, **101**, 1–6.

320 E. Krucker-Velasquez and J. W. Swan, Underscreening and hidden ion structures in large scale simulations of concentrated electrolytes, *J. Chem. Phys.*, 2021, **155**, 134903.

321 P. Jones, F. Coupette, A. Härtel and A. A. Lee, Bayesian unsupervised learning reveals hidden structure in concentrated electrolytes, *J. Chem. Phys.*, 2021, **154**, 134902.

322 F. Coupette, A. A. Lee and A. Härtel, Screening Lengths in Ionic Fluids, *Phys. Rev. Lett.*, 2018, **121**, 75501.

323 S. W. Coles, C. Park, R. Nikam, M. Kanduč, J. Dzubiella and B. Rotenberg, Correlation Length in Concentrated Electrolytes: Insights from All-Atom Molecular Dynamics Simulations, *J. Phys. Chem. B*, 2020, **124**, 1778–1786.

324 R. M. Adar, S. A. Safran, H. Diamant and D. Andelman, Screening length for finite-size ions in concentrated electrolytes, *Phys. Rev. E*, 2019, **100**, 42615.

325 B. Rotenberg, O. Bernard and J. P. Hansen, Underscreening in ionic liquids: a first principles analysis, *J. Phys.: Condens. Matter*, 2018, **30**, 054005.



326 R. Heyrovská, Equations for Densities and Dissociation Constant of NaCl(aq) at 25 °C from “Zero to Saturation” Based on Partial Dissociation, *J. Electrochem. Soc.*, 1997, **144**, 2380–2384.

327 M. Landstorfer, On the dissociation degree of ionic solutions considering solvation effects, *Electrochem. Commun.*, 2018, **92**, 56–59.

328 Z. A.-H. Goodwin and A. A. Kornyshev, Underscreening, overscreening and double-layer capacitance, *Electrochem. Commun.*, 2017, **82**, 129–133.

329 R. Kjellander and D. J. Mitchell, An exact but linear and Poisson–Boltzmann-like theory for electrolytes and colloid dispersions in the primitive model, *Chem. Phys. Lett.*, 1992, **200**, 76–82.

330 P. Kebelinski, J. Eggebrecht, D. Wolf and S. R. Phillpot, Molecular dynamics study of screening in ionic fluids, *J. Chem. Phys.*, 2000, **113**, 282–291.

331 C. W. Outhwaite and L. B. Bhuiyan, On the modified Poisson–Boltzmann closure for primitive model electrolytes at high concentration, *J. Chem. Phys.*, 2021, **155**, 14504.

332 D. R. MacFarlane, A. L. Chong, M. Forsyth, M. Kar, R. Vijayaraghavan, A. Somers and J. M. Pringle, New dimensions in salt-solvent mixtures: a 4th evolution of ionic liquids, *Faraday Discuss.*, 2018, **206**, 9–28.

333 A. Sanchez-Fernandez, A. J. Jackson, S. F. Prévost, J. J. Doutch and K. J. Edler, Long-Range Electrostatic Colloidal Interactions and Specific Ion Effects in Deep Eutectic Solvents, *J. Am. Chem. Soc.*, 2021, **143**, 14158–14168.

334 D. Constantinescu, H. Weingärtner and C. Herrmann, Protein Denaturation by Ionic Liquids and the Hofmeister Series: A Case Study of Aqueous Solutions of Ribonuclease A, *Angew. Chem., Int. Ed.*, 2007, **46**, 8887–8889.

335 H. Zhao, Effect of ions and other compatible solutes on enzyme activity, and its implication for biocatalysis using ionic liquids, *J. Mol. Catal. B: Enzym.*, 2005, **37**, 16–25.

336 Z. Yang, *Hofmeister effects: an explanation for the impact of ionic liquids on biocatalysis*, Elsevier, 2009, vol. 144.

337 T. Vasantha, A. Kumar, P. Attri, P. Venkatesu and R. S. Rama Devi, The solubility and stability of amino acids in biocompatible ionic liquids, *Protein Pept. Lett.*, 2014, **21**, 15–24.

338 A. Kumar and P. Venkatesu, Does the stability of proteins in ionic liquids obey the Hofmeister series?, *Int. J. Biol. Macromol.*, 2014, **63**, 244–253.

339 H. Zhao, S. M. Campbell, L. Jackson, Z. Song and O. Olubajo, Hofmeister series of ionic liquids: kosmotropic effect of ionic liquids on the enzymatic hydrolysis of enantiomeric phenylalanine methyl ester, *Tetrahedron: Asymmetry*, 2006, **17**, 377–383.

340 E. M. Knipping, M. J. Lakin, K. L. Foster, P. Jungwirth, D. J. Tobias, R. B. Gerber, D. Dabdub and B. J. Finlayson-Pitts, Experiments and simulations of ion-enhanced interfacial chemistry on aqueous NaCl aerosols, *Science*, 2000, **288**(5464), 301–306.

341 Q. Han, K. M. Smith, C. Darmanin, T. M. Ryan, C. J. Drummond and T. L. Greaves, Lysozyme conformational changes with ionic liquids: spectroscopic, small angle X-ray scattering and crystallographic study, *J. Colloid Interface Sci.*, 2021, **585**, 433–443.

342 D. N. Fuller, J. P. Rickgauer, P. J. Jardine, S. Grimes, D. L. Anderson and D. E. Smith, Ionic effects on viral DNA packaging and portal motor function in bacteriophage  $\varphi$ 29, *Proc. Natl. Acad. Sci. U. S. A.*, 2007, **104**, 11245 LP–11250 LP.

343 C. Y. Zhang and N. H. Zhang, Size dependent correlation between structure and apparent stiffness of viral DNA during temperature variation, *J. Mech. Phys. Solids*, 2021, **154**, 104501.

344 J. Wei and Q. Wang, Hofmeister Effect-Aided Assembly of Enhanced Hydrogel Supercapacitor with Excellent Interfacial Contact and Reliability, *Small, Methods*, 2019, **3**, 1900558.

345 J. R. Pinca, W. G. Duborg and R. Jorn, Ion Association and Electrolyte Structure at Surface Films in Lithium-Ion Batteries, *J. Phys. Chem. C*, 2021, **125**, 7054–7066.

346 S. Perkin, L. Crowhurst, H. Niedermeyer, T. Welton, A. M. Smith and N. N. Gosvami, Self-assembly in the electrical double layer of ionic liquids, *Chem. Commun.*, 2011, **47**, 6572–6574.

347 B. W. Ninham, R. M. Pashley and P. Lo Nostro, Surface forces: changing concepts and complexity with dissolved gas, bubbles, salt and heat, *Curr. Opin. Colloid Interface Sci.*, 2017, **27**, 25–32.

348 A. C. Rodrigo, E. Laurini, V. M.-P. Vieira, S. Prich and D. K. Smith, Effect of buffer at nanoscale molecular recognition interfaces – electrostatic binding of biological polyanions, *Chem. Commun.*, 2017, **53**, 11580–11583.

349 A. Salis, L. Cappai, C. Carucci, D. F. Parsons and M. Monduzzi, Specific Buffer Effects on the Intermolecular Interactions among Protein Molecules at Physiological pH, *J. Phys. Chem. Lett.*, 2020, **11**, 6805–6811.

350 S. Brudar and B. Hribar-Lee, Effect of Buffer on Protein Stability in Aqueous Solutions: A Simple Protein Aggregation Model, *J. Phys. Chem. B*, 2021, **125**, 2504–2512.

351 J. H. Jordan, H. S. Ashbaugh, J. T. Mague and B. C. Gibb, Buffer and Salt Effects in Aqueous Host–Guest Systems: Screening, Competitive Binding, or Both?, *J. Am. Chem. Soc.*, 2021, **143**, 18605–18616.

352 J. D. Willott, B. A. Humphreys, G. B. Webber, E. J. Wanless and W. M. de Vos, Combined Experimental and Theoretical Study of Weak Polyelectrolyte Brushes in Salt Mixtures, *Langmuir*, 2019, **35**, 2709–2718.

353 J. D. Willott, T. J. Murdoch, F. A.-M. Leermakers and W. M. de Vos, Behavior of Weak Polyelectrolyte Brushes in Mixed Salt Solutions, *Macromolecules*, 2018, **51**, 1198–1206.

354 E. Yilmaz Topuzlu, H. I. Okur, B. Ulgut and Ö. Dag, Role of Water in the Lyotropic Liquid Crystalline Mesophase of Lithium Salts and Non-ionic Surfactants, *Langmuir*, 2021, **37**, 14443–14453.



355 D. Tatini, D. Ciardi, C. Sofroniou, B. W. Ninham and P. Lo Nstro, Physicochemical characterization of green sodium oleate-based formulations. Part 2. Effect of anions, *J. Colloid Interface Sci.*, 2022, **617**, 399–408.

356 J. Mehringer, E. Hofmann, D. Touraud, S. Koltzenburg, M. Kellermeier and W. Kunz, Salting-in and salting-out effects of short amphiphilic molecules: a balance between specific ion effects and hydrophobicity, *Phys. Chem. Chem. Phys.*, 2021, **23**, 1381–1391.

357 G. Hantal, M. Segá, G. Horvai and P. Jedlovszky, Contribution of Different Molecules and Moieties to the Surface Tension in Aqueous Surfactant Solutions. II: Role of the Size and Charge Sign of the Counterions, *J. Phys. Chem. B*, 2021, **125**, 9005–9018.

